1 Contributions

1.1 Primary Particles – Agglomerates – Aggregates

Dirk Walter

Laboratories for Chemistry and Physics, Institute for Occupatinal and Social Medicine, Justus-Liebig-University

Gießen, Germany

Introduction

The existence of nanosized particles at the workplace is not a new phenomenon. As early as in 1997, the Deutsche Forschungsgemeinschaft, Commission for the investigation of Health Hazards of chemical compounds in the work area, defined the term "ultrafine particles" in its List of *Maximale Arbeitsplatz-Konzentration* (MAK) and *Biologischer Arbeitsstoff-Toleranzwert* (BAT) Values. The definition of "ultrafine particles" as it relates to the workplace corresponds primarily to the term nanoparticles as it is currently being used in research and technology.

Nanoparticles are not a new discovery of science, nor are they an innovation, as regards their definition based on their particle size or as a technical achievement. They have, however, always been components of smoke. Their use as natural iron oxide and carbon black particles has already been applied in prehistoric cave paintings, such as in Altamira, etc. Nanosized particles differ from coarser particles by their increasing tendency to form agglomerates. Such agglomerates are macroscopically perceived as one particle and may break down into their primary particles in biological material; this dissociation is of toxicological relevance (Oberdörster et al. 2005).

Definition

In literature, the terms agglomerate, aggregate and primary particle are not always used unambiguously and the relation of the terms between each other is often described incorrectly, although research has long been dealing with phenomenona such as agglomeration in the field of synthetic pigments (Buxbaum and Pfaff 2005; Ullmann's Encyclopedia industrial chemistry 1992).

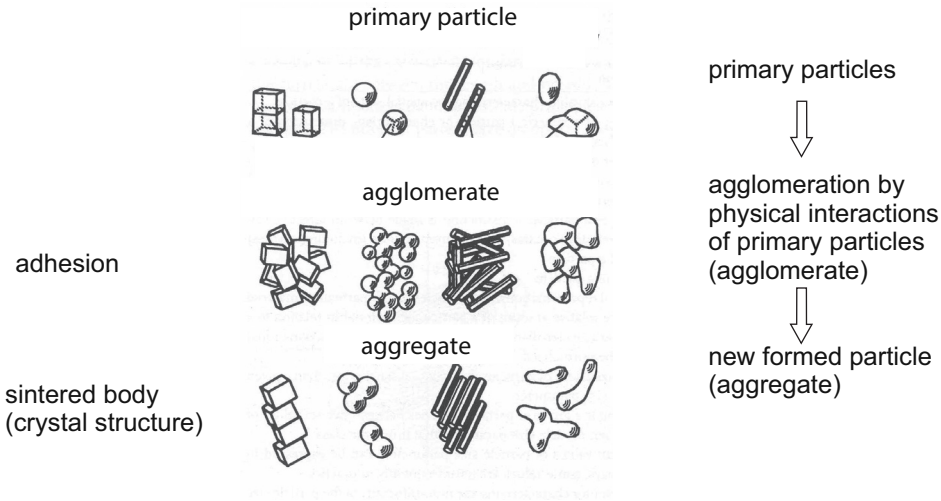

Figure 1: Relationships between primary particles, agglomerates and aggregates.

Figure 1 shows the relevant relationships.

Primary particles occur in different geometrical forms, for example in spherical, cuboidal or rod-like geometry. Particles without defined geometry are generally referred to "bulk" or "bulk-material". Primary particles characteristically agglomerate to larger units (agglomerates) by adhesion (weak physical interactions).

Agglomerates are an assembly of primary particles (e. g. joined together at the corners or edges), and/or aggregates whose total surface area does not differ appreciable from the sum of specific surface areas of primary particles.

In consequence agglomerates are not fixed units, but could change their size and shape. Altering conditions (temperature, pressure, pH-value, viscosity, etc.) of the surrounding medium result in varied agglomerates. Larger agglomerates may also break down into smaller agglomerates or, vice versa, smaller agglomerates may again form larger agglomerates. The density of agglomerates depends on the particle size distribution of the primary particles (assumption of equal geometry and chemical composition).

Aggregates develop when primary particles begin to form a common crystalline structure. From a physico-chemical point of view, the formation of aggregates corresponds to a sintering process like the formation of compact ceramic solids from several smaller (primary) particles.

Aggregates are an assembly of primary particles that have grown together and are aligned side by side; the total specific surface area is less than the sum of the surface areas of the primary particles.

For example, five primary particles form an agglomerate by adhesion. When crystal growth begins, the agglomerate is converted into a new larger formed particle (aggregate). Although the original geometry of the primary particles is still visible in the aggregate, the particles are firmly fused together. The surface area of the new particle (aggregate) compared with the sum of the surface areas of the former primary particles is reduced.

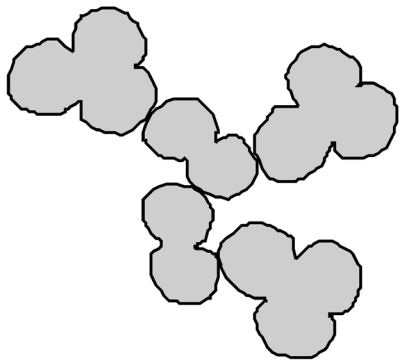

Figure 2: Diagram of an agglomerate consisting of two different aggregates. The number of original primary particles is still visible in the aggregates.

Consequently, the term "aggregate" could be defined as follows:

> The specific surface area of an aggregate is smaller than the sum of its original primary particles!

Figure 2 shows that smaller aggregates may also again form agglomerates.

Preparation of Nanoparticles

Nanoparticles are generally formed by two different processes. Based on coarser particles, the *top-down process* leads to smaller particles mainly by mechanical comminution. In *bottom-up processes*, nanosized particles are formed by gas-phase or liquid-phase reactions.

The fundamental difference between the two processes is that the top-down method generally leads to crystalline samples, such as small single crystals or polycrystalline material from a previously, "thermodynamically" formed starting material. In a crystalline solid, a "thermodynamically" formed product usually complies with the ideal crystal structure (ideal structure) of the specific compound (e. g. NaCl, CsCl, rutile, and corundum structures).

The bottom-up procedure results in the formation of small particles from crystalline areas that do not correspond to the ideal lattice (defect structure). These structures, which are difficult to describe, are typical of "kinetic" products, i. e. products that did not have enough time for an ideal crystal growth (Galway and Brown 2000). Therefore, a "kinetic" product leads to a "defect structure", which is also referred to as a real structure in literature. Such defect or real structures are classified according to different defect classes: 0-dimensional defects (non-stoichiometry), 1-dimensional defects (dislocations), 2-dimensional defects (grain boundaries) and 3-dimensional defects (pores) (Schmalzried and Navrotsky 1975).

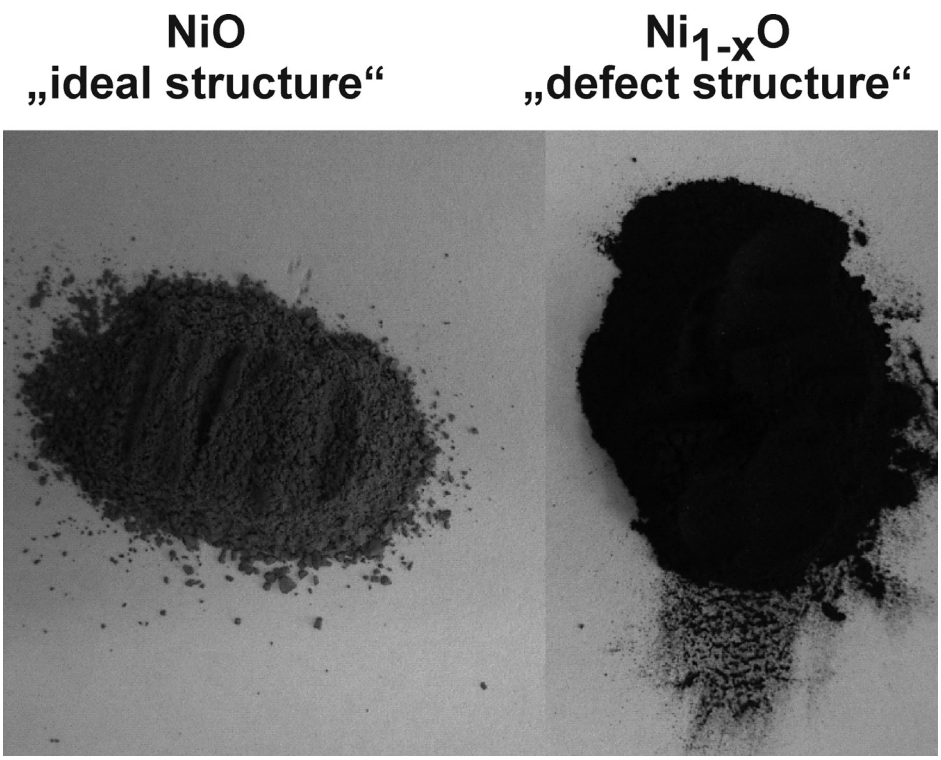

Figure 3: "Ideal" NiO (left) and "defective" $Ni_{1-x}O$ (right). The structure is determined by the process of preparation (partial pressure of oxygen).

Defect Structures

Non-stoichiometry

Figure 3 shows nickel oxide in its almost ideal sodium chloride structure as a green powder compared with "defect" = non-stoichiometric nickel oxide ($Ni_{1-x}O$) with a deficiency of cations in the metallic sublattice.

The Ni^{2+} deficiency can only be compensated electronically by the formation of Ni^{3+} ions (all lattice sites corresponding to the ideal structure are occupied by O^{2-} ions in the O^{2-}ion sublattice). However, the Ni^{3+} ions that have formed are not localized (i. e. they are not assigned to definite lattice places) and lead to a bathochromic shift or to the perception of "black" due to charge-transfer interactions (Moore 1967).

Dislocations, grain boundaries and pores

Figures 4–6 show examples of edge dislocations, grain boundaries and pores.

For particles prepared by *bottom-up procedures*, the occurrence of defects, i. e. a deviation from the ideal crystal structure, leads to altered physico-chemical properties (Schmalzried and Navrotsky 1975).

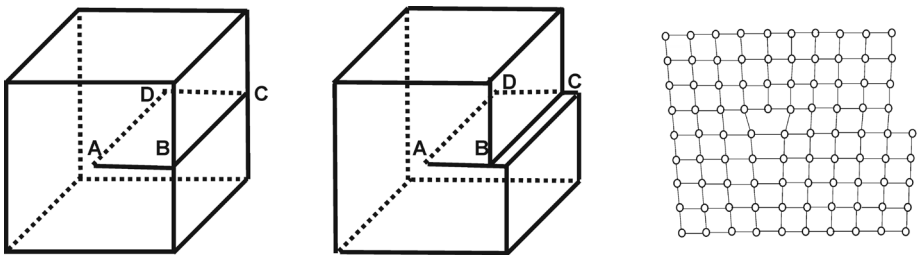

Figure 4: Diagram of an edge dislocation.

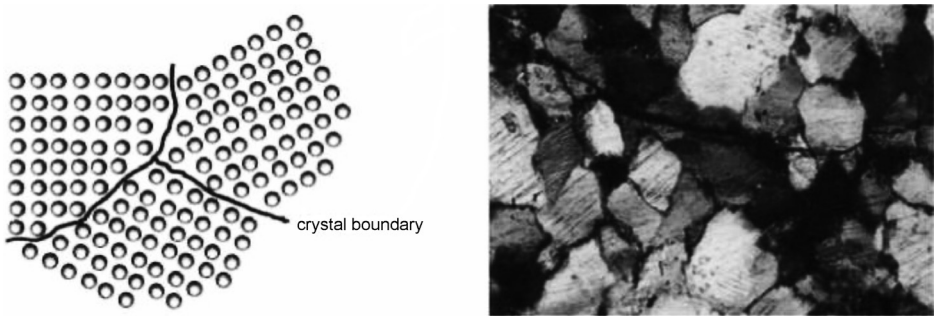

Figure 5: Diagram of grain boundaries (left); light microscopy images (thin section).

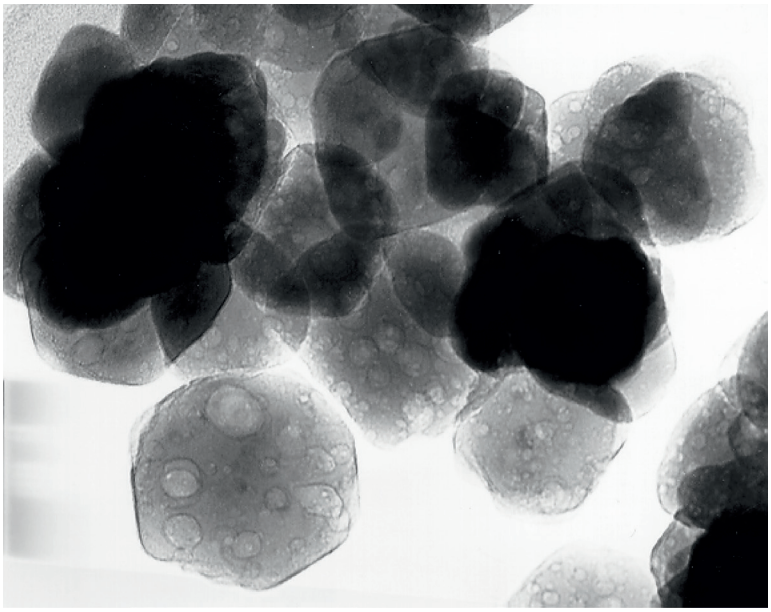

Figure 6: TEM image of pores (hematite pigments, magnification 275 000 x) on solid surfaces (Walter 2006).

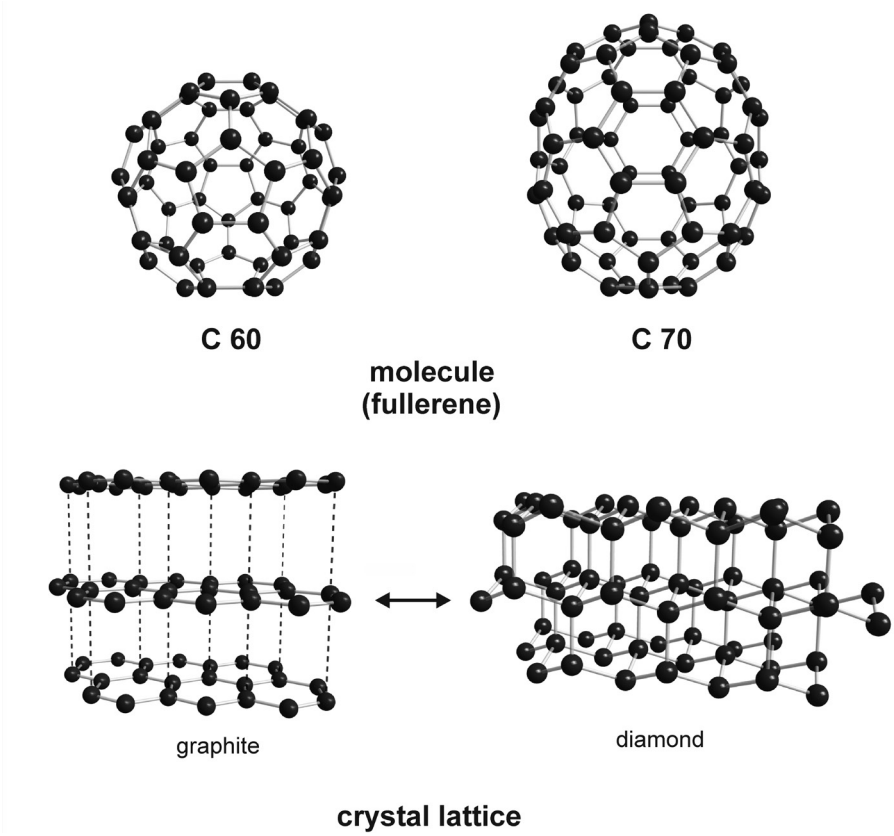

Figure 7: Modifications of carbon; molecular compounds (fullerenes above) and crystal lattices of graphite and diamond (below).

Bottom-up processes may also form molecular structures resulting in clusters. Clusters are units consisting of several atoms or compounds whose physicochemical properties depend on the size of the clusters. For example, gold clusters with fewer than 50 atoms have a molecular character, whereas clusters with more than 50 atoms have a metallic character.

Fullerenes, such as C 60, C 70 and C 84 molecules, are better known molecular carbon compounds that are prepared by *bottom-up processes*. The physicochemical properties of fullerenes (molecules) held together by covalent bindings clearly differ from the classical crystalline carbon modifications graphite and diamond (Figure 7). It must be pointed out that *bottom-up processes* may lead to the formation of both defective crystalline structures and molecular compounds in the nanoscale size range.

Problems of Detection and Measurement

As regards concentration measurements of ultrafine dusts or nanosized particles, it should be pointed out here that particle counter or particle sizer types are generally used for concentration measurement. Both particle counters each

have two disadvantages regarding toxicological aspects. First, they cannot differentiate between different substances (the difference between pollen, water droplets (= mist) and diesel soot, for example, is not detected). Second, they do not differentiate between primary particles and agglomerates or aggregates (Rödelsperger et al. 2009). This means that an agglomerate is recorded in the same way as a primary particle, i. e. as an individual particle! Therefore, the detected particles require further characterization.

Methods for the Characterization of Nanoparticles

What methods are actually suitable for characterizing nanoparticles? X-ray diffraction (XRD) is generally used to characterize solids. However, in the case of particles < 100 nm, XRD measurements are not very conclusive due to the effects of scattering and are therefore not suitable for characterizing nano-dusts. An appropriate X-ray method seems to be the use of highly monochromatic synchrotron radiation as applied for example at the DESY linear accelerator in Hamburg, Germany. However, the time of measurement is available only in individual cases on request. Electron microscopy, in particular transmission electron microscopy (TEM) with subsequent elemental analysis (EDX), is another suitable method (Rödelsperger et al. 2003 a). On account of the relatively sophisticated sample preparation, TEM analyses are only of limited suitability for routine measurements. In addition to electron microscopy, thermal analysis (TG-FTR and TG-MS) has recently been used to investigate different agglomerate/aggregate constellations of nanoscale dusts (Eichholz et al. 2012). Determination of the specific surface by nitrogen adsorption according to the Brunauer, Emmett, and Teller (BET) adsorption is another method frequently used for characterization. The BET adsorption is based on a relationship between the number of adsorbed nitrogen molecules and the specific surface (Brunauer et al. 1938).

Problem of Data on the Specific Surface

The following will explain why data published on the specific surface of dust samples are hardly a characteristic parameter and must be reviewed critically.

It is common practice to use the specific surface [m^2/g] as a synonym for the size (geometry) of the particles (Buxbaum and Pfaff 2005). However, this requires a very narrow particle size distribution within the sample. In other words: the specific surface can be used as a synonym for the particle size only if the sample consists of particles of the same size and same geometry! As a rule, only synthetic pigments with an even surface morphology sufficiently meet these requirements. Particles with a fissured surface morphology and/or pore structure (inner surface) no longer readily fulfil this requirement (Walter et al. 2001) (Figure 8).

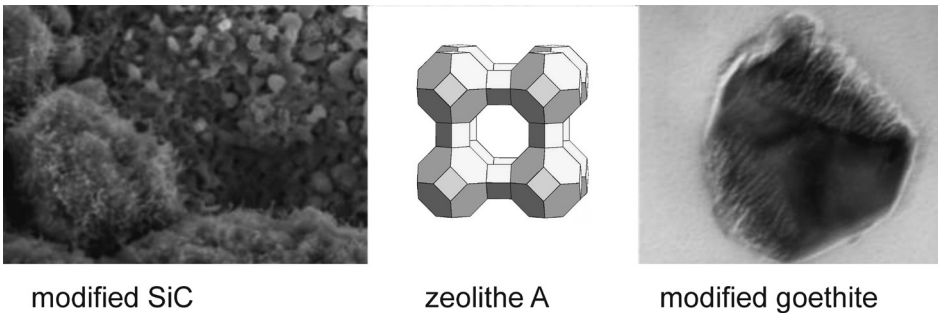

Figure 8: Samples for which BET analyses cannot be used as a synonym for particle size: differently fissured surface (left), inner surface (middle) and pores (right).

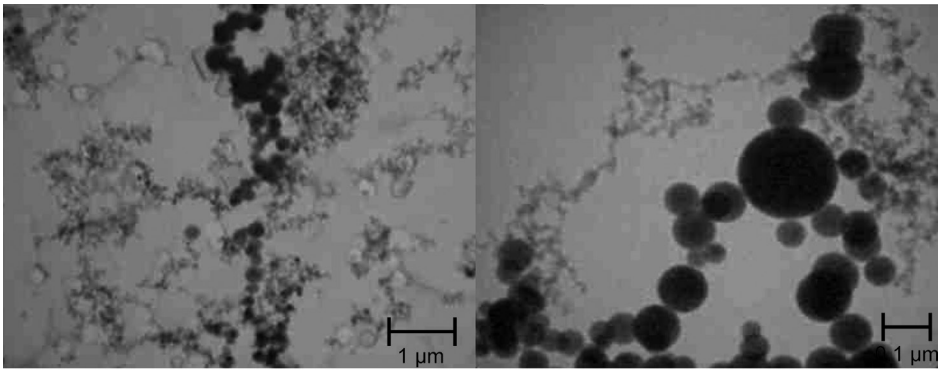

Figure 9: Welding fume sample consisting of primary particles, agglomerates and aggregates of different particle sizes.

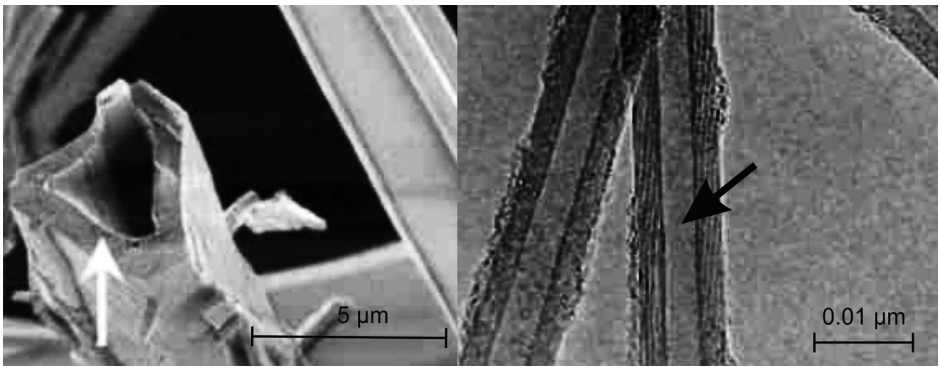

Figure 10: Electron microscopy images of fibre cavities of different sizes

Applied to a real workplace sample (welding fume; Figure 9), this means that differently sized particles within one sample cannot be characterized by simple BET measurements.

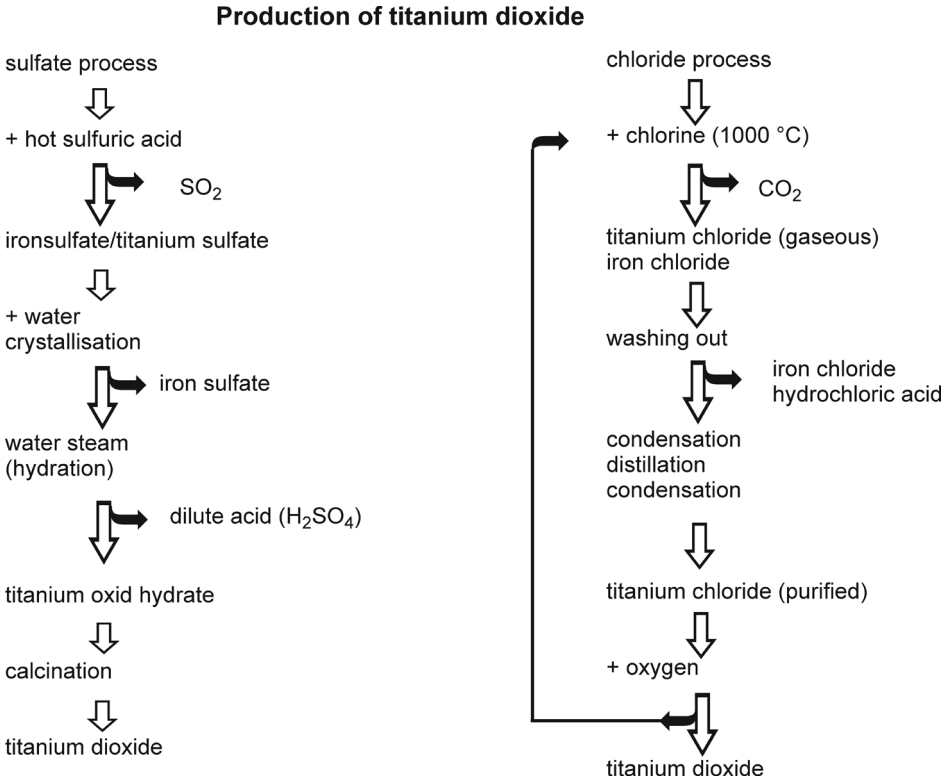

Figure 11: Simplified process diagrams of titanium dioxide production.

Another point is the toxicological relevance of the inner surface. For example, if cavities are too small for macrophage entry, this fraction of the inner surface loses its toxicological relevance (Figure 10).

Titanium Dioxide and Carbon Black as Representatives of Technically Relevant Nanoparticles

Titanium dioxide

1. Use of titanium dioxide (TiO_2) pigments:
   - UV absorber. Small TiO_2 particles (10–50 nm) absorb UV radiation in a wavelength range of 280–400 nm. Therefore, they are mainly used for cosmetics (sunscreens) and polymers (protection from UV radiation).
   - Paper. High-quality paper contains titanium dioxide pigments as fillers. Glossy paper is coated with titanium dioxide pigments.
   - Catalysts. (TiO_2) pigments are used in heterogeneous catalysis either directly or as a carrier material, e. g. for rare metals.
2. Technical preparation:
   Titanium dioxide occurs in the form of the modifications (identical molecular formulas, but different binding of the atoms or ions in the crystal

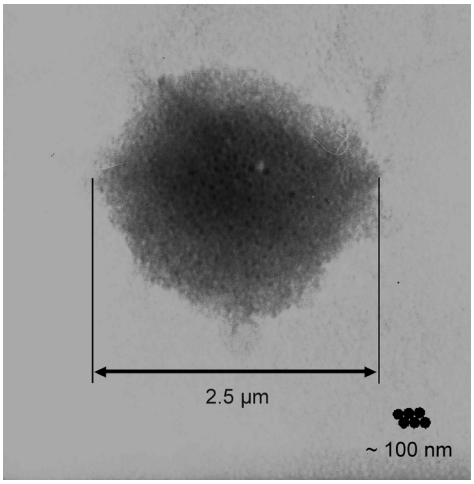

Figure 12: TEM image of a TiO_2 agglomerate.

lattice) rutile, anatase and brookite. Technically, two different processes are used to produce titanium dioxide: On the one hand, the "sulfate process", in which titanium dioxide is produced via titanium sulfate starting from ilmenite and sulfuric acid, and, on the other hand, the "chloride process", in which a solids mixture of titanium oxide and coke is converted into titanium chloride at high temperatures by means of chlorine. Subsequently, titanium chloride reacts with oxygen to produce titanium dioxide. Ultimately, this means that the titanium dioxide sample may still carry traces of sulfate/SO_2 and chloride – incorporated in the crystal lattice and attached to the surface, respectively – depending upon which of these divergent production processes is used.

The tendency of titanium dioxide to form agglomerates can clearly be seen in Figure 12. Primary particles of a diameter of ~ 5 nm form agglomerates of a diameter of 2.5 µm.

Carbon black (industrial soot)

Soot is a manifestation of carbon appearing in the incomplete combustion of carbon-containing substances. This leads to aggregates consisting of practically spherical primary particles with a diameter of 5–500 nm. The formation of these aggregates is of decisive importance for the properties of use of carbon black and is also called carbon black structure in technology (Greim 1999). The primary particles consist of six-membered carbon ring layers that are arranged around the particle centre. The distances between the layers are somewhat greater than in the graphite lattice; see Figure 13.

At ~ 85 %, the major fraction of carbon black is used in the rubber industry. Carbon black optimizes the properties of rubber mixtures for tyres. Elasticity,

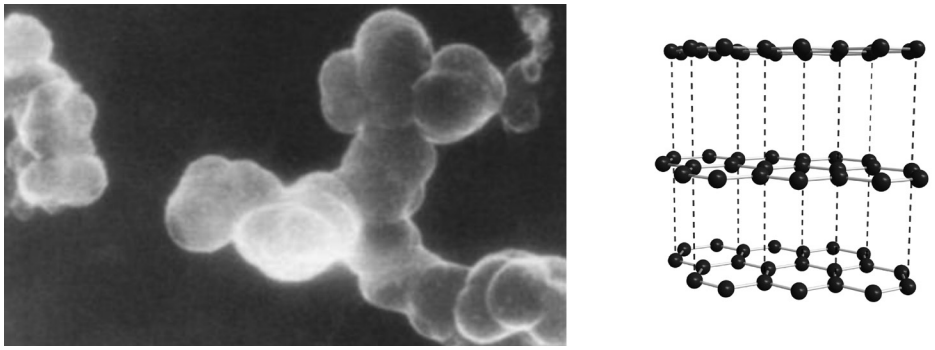

Figure 13: TEM image of carbon black aggregates (carbon black structure on the left); diagram of the distances between the six-membered carbon ring layers in carbon black.

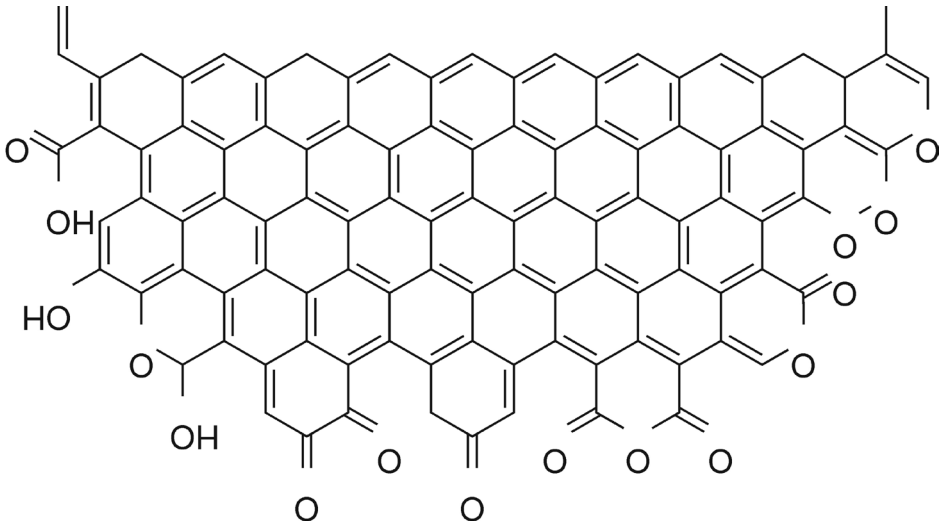

Figure 14: Possible functionalization of the margins of six-membered carbon ring layers in carbon black.

wheel grip, abrasion, etc. can be controlled via the particle size, surface characteristics, and agglomerate and aggregate state. The remaining 15 % of carbon black produced is used for products such as printing ink, polymer dyes, etc. Technically, carbon black is most commonly prepared according to the furnace black process, i. e. a continuous process using the combustion of oil vapour, which allows carbon black to be manufactured with specific surfaces between 20–1000 m^2/g. Modifications at the margins of such six-membered carbon ring layers present a problem for technical preparation. Different functional groups such as ether, peroxide, lactone, carboxyl, phenol, and anhydride may be formed there; see Figure 14.

Furthermore, the formation of polycyclic aromatic hydrocarbons (PAH) cannot be ruled out.

Distinction between Agglomerates and Aggregates

In order to be able to distinguish between agglomerates and aggregates, nanoscale dusts are transferred into aqueous or alcoholic suspension and examined by electron microscopy after ultrasonic treatment. Here, the example of welding fumes shows that 10-minute ultrasonic treatment leads to a more than tenfold increase in the number of agglomerates on an exactly defined area under the transmission electron microscope (TEM). For example, 21 agglomerates observed before ultrasonic treatment become 245 agglomerates after ultrasonic treatment, or, in other words, a few large agglomerates become several smaller agglomerates. Agglomerates disagglomerate in aqueous solution (Rödelsperger et al. 2003 b).

Comparison of Workplace Air Measurements with Results from Electron Microscopy

Table 1 shows the airborne concentrations of nanoscale particles from different work areas.

A comparison of these samples under the electron microscope shows that the different materials consist of a varying number of primary particles (Figure 15).

The mean number of primary particles per agglomerate of a specific substance can be determined under the transmission electron microscope (Table 2).

Table 1: Particle concentrations by particle sizer measurements in different work areas.

Workplace	**Particle concentrations [particles/mg]**
Carbon black	0.7×10^9
Sandstone	1.3×10^9
MIG* welding	15.0×10^9
MMA** welding	62.0×10^9
Diesel soot	740.0×10^9

*metal inert gas (MIG) welding; **manual metal arc (MMA) welding

Table 2: Mean number of primary particles per agglomerate in samples from different work areas.

Workplace	**Primary particles/ agglomerate**
Sandstone	3
Diesel soot	20
MMA welding	20
MIG welding	300
Carbon black	10 000

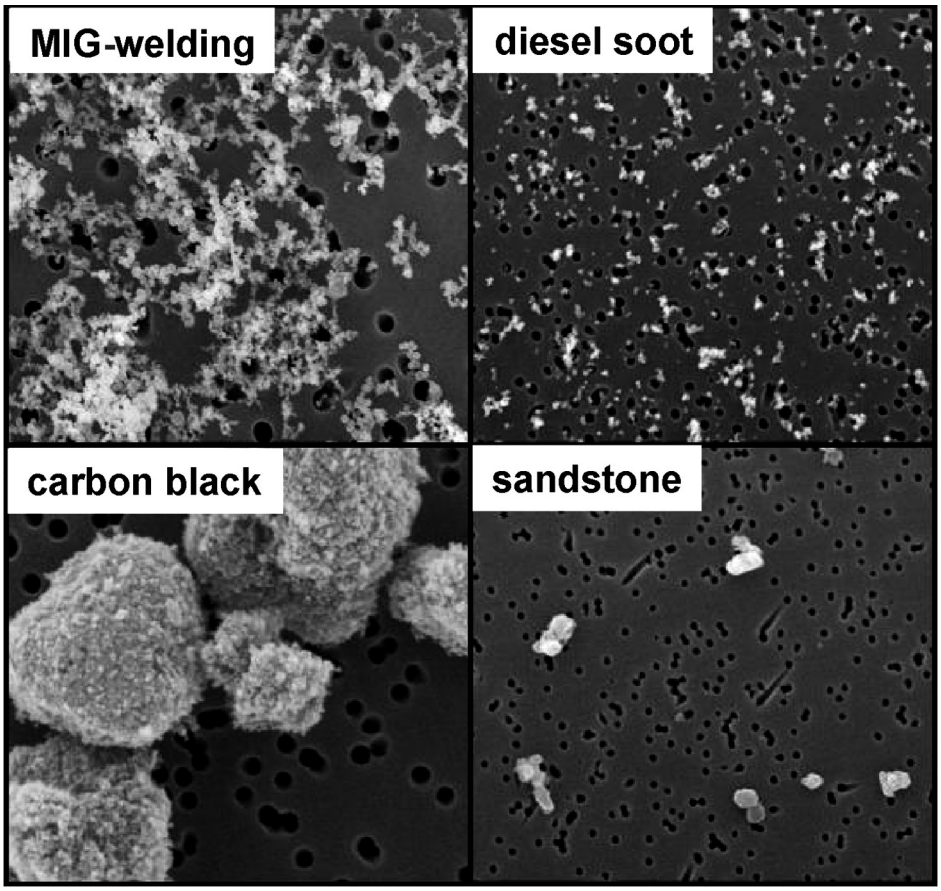

Figure 15: SEM images of different dust samples.

A diesel soot agglomerate consists of an average of 20 primary particles, whereas a carbon black agglomerate is composed of 10 000 primary particles. Under the worst case assumption that agglomerates completely break down into their primary particles, the number of primary particles per agglomerate is to be multiplied with the particle concentrations mediated by particle sizer measurement. Table 3 shows the results of such a worst case assumption

Table 3: Results of particle size counts by measurements and transmission electron microscopy in samples from different work areas.

Workplace	**Results (Scanning Mobility Particle Sizer) [particles/mg]**	**Results (TEM) [(tr) particles/mg]**
Carbon black	0.7×10^9	7.0×10^{12}
Sandstone	1.3×10^9	3.9×10^9
MIG welding	15.0×10^9	4.5×10^{12}
MMA welding	$62{,}0 \times 10^9$	1.2×10^{12}
Diesel soot	740.0×10^9	1.5×10^{13}

(*tr* = maximum *t*oxicologically *r*elevant primary particle concentration). The difference between the measured particle concentration (particle sizer) and the primary particle concentration determined under the electron microscope is caused by the agglomeration behaviour of the ultrafine particles (Rödelsperger et al. 2009).

Diversity of Primary Particles

Primary particles may be structured differently depending on the preparation process. A primary particle could consist of

1. a molecule.

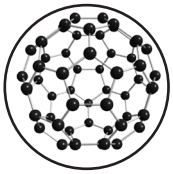

2. an ideal crystal.

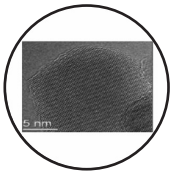

3. a real crystal with defects, although they have a homogeneous, intact surface.

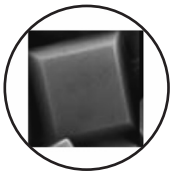

4. a real crystal with defects and have a fissured, porous surface.

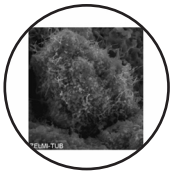

5. a real crystal with defects and have pores or an inner surface (zeolite).

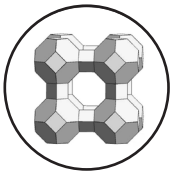

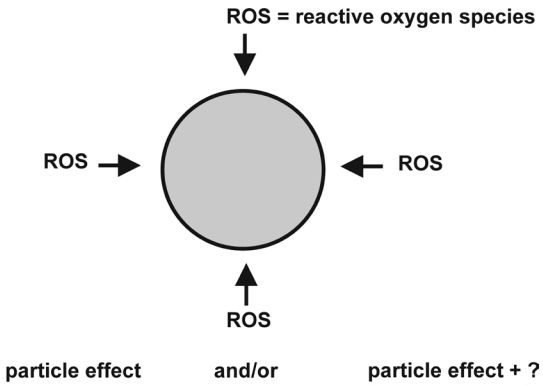

Figure 16: Possible behaviour of poorly soluble particles.

Effect of Primary Particles

Primary particles may be poorly soluble and may correspond to a granular biopersistent dust (GBD) and thus cause a "particle effect" (macrophages/reactive oxygen species (ROS)) with a local effect (Figure 16). ROS can interfere with the complete area of the surface.

They may also induce a particle effect with a systemic effect, for example by phagocytosis. Highly soluble primary particles lead to a local and/or systemic availability of metal ions.

General Tendencies of Primary Particles

Figure 17 shows the general tendencies of primary particles. In particular, the agglomeration behaviour increases with a decrease in particle size. Solubility generally also increases with a decrease in particle size.

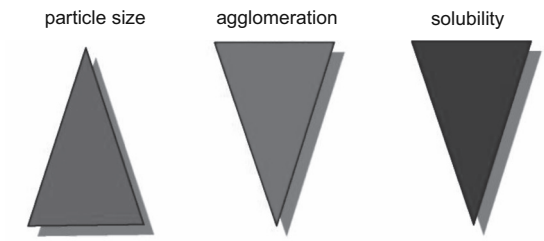

Figure 17: Diagram of the associations between agglomeration behaviour/solubility and particle size.

References

Brunauer S, Emmett PH, Teller, E (1938) Adsorption of gases in multimolecular layers. J Am Chem Soc 60: 309–319

Buxbaum G, Pfaff G (2005) Industrial inorganic pigments. Wiley-VCH Verlag, Weinheim

Eichholz S, Lerch M, Heck M, Walter D (2012) Various carbon dust particles – studies on thermal behaviour. J Therm Anal Calorim, DOI 10 1007/s 10973–011–2188-z

Galwey AK, Brown ME (2000) Thermal decomposition of ionic solids. Elsevier, Amsterdam

Greim H (Hrsg) (1999) Industrieruße (Carbon Black) in Form atembarer Stäube. Gesundheitsschädliche Arbeitsstoffe, Toxikologisch-arbeitsmedizinische Begründung von MAK-Werten 29. Lieferung. VCH, Weinheim List of MAK and BAT Values (2009) Wiley-VCH Verlag, Weinheim

Moore WJ (1967) Seven solid states. WA Benjamin, Inc., New York

Oberdörster G, Oberdörster E, Oberdörster J (2005) Nanotoxicology: An emerging discipline evolving from studies of ultrafine particles. Environ Health Perspect 113: 823–839

Rödelsperger K, Podhorsky S, Brückel B, Dahmann D, Hartfiel GD, Woitowitz H-J (2003 a) Measurements of granular ultrafine bio-durable particles for workplace protection. Eur J Oncol 8: 103–112

Rödelsperger K, Podhorsky S, Brückel B, Dahmann D, Hartfiel GD, Woitowitz H-J (2003 b) Charakterisierung von Aerosolen ultrafeiner Teilchen für den Arbeitsschutz, Abschlussbericht des Projektes F 1804 (Characterization of ultrafine particle aerosols for occupational safety, final report of project F 1804) (German), ISBN 3–88261–050–6 Dortmund-Berlin-Dresden

Rödelsperger K, Brückel B, Podhorsky S, Schneider J (2009) Charakterisierung ultrafeiner Teilchen für den Arbeitsschutz – Teil 2, BAUA-Abschlussbericht des Projektes F 2075 der Bundesanstalt für Arbeitsschutz und Arbeitsmedizin (Characterization of ultrafine particles for occupational safety, BAUA final report of project F 2075 of the Federal Institute for Occupational Safety and Health) (German)

Schmalzried H, Navrotsky A (1975) Festkörperthermodynamik/Chemie des festen Zustandes. Verlag Chemie, Weinheim

Ullmann's Encyclopedia industrial chemistry VCH (1992), Vol. 20, Weinheim

Walter D, Buxbaum G, Laqua W (2001) The mechanism of the thermal transformation from goethite to hematite. J Therm Anal Cal 63: 733–748

Walter D (2006) Characterization of synthetic hydrous hematite pigments. Thermochim Acta 445: 195–199

1.2 Exposure during Production and Handling of Manufactured Nanomaterials

Markus G. M. Berges

Institute for Occupational Safety and Health (IFA)

Sankt Augustin, Germany

In the traditional risk framework, risk management decisions concerning occupational safety and health rely on site-specific risk assessment and information about the effectiveness of available measures to mitigate exposure. In its turn, risk assessment builds on hazard and exposure assessments (Murashov et al. 2009). Though there is mounting evidence that some manufactured nanomaterials may impose a health hazard to humans the target organs and endpoints and the specific dose-response relationship are not clearly delineated. In view of the uncertainty regarding the hazard of manufactured nanomaterials the assessment and control of the potential exposure of workers become crucial in occupational health and safety in order to minimize the risk of the workers.

The current method of assessing worker exposure to airborne particles in the workplace involves the measurement of mass concentration of health-related fractions of particles in the worker's breathing zone. The main exceptions to this methodology are particle-number-based metrics for exposure for fibres and for microorganisms (ISO/TR 12885, 2008; ISO 13794, 1999). However nanoparticles carry only very small masses and therefore generally contribute negligibly to the integral mass concentration of the inhalable or respirable dust fraction. Furthermore, there is evidence that other metrics such as particle number concentration or surface area may be better descriptors for the biological effects of nanoparticles. The issue of exposure metrics has extensively been addressed by Maynard and Aitken (2007). Reflecting the state of the art they conclude that effective approaches to measuring exposure to a wide range of manufactured nanomaterials/nanoobjects will require methods for measuring aerosol number, surface area and mass concentration.

Back in 1998 several European OSH Institutes in collaboration with the DFG (the German Research Foundation) agreed on a convention (Möhlmann 1998, revised 2007, Riediger and Möhlmann 2001) for the measurement of ultrafine particles in order to permit comparison of measurements. The core points of this convention were:

- An ultrafine aerosol particle is a particle with a mobility equivalent diameter of < 0.1 µm
- The particle number concentration should be measured in the range from approximately 10 to 600 nm.
- The entire particle size distribution should be measured if possible.
- A concentration range of up to approximately 1×10^8 particles/cm³ should be covered.

In the meantime the most widespread method that evolved to determine airborne submicron particle number concentrations as a function of particle size, i. e., particle number size distributions, is based on electrical mobility analysis of the particles (Asbach et al. 2009). These techniques usually comprise three main components: (1) a particle charger that predictably charges particles depending on their size; (2) a mobility analyzer that classifies the particles of one polarity according to their electrical mobility; and (3) a particle counter that determines the number concentration of mobility-classified particles. These three techniques are usually employed in what has become the workhorse for occupational exposure measurements the Scanning Mobility Particle Sizer (SMPS). ISO/TR 27628 (2007) further describes the available methods to measure the above mentioned metrics of nanoobjects.

Historically the methods and instruments were first used at the workplace to measure ultrafine particles and later on as nanotechnology evolved to measure nanoparticles. In the absence of occupational exposure limits for nanoparticles or species of nanoparticles the exposure to nanoparticles is often put into perspective by comparing it with the ultrafine exposure of workers at the workplace or with the so called ambient or background concentration of ultrafine particles.

The Institute for Occupational Safety and Health (IFA) in Germany published results on the ultrafine exposure of workers performing a variety of tasks (Riediger and Möhlmann 2001; Möhlmann 2005, Möhlmann 2007). Wake et al. (2002) reported on number concentrations and particle sizes during handling of high specific surface area materials (carbon black, precious metal black, nickel powder), ultrafine TiO_2 and of unwanted ultrafine particles. Dasch et al. (2005) characterized fine particles from machining in automotive plants by employing several devices including an Aerodynamic Particle Sizer (APS) for a size range from 0.5 µm to 20 µm and a Micro-orifice Uniform Deposit Impactor (MOUDI) for the particle mass distribution between 0.06 µm to about 20 µm. Ukkonen et al. (2005) employed an Electrical Low Pressure Impactor (ELPI™) during plasma arc cutting and reported particle number concentrations between 40 000 and 800 000 particles/cm³ with a number median diameter in the range of 40 nm to 60 nm.

Schneider et al. (2007) review the exposure to ultrafine particles and summarize most of the measurements as given in table 1 and 2.

Although these measurements are more task related and not representative of the real exposure of the workers during a shift, it can be concluded that the exposure to ultrafine particles easily exceeds background concentrations with maximum of millions of particles/cm³ during welding. Thus the identification of the source of ultrafine particles is in general fairly easy; however the identification of the individual particles by further chemical methods and imaging methods like electron microscopy still remains a challenge.

An alternative approach to give the measurement of nanoparticles at the workplace a meaning by the use of benchmark levels was proposed by the Institute for Occupational Safety and Health (IFA) (http://www.dguv.de/ifa/en/fac/nanopartikel/beurteilungsmassstaebe/index.jsp). The feasibility of this concept

Table 1: Particle number and mass concentrations at industrial sites from Ukkonen (2005), Riediger and Möhlmann (2005).

Process	Geometric mean [Number of particles/ $cm^3 \times 1000$]	Median diameter [nm]	Mass [mg/m^3] *	Reference
Plasma cutting §	40–800	40–60	0.3–1.3 ($PM_{2.5}$,S)	Ukkonen et al. (2005); Riediger and Möhlmann (2005)
Plasma cutting	40–230	140–180	4.2 (I)	
Laser welding	5 000–40 000		0.17–0.48 (I)	
Aluminum welding	20–640	256–411	2.8–15 (R,P)	
Soldering	28–390	43–62	< 0.76 (I,P)	
Cutting aluminium, minimal MVF	10–260	30–111	< 0.95 (I,P)	
Iron foundry	290–580	54–70	1.5–1.7 (I)	
Plastic casting	20	45	< 0.25 (R,S)	
Grinding metal	10–130	32–155	1.8 (I)	
Grinding granite baking	26–60	< 10	Up to 41 (I,P)	
Out-door	5–640 26–700	55–83 < 41	0.3 (I) 0.07 (I,S)	

All measurements with SMPS: Scanning Mobility Particle Sizer, except (§) made with ELPI: Electrical Low Pressure Impactor.

* I: Inhalable, R: Respirable, P: Personal sample, S: Stationary sample. MVF: metalworking fluid.

is currently tested by the Dutch government under the term "nano reference values".

In 2009 the European Agency for Safety and Health at Work reviewed the literature on the workplace exposures to nanoparticles available till early 2008 (Kosk-Bienko 2009). Brouwer et al. (2009) discuss the literature available till early 2009 (14 studies) with emphasis on possible ways to cope with the problem of background distinction. One major finding of most studies is that during production and handling of nanoparticles the workplace particle number concentration of particles below 100 nm is close to the background concentration in companies. This background aerosol consists of ubiquitous ambient particles and of ultrafine particles from sources in or outside a company e. g. particles emitted from diesel engines by trucks or forklifts, welding fumes or even vacuum cleaners with electric motors close to the process. During the event of a leakage at the bin filling station in the production line of nano titanium dioxide

Table 2: Number concentrations and particles sizes from Wake et al. (2002).

Material or type of industry	Outside	Workplace	Outside	Workplace	Activity
	Range/ $cm^3 \times 1000$	Range/ $cm^3 \times 1000$	Number median, nm (GSD)	Number median, nm (GSD)	
Carbon black	649–3836	3.5–50	44 (3.2)	51–400 (2.4)	Bagging
Nickel powder	3.3–16	3.7–212	23 (1.9)	49 (3.3)	Bagging
Titanium dioxide	10–58	4.2–17			Bagging
Precious metal	19–62	23–71			Sieving
blacks					
Zinc refining	20–23	12–24	503 (5.3)	70 (2.2)	Sintering
Zinc refining	20–23	56	100		Casting
Plasma coating	2.3–8.0	2.8–905	41 (2.2)	587 (1.3)	Wire coating
Galvanizing	15–37	10–683	64 (2.0)	99 (2.1)	Galvanizing
Steel foundry	13–72	118→ 500	46 (1.9)	66 (2.0)	Fettling
Welding	10–19	117→ 500	53 (2.1)	179 (2.2)	MIG „Metal-Inert-Gas" welding
Plastic welding	1.2–5.2	111–3766	31 (2.0)	37 (1.7)	Welding
Hand soldering	2.2–11	12→500	41 (2.0)	72 (2.3)	Tinning

GSD: Geometric Standard Deviation

up to 130 000 particles/cm^3 have been encountered. The chemical identity of the nanoparticles was verified by transmission electron microscopy. Another common finding is that aggregates or agglomerates above 100 nm in size were quite often detected at the workplace and correlated with the operations.

High aspect ratio nanoparticles (HARN) such as carbon nanotubes (CNT) present an additional challenge to the employed SMPS (Scanning Mobility Particle Sizer) as they clearly are not spherical particles for which the SMPS has been designed in the first place. The manufactures usually calibrate these instruments only with spherical particles. The SMPS response is in direct relation with the CNTs transport through its differential mobility analyzer (DMA). This is influenced by the peculiar shape of the CNT and their orientation in the electric field of the DMA. Kim et al. (2005) show exemplary CNTs correlations between CNT lengths and electrical mobility diameter. By using Multi-Walled Carbon Nanotubes (MWCNTs) of approximately 15 nm diameter and irregular alignment, the electrical mobility diameter chosen by a DMA underestimates the geometri-

cal length of a CNT by factors of 2.5 to 7. 4. Golanski et al. (2009) evaluate the detection of CNTs with the SMPS and explore a theoretical approach for unitary and straight CNTs to predict the equivalent spherical diameter given by SMPS for CNTs with different aspect ratios. However commercially mass-produced pellets of MWCNT are entangled and form bigger structures further complicating matters. Lee et al. (2010) examine the size responses of aerosol instruments consisting of both a scanning mobility particle sizer (SMPS) and an aerodynamic particle sizer (APS) using five types of commercial MWCNTs. Regardless of the phase and purity, the aerosolized MWCNTs showed consistent size distributions with both SMPS and APS. The SMPS and APS measurements revealed a dominant broad peak at approximately 200–400 nm and a distinct narrow peak at approximately 2 µm, respectively. They propose that the APS response could be a fingerprint of the MWCNTs in a real workplace environment. From the beginning other methods to measure CNTs were also explored. Maynard et al. (2004) reported CNT concentration levels from 0 to 53 µg/m³ based on determination of metals from the catalyst and backward calculations assuming a known percentage of metals of the CNT material. This method is currently pursued by Bayer Material Science in controlling their recommended exposure limit value of 0.05 mg/m³ for Baytubes C 150 P (Bayer Material Science, MSD, version 2.1 of 3 December 2009). Han et al. (2008) and Ono-Ogasawara et al. (2009) employed methods to detect elemental carbon (EC). The former uses an Aethalometer, as an optical method and the latter the combination of a thermal/optical instrument with the final temperature of carbon analysis of 920 °C. Han et al. (2008) also analyzed air samples according to the NIOSH (National Institute for Occupational Safety and Health) method 7402 for asbestos. MWCNT fibres with aspect ratios larger than 3:1 were counted in more than 50 grid openings. The MWCNT fibres were distinguished from asbestos by Scanning Electron Microscope/Energy Dispersive X-ray Spectroscopy (SEM/EDX) analysis. The reported number of MWCNT fibres ranged from 173 to 194/cm³ before the control measures and decreased to 0.018–0.05/cm³ (equivalent to 18 000–5 000/m³) after protective improvements had been implemented. They also conclude that conventional engineering controls work well.

However due to the different properties of CNT fibres compared to asbestos fibres e. g. much smaller diameter and different morphology, current conventions for counting single asbestos fibres and rules for the statistical calculation cannot simply be transferred to the counting of carbon nanotubes (Methner et al. 2010).

In summary all studies are more explorative in character and focused on the potential for emission of manufactured nanoparticles. No shift averages were presented based on particle number concentration or surface area concentration (Brouwer et al. 2009) or fibre concentration.

For the most widespread used instrument for the measurement of particle number concentration and size distribution (SMPS) no standard method has been agreed on to produce reference particle number concentration (Asbach et al. 2009). In addition the response function to non-spherical particles like aggregates and tubes are still under scrutiny. Furthermore, due to the encoun-

tered rather low concentrations in comparison to those of ultrafine particles at the workplace additional analytical methods to determine the morphology and chemical composition of the nanoparticles are necessary in order to cope with the problem of background distinction. The SMPS is still too bulky, complicated to use and too expensive for routine operation by small and medium sized companies. Smaller handheld instruments can however be successfully used to monitor the efficiency of engineering controls which up to now have proven to effectively control the exposure of workers against nanoparticles at the workplace.

References

Asbach C, Kaminski H, Fissan H, Monz C, Dahmann D, Mülhopt S, Paur HR, Kiesling HJ, Herrmann F, Voetz M, Kuhlbusch TAJ (2009) Comparision of four mobility particle sizers with different time resolution for stationary measurement. J Nanopart Res 11: 1593–1609

Brouwer D, van Duuren-Stuurman B, Berges M, Jankowska E, Bard D, Mark D (2009) From workplace air measurement results towards estimates of exposure? Development of a strategy to assess exposure to manufactured nano-objects. J Nanopart Res 11: 1867–1881

Dasch J, D'Arcy J, Gundrum A, Sutherland J, Johnson J, Carlson D (2005) Characterization of fine particles from machining in automotive plants. J Occup Environ Hyg 2: 609–625

Golanski L, Bernard S, Guiot A, Poncelet O, Le Poche H, Tardif F (2009) Specific response of SMPS particle counter to CNT. J Physics: Conference Series 170

Han JH, Lee EJ, Lee JH, So KP, Lee YH, Bae GN, Lee S-B, Ji JH, Cho MH, Yu IJ (2008) Monitoring multiwalled carbon nanotube exposure in carbon nanotube research facility. Inhal Toxicol 20: 741–749

ISO/TR 27628 (2007) Workplaces atmospheres – Ultrafine, nanoparticle and nano-structured aerosols – Inhalation exposure characterization and assessment, ISO copyright office, Case postale 56, CH-1211 Geneva 20

ISO/TR 12885 (2008) Nanotechnologies – Health and safety practices in occupational settings relevant to nanotechnologies, ISO copyright office, Case postale 56, CH-1211 Geneva 20

ISO 13794 (2005) Ambient air – Determination of asbestos fibres – Indirect transfer transmission electron microscopy method

Kim SH, Zachariah MR (2005) In-flight size classification of carbon nanotubes by gas phase electrophoresis. Nanotechnology 16: 2149–2152

Kosk-Bienko J (2009) Workplace exposure to nanoparticles. European Agency for Safety and Health at work (EU-OSHA)

Lee SB, Lee JH, Bae GN (2010) Size response of an SMPS-APS system to commercial multi-walled carbon nanotubes. J Nanopart Res 12: 501–512

Maynard AD, Baron PA, Foley M, Shvedova AA, Kisin ER, Castranova V (2004) Exposure to carbon nanotube material: aerosol release during the handling

of unrefined single-walled carbon nanotube material. J Toxicol Environ Health A 67: 87–107

Maynard AD, Aitken RJ (2007) Assessing exposure to airborne nanomaterials; current abilities and future requirements. Nanotoxicology 1: 26–41

Methner M, Hodson L, Dames A, Geraci C (2010) Nanoparticle assessment technique (NEAT) for the identification and measurement of potential inhalation exposure to engineered nanomaterials – Part B: Results from 12 Field Studies. JOEH 7: 163–176

Möhlmann C (2005) Vorkommen ultrafeiner Aerosole an Arbeitsplätzen. Gefahrstoffe – Reinhalt. Luft 65: 469–471

Möhlmann C (2007) Ultrafeine (Aerosol-)Teilchen und deren Agglomerate und Aggregate, Kennziffer 0425/5 38. Lfg. IV/07, 4 S. In: Messung von Gefahrstoffen – BGIA-Arbeitsmappe (Hrsg) Berufsgenossenschaftliches Institut für Arbeitsschutz – BGIA. Erich Schmidt Verlag, Berlin 1989 – Loseblatt-Ausgabe. ISBN: 978 3 503 02085 3

Möhlmann C (2007) Ultrafeine Aerosole am Arbeitsplatz, Kennzahl 120130. Lfg. IX/2007. In: BGIA-Handbuch Sicherheit und Gesundheitsschutz am Arbeitsplatz (Hrsg) Berufsgenossenschaftliches Institut für Arbeitsschutz – BGIA. Erich Schmidt Verlag, Berlin 1989 – Loseblatt-Ausgabe. ISBN: 978 3 503 02085 3

Murashov V, Engel S, Savolainen K, Fullam B, Lee M, Kearns P (2009) Occupational safety and health in nanotechnology and organisation for economic cooperation and development. J Nanopart Res 11: 1587–1591

Ono-Ogasawara M, Serita F, Takaya M (2009) Distinguishing nanomaterial particles from background airborne particulate matter for quantitative exposure assessment. J Nanopart Res 11: 1651–1659

Riediger G; Möhlmann C (2001) Ultrafeine Aerosole an Arbeitsplätzen – Konventionen und Beispiele aus der Praxis. Gefahrstoffe – Reinhalt Luft 61: 429–434

Schneider T (2007) Evaluation and control of occupational health risks from nanoparticles. Tema Nord 2007: 581, Nordic Council of Ministers, Copenhagen

Ukkonen A, Lamminen E, Kasurinen H (2005) Measuring the size distribution and concentration of particles formed in plasma arc cutting. NOSA Aerosol Symposium, Göteborg, Sweden

Wake D, Mark D, Northage C (2002) Ultrafine Aerosols at the workplace. Ann Occup Hyg 46 (Suppl 1): 235–238

1.3 Toxicokinetics of Inhaled Nanoparticles

Wolfgang G. Kreyling

Helmholtz Center Munich – Research Center for Environmental Health; Institute for Lung Biology and Disease, Focus Network: Nanoparticles and Health

Neuherberg/Munich, Germany

Nanoparticles are increasingly used in a wide range of applications in science, technology and medicine. Since they are produced for specific purposes which cannot be met by larger particles and bulk material they are likely to be highly reactive, in particular, with biological systems. On the other hand a large body of know-how in environmental sciences is available from adverse effects of ultrafine particles after inhalative exposure. Since nanoparticles elicit the same responses as ultrafine particles, adverse health effects cannot be excluded and a safe and sustainable development of new emerging nanoparticles is required.

Inhaled nanoparticles deposit preferentially in the alveolar region of the lungs with a maximum at 20 nm. Below that size, increasing fractions deposit in the airways of the head and thorax according to their increasing diffusivity with decreasing size. Once deposited in the peripheral lungs nanoparticles are not only subject to phagocytosis by alveolar macrophages but also by epithelial cells. It appears plausible that macrophages take up all nanoparticles deposited in their immediate vicinity while distant nanoparticles are not recognized. As a result a major fraction (> 80 %) of the nanoparticles in the peripheral rodent lung enter the epithelium and penetrate into interstitial spaces (Semmler-Behnke et al. 2007). Hence, nanoparticles behave differently compared to micro-sized particles which are retained on the rodent epithelium leaving the lungs by macrophage-mediated clearance at a rate of 2–3 % per day. Surprisingly, nanoparticles are cleared by the same clearance rate via this macrophage-mediated transport process indicating relocation of the nanoparticles from the interstitial spaces and epithelium to top of the epithelium. Therefore, macrophage-mediated clearance is the most prominent long-term clearance mechanism in the peripheral lung of rodents. In fact, while the nanoparticles are retained in the interstitium close to lymphatic drainage and blood vessels only rather small fractions are removed via these two pathways. Particle clearance from the human peripheral lungs and from those of dogs and monkeys differ from that in rodents: in the three large species even micron-sized particles enter the epithelium and penetrate into interstitial spaces and macrophage-mediated clearance occurs at a rate which is one order of magnitude lower than that of rodents (Kreyling and Scheuch 2000). Yet, since micron-sized particles penetrate into interstitial spaces it appears plausible that nanoparticles also follow this pathway. Unfortunately for humans neither macrophage-mediated clearance kinetics data nor translocation data of nanoparticles into the circulation are available. Existing data suggest that translocation fractions of nanoparticles must be below 1 % of the deposited nanoparticles according to the lower limit

of experimental detection as no accumulation was observed in any secondary target organ (Möller et al. 2008). An important underlying mechanism of the special behaviour of nanoparticles may be selected binding of proteins and nanoparticles affecting the biokinetic fate of the nanoparticles. In other words, coating of nanoparticles with selected proteins can influence their uptake and distribution and direct them to specific locations.

Cardio-vascular effects observed in epidemiological studies triggered the discussion on enhanced translocation of ultrafine particles from the respiratory epithelium towards the circulation and subsequent target organs, such as heart, liver, spleen and brain, eventually causing adverse effects on cardiac function and blood coagulation, as well as on functions of the central nervous system. There is clear evidence that nanoparticles can cross body membranes and reach in the above mentioned secondary target organs and accumulate there.

To determine accumulated fractions in such organs the ultimate aim is to quantitatively balance the fractions of nanoparticles in all relevant organs and tissues of the body and include the remainder body and total excretion collected between application and autopsy. Otherwise substantial uncertainty remains if only selected organs are analysed. Since these gross determinations of nanoparticle contents in organs and tissues do not provide microscopic information on the anatomical and cellular location of nanoparticles such studies are to be complemented by electron microscopy analysis using elemental mapping technology.

Based on quantitative biokinetic analysis after nanoparticle application to the lungs of a rat model, small fractions of nanoparticles (iridium, carbon, gold, and preliminary results on titanium dioxide) were found in all secondary organs studied including the brain, heart and even in the foetus (Kreyling et al. 2002; Semmler et al. 2004; Semmler-Behnke et al. 2007 a, b, 2008; Kreyling et al. 2009). All nanoparticles were radio-labelled with the label firmly fixed to the particle core. Fractions in each of the secondary target organs were usually below 0.5 % of the administered dose to the lungs but depended strongly on particle size in an inverse fashion. However, nanoparticle fractions in soft tissue and skeleton (without blood content) increased the totally translocated fraction to 5–10 % of the administered dose. Also negatively ionic surface charged nanoparticles translocated more rapidly than positively charged nanoparticles of the same size. In addition, strong differences of the totally translocated fractions between chain-aggregated/agglomerated iridium and carbon nanoparticles versus gold spheres of same size highlights the importance of nanoparticle material, morphological and/or surface properties. Furthermore, nanoparticle accumulation in the rat brain results from both pathways: via the olfactory bulb versus circulation.

The inhalation study using 20 nm iridium nanoparticles was extended to follow the fate of the nanoparticles over six months after a single one-hour inhalation and yielded significant retention in secondary target organs such as liver, spleen, kidneys, heart and brain (Semmler et al. 2004; Semmler-Behnke et al. 2007 a). In this study, we found evidence for considerable particle relocation within the pulmonary tissue during the six-month period. Combining ex-

haustive bronchoalveolar lavages (BAL) with our long-term biokinetics studies we observed three days after inhalation nanoparticles were only to 10–20 % accessible to BAL and more than 80 % had already been relocated into the epithelial and interstitial tissue. Even more surprising, these interstitially retained nanoparticles were predominantly cleared by macrophage mediation back to the luminal side of the epithelium and towards the mucociliary escalator of the bronchiole and bronchi to the larynx (from where they were swallowed and excreted) (Semmler-Behnke et al. 2007 a). Translocation to the lymphatic drainage and to blood circulation remained to be rather low even though the nanoparticles were retained rather closely to the lymphatic system and the blood vessels.

While these macroscopic studies do not provide insight into which cells or cell compartments the nanoparticles are retained or relocated within an organ, complementary microscopic studies are required to fill this gap. Recently we performed a microscopic study directly after and 24 hours after inhalation of 20 nm chain-aggregated/agglomerated titanium dioxide (TiO_2) nanoparticles showing rapid penetration of nanoparticles into the epithelial cell layer as well as translocation into interstitial spaces and the vascular endothelium (Kapp et al. 2004; Geiser et al. 2005 and 2008). But at that time no macroscopic inhalation study was available using the same TiO_2 nanoparticles since the radio-labelling technology of the aerosolized TiO_2 nanoparticles was not yet developed. This has now been achieved and first results indicate that modest nanoparticle accumulation in all secondary target organs occurs but that total 24-hour translocation of these chain-aggregated/agglomerated TiO_2 nanoparticles is significantly lower by a factor of 5 from that of similar 20 nm sized iridium nanoparticles (Kreyling, personal communication). The aerosolized TiO_2 nanoparticles used were generated by spark ignition and are currently carefully characterized showing 20 nm chain-aggregates/agglomerates of polycrystalline primary anatase TiO_2 particles of 3–5 nm size. As a result they are different from commercially available TiO_2 nanoparticles. However, they are designed to challenge the nanoscale size to the lower limits and to study the biokinetics of inhaled 20 nm nanoparticles. Commercially available TiO_2 nanoparticle powders cannot be dispersed to such small entities yet. On the other hand disagglomeration of micron-sized commercial TiO_2 nanoparticle agglomerates has been shown (Ferin et al. 1991) and cannot be excluded neither in nanotechnological processes leading to human exposure nor after incorporation of those nanomaterials in the body.

These data suggest nanoparticle parameters such as material, size, morphology, hydrophilicity/lipophilicity, surface charge, surface ligands and their possible exchange in various body fluids need to be considered. Unfortunately, quantitative biokinetic studies are not possible in human subjects. Existing data only confirm that translocated fractions to secondary target organs do not exceed the fractions found in the rat model. However, precise fractions in humans are still lacking.

Currently no biokinetic data exist on carbon nanotubes or nanowires while there are a few data on carbon black nanoparticles yet, there is considerable

data on the toxicological effects of carbon black nanoparticles *in vitro* and *in vivo* as a result of the scientific interest of the effects of ambient ultrafine aerosol particles in air pollution (Donaldson et al. 2005, 2006, Poland et al. 2008). However, there is growing evidence, that inhalation exposure to carbon nanotubes at elevated doses induce oxidative stress and pro-inflammatory reactions in mouse models (Shvedova et al. 2009).

Acute effects resulting directly from translocated nanoparticles in secondary target organs of humans are likely to be rather low because of the estimated rather low accumulation fractions of nanoparticles tested so far. Chronic exposure will lead to cumulative accumulation of insoluble nanoparticles in some secondary target organs which may well mediate adverse health effects including inflammatory diseases in those secondary target organs. In addition, beyond the direct effect of translocated nanoparticles it appears worthwhile to investigate the effects caused by mediators released from the lungs as the primary organ of intake to blood as a result of the interaction of freshly inhaled nanoparticles with lung tissues even after short term exposures.

Hence there are gaps of knowledge which need to be addressed in due course for a comprehensive risk assessment. The following is a limited list of issues:

- Mechanisms determining the transport of nanoparticles through cell membranes and biological membranes such as the air-blood barrier of the lungs, the epithelium of the intestine, the blood-brain-barrier, the placental barrier, etc. and the role of nanoparticle properties and appropriate metrics.
- Toxicological responses of cells and membranes to nanoparticles using well defined and relevant nanoparticle doses.
- Repeated or chronic nanoparticle exposure studies with subsequent accumulation of nanoparticles in secondary target organs for dose estimates to plan subsequent toxicological testing.
- Mediator release in circulation after nanoparticle exposure to the lungs and their role in triggering adverse cardio-vascular effects.
- Dose-response studies in case of toxic outcomes in primary or secondary target organs.

References

Donaldson K, Tran L, Jimenez LA, Duffin R, Newby DE, Mills N, Macnee W, Stone V (2005) Combustion-derived nanoparticles: A review of their toxicology following inhalation exposure. Part Fibre Toxicol 2: 10, doi 10.1186/1743-8977-2-10

Donaldson K, Aitken R, Tran L, Stone V, Duffin R, Forrest G, Alexander A (2006) Carbon nanotubes: a review of their properties in relation to pulmonary toxicology and workplace safety. Toxicol Sci 92: 5–22

Ferin, J.; Oberdöster, G.; Soderholm, S. C.; Gelein, R. Pulmonary tissue access of ultrafine 450 particles. Journal of Aerosol Medicine 1991, 4, 57-68.

Geiser M, Casaulta M, Kupferschmid B, Schulz H, Semmler-Behnke M, Kreyling W (2008) The role of macrophages in the clearance of inhaled ultrafine titanium dioxide particles. Am J Resp Cell Mol 38: 371–376

Geiser M, Rothen-Rutishauser B, Kapp N, Schurch S, Kreyling W, Schulz H, Semmler M, Im Hof V, Heyder J, Gehr P (2005) Ultrafine particles cross cellular membranes by nonphagocytic mechanisms in lungs and in cultured cells. Environ Health Perspect 113: 1555–1560

Kapp N, Kreyling W, Schulz H, Im Hof V, Gehr P, Semmler M, Geiser M (2004) Electron energy loss spectroscopy for analysis of inhaled ultrafine particles in rat lungs. Microsc Res Tech 63: 298–305

Kreyling W, Scheuch G (2000) Clearance of particles deposited in the lungs. In: Heyder J, Gehr P (ed) Particle Lung Interactions, Marcel Dekker, New York, USA, 323–376

Kreyling WG, Semmler M, Erbe F, Mayer P, Takenaka S, Schulz H, Oberdörster G, Ziesenis A (2002) Translocation of ultrafine insoluble iridium particles from lung epithelium to extrapulmonary organs is size dependent but very low. J Toxicol Environ Health 65: 1513–1530

Möller W, Felten K et al. (2008) Deposition, retention, and translocation of ultrafine particles from the central airways and lung periphery. Am J Resp Crit Care Medicine 177: 426–32

Poland CA, Duffin R, Kinloch I, Maynard A, Wallace WAH, Seaton A, Stone V, Brown S, MacNee W, Donaldson K (2008) Carbon nanotubes introduced into the abdominal cavity of mice show asbestos-like pathogenicity in a pilot study. Nat Nanotechnol advanced online publication, doi:10 1038/nnano.2008 111

Semmler M, Seitz J, Erbe F, Mayer P, Heyder J, Oberdörster G, Kreyling WG (2004) Long-term clearance kinetics of inhaled ultrafine insoluble iridium particles from the rat lung, including transient translocation into secondary organs. Inhal Toxicol 16: 453–459

Semmler-Behnke M, Takenaka S, Fertsch S, Wenk A, Seitz J, Mayer P, Oberdorster G, Kreyling WG (2007 a) Efficient elimination of inhaled nanoparticles from the alveolar region: evidence for interstitial uptake and subsequent reentrainment onto airways epithelium. Environ Health Perspect 115: 728–733

Semmler-Behnke M, Fertsch S, Schmid O, Wenk A, Kreyling WG (2007 b) Uptake of 1.4 mm versus 18 mm Gold particles by secondary target organs is size dependent in control and pregnants rats after intertracheal or intravenous application. Proceedings of Euro Nanoforum – Nanotechnology in industrial application: 102–104

Semmler-Behnke M, Kreyling W, Lipka J, Fertsch S, Wenk A, Takenaka S, Schmid G, Brandau W (2008). Biodistribution of 1.4- and 18-nm Gold Particles in Rats. Small 4: 2108–2111

Shvedova AA, Kisin ER, Porter D, Schulte P, Kagan VE, Fadeel B, Castranova V (2009) Mechanisms of pulmonary toxicity and medical applications of carbon nanotubes: Two faces of Janus? Pharmacological & Therapeutics 121: 192–204

1.4 Penetration of Nanoparticles through Intact and Compromised Skin

Gintautas Korinth and Hans Drexler

Institute and Outpatient Clinic of Occupational, Social and Environmental Medicine of University of Erlangen-Nuremberg

Erlangen-Nuremberg, Germany

Depending on their physicochemical properties, nanoscale chemical compounds are used, for example, to protect the skin from external exposure or as transdermal transport systems for medications. Metallic nanoparticles are of most significance for dermal exposure. They are used among others in cosmetics, sunscreens, toiletries, textiles and wound dressing materials and are thus accessible to the human organism via the skin. Application in nanoparticle (NP) form results in a more effective epidermal distribution of a compound or a higher topical release rate. Although dermal absorption of NP, particularly of titanium dioxide (TiO_2), has been intensively investigated since the 1990s, the data are still insufficient. Since NP have a high readiness to agglomerate/aggregate, it cannot be ruled out that, even before exposure, large particles may be formed that can barely be absorbed through the skin. Older studies provide only little data on the particle size or form in the application phase, nor are such data declared in consumer products in most cases. Therefore, studies in which particles are characterized according to size, form and stability in the application phase are of special interest.

There are numerous studies on the dermal penetration of TiO_2 and zinc oxide (ZnO) from cosmetic formulations. Both compounds are added to sunscreens as UV radiation filters. Reviews suggest that, after short-term exposure, TiO_2 and ZnO barely penetrate the skin beyond the stratum corneum *in vitro* as well as *in vivo* (Crosera et al. 2009; Newman et al. 2009). Long-term dermal exposure may, however, lead to a systemic bioavailability and accumulation of TiO_2 in various organs. Wu et al. (2009) demonstrated dermal absorption of nanoscale TiO_2 in two animal models (hairless mice and pigs) *in vivo*. After dermal exposure (60 days for 3 hours daily) of hairless mice, the nanoscale TiO_2 level was considerably increased in various organs as compared with the control group and the group exposed to normal-scale TiO_2. Moreover, histopathological investigations showed severe skin damage in all mouse groups exposed to TiO_2 NP formulations; it was not observed in the mouse groups exposed to the vehicle (control group) and to normal-scale TiO_2. Penetration of TiO_2 into the epidermis, but not into the dermis, was observed in the porcine skin, which should be more similar to the human skin. Additionally, it was demonstrated that the penetration capacity of TiO_2 into deeper epidermal layers of porcine skin depends on the particle size, where smaller NP showing higher penetration (Wu et al. 2009). Sadrieh et al. (2010) were not able to confirm a significant penetration of nanoscale TiO_2 through the intact skin using a comparable study design

in mini pigs; their results thus do not significantly differ from the results of Wu et al. (2009) in pig skin. In a diffusion cell study using excised human skin, Mavon et al. (2007) also showed nanoscale (~20 nm) TiO_2 in the dermis from a sunscreen formulation. After a 5-hour exposure, ~5 % of the applied TiO_2 was recovered in the epidermis. The authors assumed, however, that there was no relevant TiO_2 penetration beyond the stratum corneum. In the absence of a negative control and in consideration of data in porcine skin from literature, Mavon et al. (2007) explained their results by stating that the NP found were deposits of TiO_2 in deeper furrows or that the values were in the range of the analytical detection limit.

In a diffusion cell study with human epidermal membranes, Cross et al. (2007) detected significantly higher NP levels in the receptor phase in treated skin as compared to the control after 24-hour exposure to nanoscale ZnO in sunscreens. Since it was not possible to detect ZnO by electron microscopy in the lower stratum corneum or epidermis, Cross et al. (2007) interpreted the spectrometric evidence of Zn in the receptor phase, suggesting that a small fraction of Zn must have been present in solution and penetrated the skin barrier as metallic zinc. In a diffusion cell study by Gamer et al. (2006) in porcine skin with nanoscale ZnO (< 160 nm) applied in an oil/water emulsion, the background exposure was higher than the amount of ZnO in the stratum corneum, skin and receptor phase. This shows the importance of a physicochemical characterization of the particles and the necessity of negative controls.

A diffusion cell study with gold NP in excised rat skin also demonstrated that penetration essentially depends on NP size (Sonavane et al. 2008). Dermal penetration of small gold NP (15 nm) was many times higher than that of larger gold NP (102 and 198 nm). In that study, the dermal penetration kinetics was assessed and the penetration rates of NP of different sizes were compared semi-quantitatively by calculating permeability coefficients.

Ryman-Rasmussen et al. (2006) investigated the dermal penetration of quantum dot (QD) 565 (spherical form) and 655 (ellipsoid form) NP coated with polyethylene glycol (PEG), polyethylene glycol amine (NH_2) or carboxylic acid (COOH) through porcine skin in the diffusion cell model. After 8-hour exposure, confocal laser scanning microscopy revealed that QD 565 NP penetrated into the epidermis (PEG and COOH) or dermis (NH_2) depending on the coating. QD 655 NP were recovered in the stratum corneum (COOH) or epidermis (PEG or NH_2). After 24-hour exposure, QD 655 NP coated with COOH also penetrated into the epidermis.

The available studies are of limited reliability for assessing the risk of occupational NP exposure. Since evidence of relevant background exposure of TiO_2 (Tan et al. 1996; Wu et al. 2009) and ZnO (Cross et al. 2007; Gamer et al. 2006) NP was provided both in human skin and in animal studies, negative controls are necessary. In older studies, the method of tape stripping was often used to determine the dermal penetration of NP. However, it is difficult to interpret the results of this method, since it is based on indirect detection and it is not clear how many tape strips are required to remove the stratum corneum. Moreover, only in a few older studies the particles were characterized physicochemically

in the applied matrix. Most of the older studies did not take the high readiness of NP to agglomerate/aggregate into account.

At industrial workplaces, up to 82 % of workers may show visible damage of the epidermal barrier (for example Korinth et al. 2007). Table 1 summarizes studies that allow a comparison to be made between the penetration of NP through intact and compromised skin. In a diffusion cell study, Larese et al. (2009) investigated the penetration of silver (Ag) NP through intact and by scratch technique damaged human skin. Atomic absorption spectrometry showed five times higher penetration of Ag through damaged than through intact skin. However, this study was not reliable in differentiating Ag NP and elemental silver. Transmission electron microscopy investigations showed Ag NP in stratum corneum and in the upper epidermal layers. Since deeper skin layers were also damaged, such a model has limited reliability for the situation at workplaces and in the environment. In their diffusion cell study in excised human skin, Baroli et al. (2007) found that, a stratum corneum swelling by hydration led to the formation of depots of iron and iron oxide NP. They also observed penetration of iron-containing NP into the epidermis in experiments with intact skin. In a diffusion cell study in rat skin using two different QD NP, Zhang and

Table 1: Comparison of nanoparticle (NP) penetration through intact and compromised skin.

Nanoparticles	**Particle characterization**	**Type of study**	**Skin compromising technique**	**Skin penetration**	**Reference**
Silver	coated with polyvinylpyrrolidone (Ø up to 25 nm)	controlled diffusion cell study in human skin	skin scratching	5-fold penetration increase of silver through damaged skin	Larese et al. 2009
Fe_2O_3 (maghemite), iron	coated with organic molecules (Ø < 24 nm)	controlled diffusion cell study in human skin	swelling of the stratum corneum caused by 24-hour hydration	formation of NP depots in hydrated stratum corneum	Baroli et al. 2007
Fullerene	peptide coating (Ø ~ 4 nm)	controlled diffusion cell study in porcine skin	mechanical skin flexion	penetration enhancement by skin flexion	Rouse et al. 2007
Quantum dots (QD)	Cd/Se core and ZnS shell (Ø ≤ 18 nm)	controlled diffusion cell study in rat skin	tape stripping, abrasion and mechanical skin flexion	penetration enhancement in abraded skin	Zhang and Monteiro-Riviere 2008
Beryllium oxide*	Ø ≤ 1 µm	excised human skin	mechanical skin flexion	penetration enhancement by skin flexion	Tinkle et al. 2003

*Physicochemical characterization of beryllium oxide was not performed

Monteiro-Riviere (2008) detected neither dermal penetration after exposure of up to 24 hours nor penetration into the epidermis after repeated flexion and tape stripping of stratum corneum. QD NP were, however, recovered in the dermis of rat skin abraded with sandpaper, but most of the epidermis had been abraded as well (Zhang and Monteiro-Riviere 2008). In a diffusion cell study in excised pig skin, the same working group (Rouse et al. 2007) showed that surface-functionalized peptide NP on fullerene basis penetrated into the epidermis and dermis after 8-hour exposure. After repetitive mechanical flexing of porcine skin for 60 or 90 minutes, a penetration of fullerene NP was observed deep into the dermis that increased proportionally with the duration of flexing. After 24-hour exposure, dermal penetration of the peptide NP on fullerene basis increased considerably as compared with 8-hour exposure.

Dermal penetration of chemicals is usually enhanced in the presence of skin creams or when chemicals are applied in mixtures (Korinth et al. 2007; Korinth et al. 2008). This effect seems to be even more pronounced in creams on NP basis. For example, in diffusion cell studies with porcine skin designed for therapeutic purposes, the azo dyes rhodamin B and nile red penetrated through the skin from creams on NP basis better than from conventional creams (Küchler et al. 2009 a, b). NP incorporation into vehicle led also to dermal penetration enhancement of acridine orange 10-nonyl bromide comparing with basic emulsions (Eskandar et al. 2010). Dermal penetration enhancement was also demonstrated in porcine skin both *in vitro* and *in vivo* for fullerene NP from mixtures with low-molecular hydrocarbons, such as chloroform, toluene and cyclohexane (Xia et al. 2010). Thus, creams on NP basis show the same dermal penetration enhancement behaviour of chemicals as skin creams used in workers.

It is generally agreed that NP can induce toxic reactions in viable skin. Cytotoxic effects have been described for both metallic and carbon-containing NP for the epidermis and dermis as well as for keratinocytes and fibroblasts in cell culture experiments (Crosera et al. 2009). However, it must be verified, whether such *in vitro* data are transferable to human beings.

Summary

For chemical compounds, diffusion through stratum corneum is the decisive step in determining the absorption level. In older studies, penetration of nanoparticles (NP) beyond the stratum corneum was barely demonstrated in intact skin. Up to now, there is no evidence of NP penetration into deeper tissue through hair follicles. However, dermal penetration of NP has been demonstrated for mechanically compromised or damaged skin. The quantity of dermal absorption generally depends on exposure conditions. Since there are no data from occupational field studies, it is currently difficult to assess the toxicological relevance of dermally absorbed NP. Moreover, the exposure to NP at workplaces is often not characterized. The data on the dermal absorption of coated NP are also insufficient.

Because of the background exposure to NP and the possible contamination, negative controls should be included in skin penetration studies. At present, the skin penetration of NP can be quantified only to a limited extent, since there are no validated analytical methods. Therefore, there is only little kinetic dermal penetration data available.

In older studies, physicochemical characterization of the size and form of the particles in the exposure phase was rarely performed. Due to the methodological problems, the dermal penetration data of NP is still insufficient. Further data of well-designed studies and the development of new analytical methods are required for the quantification of dermal penetration of NP and for the risk assessment.

References

Baroli B, Ennas MG, Loffredo F, Isola M, Pinna R, López-Quintela MA (2007) Penetration of metallic nanoparticles in human full-thickness skin. J Invest Dermatol 127: 1701–1712

Crosera M, Bovenzi M, Maina G, Adami G, Zanette C, Florio C, Larese Filon F (2009) Nanoparticle dermal absorption: a review of the literature. Int Arch Occup Environ Health 82: 1043–1055

Cross SE, Innes B, Roberts MS, Tsuzuki T, Robertson TA, McCormick P (2007) Human skin penetration of sunscreen nanoparticles: *in vitro* assessment of a novel micronized zinc oxide formulation. Skin Pharmacol Physiol 20: 148–154

Eskandar NG, Simovic S, Prestidge CA (2010) Mechanistic insight into the dermal delivery from nanoparticle-coated submicron O/W emulsions. J Pharm Sci 99: 890–904

Gamer AO, Leibold E, van Ravenzwaay B (2006) The *in vitro* absorption of microfine zinc oxide and titanium dioxide through porcine skin. Toxicol In Vitro 20: 301–307

Korinth G, Weiss T, Penkert S, Schaller KH, Angerer J, Drexler H (2007) Percutaneous absorption of aromatic amines in rubber industry workers: impact of impaired skin and skin barrier creams. Occup Environ Med 64: 366–372

Korinth G, Lüersen L, Schaller KH, Angerer J, Drexler H (2008) Enhancement of percutaneous penetration of aniline and o-toluidine *in vitro* using skin barrier creams. Toxicol In Vitro 22: 812–818

Küchler S, Radowski MR, Blaschke T, Dathe M, Plendl J, Haag R, Schäfer-Korting M, Kramer KD (2009) Nanoparticles for skin penetration enhancement – a comparison of a dendritic core-multishell-nanotransporter and solid lipid nanoparticles. Eur J Pharm Biopharm 71: 243–250

Küchler S, Abdel-Mottaleb M, Lamprecht A, Radowski MR, Haag R, Schäfer-Korting M (2009) Influence of nanocarrier type and size on skin delivery of hydrophilic agents. Int J Pharm 377: 169–172

Larese FF, D'Agostin F, Crosera M, Adami G, Renzi N, Bovenzi M, Maina G (2009) Human skin penetration of silver nanoparticles through intact and damaged skin. Toxicology 255: 33–37

Mavon A, Miquel C, Lejeune O, Payre B, Moretto P (2007) *In vitro* percutaneous absorption and *in vivo* stratum corneum distribution of an organic and a mineral sunscreen. Skin Pharmacol Physiol 20: 10–20

Newman MD, Stotland M, Ellis JI (2009) The safety of nanosized particles in titanium dioxide- and zinc oxide-based sunscreens. J Am Acad Dermatol 61: 685–692

Rouse JG, Yang J, Ryman-Rasmussen JP, Barron AR, Monteiro-Riviere NA (2007) Effects of mechanical flexion on the penetration of fullerene amino acid-derivatized peptide nanoparticles through skin. Nano Lett 7: 155–160

Ryman-Rasmussen JP, Riviere JE, Monteiro-Riviere NA (2006) Penetration of intact skin by quantum dots with diverse physicochemical properties. Toxicol Sci 91: 159–165

Sadrieh N, Wokovich AM, Gopee NV, Zheng J, Haines D, Parmiter D, Siitonen PH, Cozart CR, Patri AK, McNeil SE, Howard PC, Doub WH, Buhse LF (2010) Lack of significant dermal penetration of titanium dioxide from sunscreen formulations containing nano- and submicron-size TiO_2 particles. Toxicol Sci 115: 156–166

Sonavane G, Tomoda K, Sano A, Ohshima H, Terada H, Makino K (2008) *In vitro* permeation of gold nanoparticles through rat skin and rat intestine: effect of particle size. Colloids Surf B Biointerfaces 65: 1–10

Tan MH, Commens CA, Burnett L, Snitch PJ (1996) A pilot study on the percutaneous absorption of microfine titanium dioxide from sunscreens. Australas J Dermatol 37: 185–187

Tinkle SS, Antonini JM, Rich BA, Roberts JR, Salmen R, DePree K, Adkins EJ (2003) Skin as a route of exposure and sensitization in chronic beryllium disease. Environ Health Perspect 111: 1202–1208

Wu J, Liu W, Xue C, Zhou S, Lan F, Bi L, Xu H, Yang X, Zeng FD (2009) Toxicity and penetration of TiO_2 nanoparticles in hairless mice and porcine skin after subchronic dermal exposure. Toxicol Lett 191: 1–8

Xia XR, Monteiro-Riviere NA, Riviere JE (2010) Skin penetration and kinetics of pristine fullerenes (C 60) topically exposed in industrial organic solvents. Toxicol Appl Pharmacol 242: 29–37

Zhang LW, Monteiro-Riviere NA (2008) Assessment of quantum dot penetration into intact, tape-stripped, abraded and flexed rat skin. Skin Pharmacol Physiol 21: 166–180

1.5 Studies on the Inhalation Uptake and Effects of Nanomaterials

Robert Landsiedel

BASF SE, Ludwigshafen, Germany

Hypothesis

Exposure to nanomaterials could occur during production, subsequent processing and use of the end product. For most nanomaterials in our industry, inhalation uptake is regarded the most critical route of exposure. We aimed to assess the toxicity of inhaled nanomaterials. Our hypotheses were:

- Nanomaterials usually exist as agglomerates (and aggregates).
- Inflammation processes in the lung are the dominating effects of inhaled biopersistent nanomaterials.
- Desagglomeration in the lung and translocation to other organs does not occur.

Aerosols from Nanomaterials

We characterized the aerosols of various nanomaterials using different dispersion methods. Typically the number concentration of particles below 100 nm in diameter was 10 to 20 % in these aerosols, with the majority of particles being agglomerates (or aggregates) above the nano-range (Ma-Hock et al. 2007).

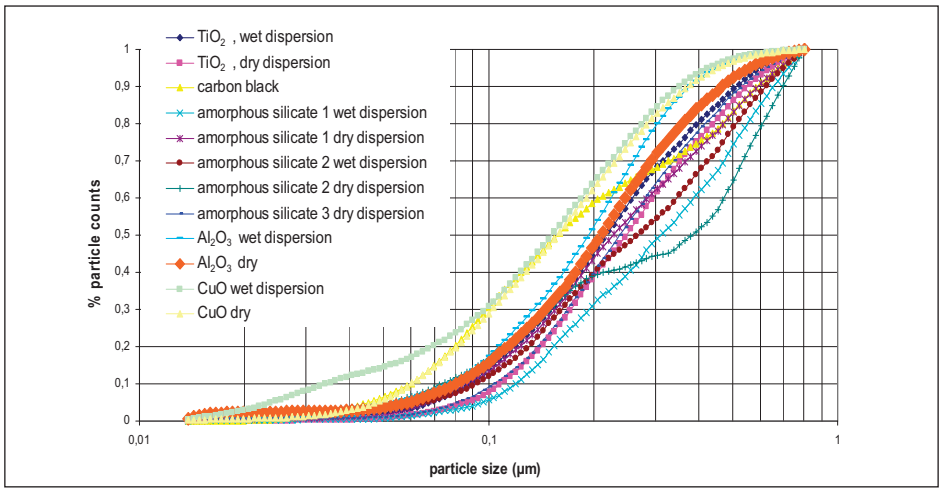

Figure 1: Particle size distribution of aerosols from nanomaterials by wet or dry dispersion. Particles were analyzed by SMPS (Scanning Mobility Particle Sizer) and hence particles larger than 1 µm were not counted; the particle count fraction of these particles is, however, negligible.

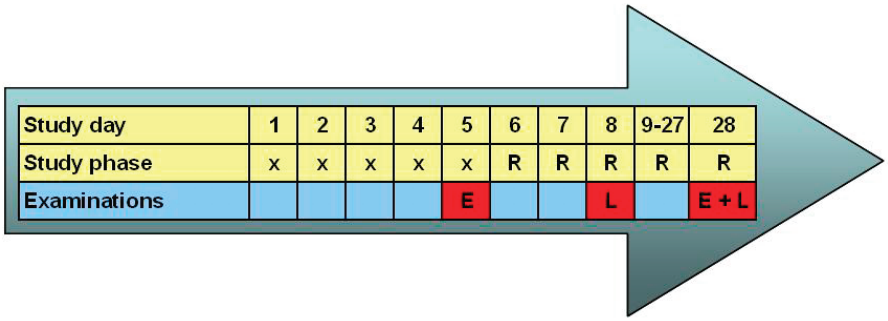

Figure 2: Study design of short-term inhalation method
X: Head-nose exposure to aerosols for 6 hours per day on 5 consecutive days
R: Recovery period
E: Examinations (histology of selected organs, organ burden, distribution and translocation, particle size distribution within the lung
L: Cytological and biochemical parameters in the bronchoalveolar lavage fluid

Toxicological Test Method

We used these aerosols to test the inhalation uptake and toxicity of 15 substances in rats. 11 Nanomaterials were tested (SiO_2, surface coated SiO_2, TiO_2 P 25, coated TiO_2, CeO_2, doted CeO_2, ZrO_2, $BaSO_4$, carbon black, MWCNT1, MWCNT2) and – for comparison – four micron-scaled materials (quartz, TiO_2, CeO_2, ZnO). All materials were sufficiently characterized and tested by the well-established short-term inhalation toxicity protocol for nanomaterials (Ma-Hock et al. 2008). For method development over 70 biological parameters were used. Total protein concentration and polymorphonuclear neutrophils in bronchoalveolar lavage fluid was, however, the most sensitive indicator of lung inflammation (in addition to histopathology). The method was developed and used within the German BMBF project *nanoCare*, the EU project *NanoSafe2* and BASF-internal research projects.

Deposition and Fate

The amount of the test materials in the lungs as well as the blood, lymph nodes, liver, kidney, spleen and basal brain with olfactory bulb was determined by ICP-AES and by TEM. The examinations were carried out shortly after the exposure and at different times within three weeks after the first inhalation.

For the TiO_2 nanomaterial deposition was studied in detail and compared to the micron-scale material: Both materials deposited similarly in the lungs due to similar aerodynamic size. The material was retained in the lungs (extracellularly and in macrophages); the particles were mostly agglomerates of about the same size as found in the atmosphere; there were no signs of desagglomeration in the lungs (Morfeld et al. 2012). Clearance from the lungs and a translocation to the mediastinal lymph nodes was noted, though in smaller amounts than those exposed to micron-scale TiO_2 (Ravenzwaay et al. 2009). There was no indication of a translocation into other organs.

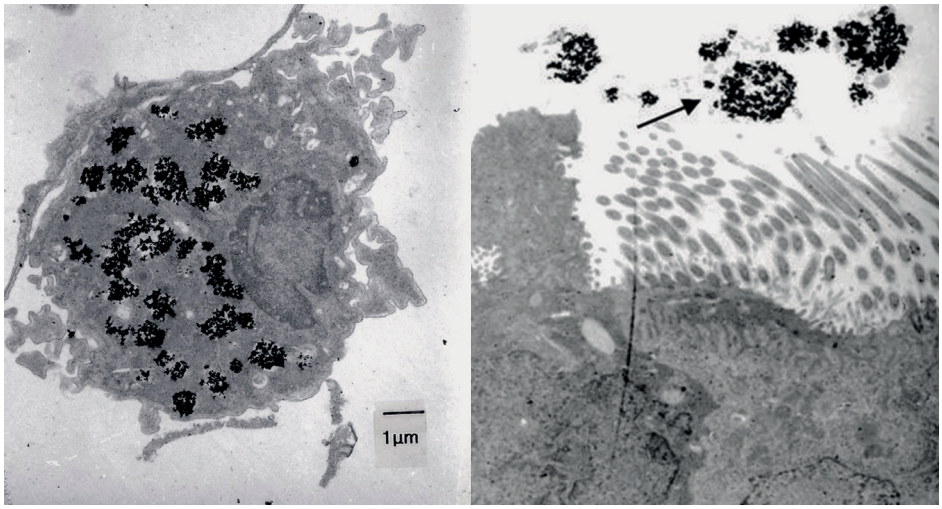

Figure 3: TEM images of inhaled nanomaterial (TiO_2) in the lungs. Agglomerates of nanoparticles were found in macrophage (left) and on the lung surface (right).

All 15 materials were deposited in the lungs and no translocation to other tissues than the draining lymph nodes was detected. With two exceptions: (1) Coated silica particles were additionally found in the spleen, whereas the uncoated particles were not. (2) With zinc oxide elevated zinc ion concentrations were found in various tissues, due to the solubility of the material.

Effects

For insoluble nanomaterials the inflammation of the lungs was the main effect and no systemic toxicity was observed. When the nanomaterial was compared to the micron-scale material, effects at the same mass-concentration were generally stronger with the nanomaterial. Soluble zinc oxide particles additionally caused necrosis in the upper respiratory tract. The concentrations which caused the local effects in the lung varied over two orders of magnitude when using mass concentration as dosimetry (Landsiedel et al. 2010). Effects of MWCNT observed in the short-term test were confirmed in a subchronic inhalation study according to OECD test guideline 413 (Ma-Hock et al. 2009).

Conclusions

Inflammatory effects and translocation of different nanomaterials can be studied and compared in short-term inhalation studies.

From the results of 15 inhalation studies we conclude:

- Aerosols of nanomaterials are mixtures of nanoparticles as well as small and larger agglomerates (and aggregates).

Table 1: Summary of results of short-term inhalation studies with nanomaterials (yellow) and micro-scale materials (blue).

Material	Conc. [mg/m³]	NOAEC [mg/m³]	BAL	Pathology	Reversibility	Translocation
Quartz	100	**-**	pronounced inflammation	diffuse histocytosis increased apoptosis granulomatous inflammation	not complete	no indication
SiO_2	0.5; 2.5; 10	**10**	no effects	no effects	–	no indication
SiO_2 coated	0.5; 2.5; 10	**10**	no effects	no effects	–	yes: in spleen
$pTiO_2$	250	**-**	no effects	diffuse histocytosis increased apoptosis	not complete	no indication
TiO_2	2, 10, 50	**2**	inflammation	histocytosis	not complete	no indication
pZnO	12.5	**–**	Inflammation	mild diffuse histocytosis nose: necrosis	yes	yes (Zn ions?)
ZnO	0.5; 2.5; 12,5	**≤ 0.5**	Inflammation	lung: inflammation, cell death; nose: necrosis	yes	yes (Zn ions?)
CeO_2	0.5; 2.5; 10	**< 0.5**	Inflammation	histocytosis, mild inflammation	not complete	n. d.
CeO_2 doped	0.5; 2; 10	**< 0.5**	inflammation	histocytosis, mild inflammation	not complete	n. d.
$BaSO_4$	2, 10, 50	**50**	no adverse finding	no adverse finding	–	n. d.
Carbon-black	0.5; 2.5; 10	**10**	no effects	no effects	–	n. d.
MWC-NT	0.1; 0.5; 2.5	**≤ 0.1**	inflammation	inflammation	no	no indication

BAL bronchoalveolar lavage
n. d. not determined
SiO_2 polyacryl-coated amorphous silica
pZnO, **$pTiO_2$** pigmentary (non-nano, micro-scale) ZnO, TiO_2

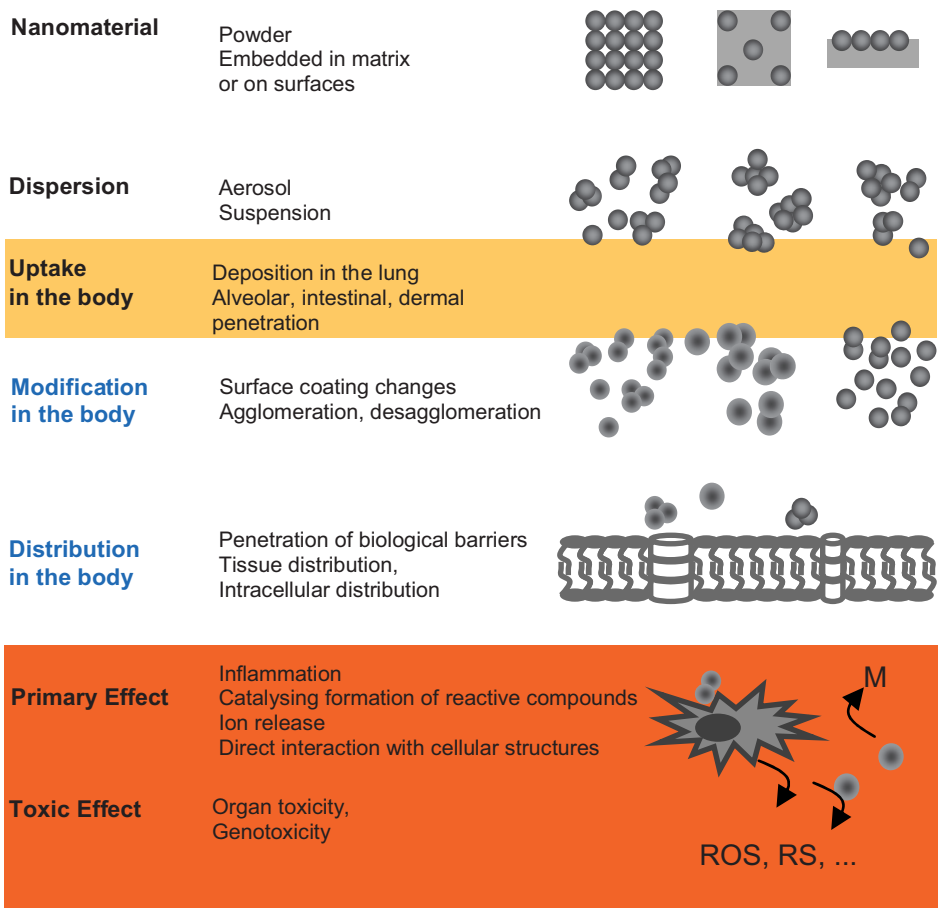

Figure 4: Release, uptake, distribution and effects of nanomaterials in the body.

- Inflammation processes in the lung are indeed the dominating effects of inhaled biopersistent nanomaterial. Whereas the toxicity of the released ions dominates the effects of soluble metal-containing nanomaterials. The effects of a nanomaterial could not be attributed to a single material property (chemical composition, size, shape, surface area, surface coating).
- Desagglomeration in the lung was not observed. Translocation seems to be triggered by specific material properties (in our studies it was the surface-coating of a silica-material).

The observed effects of nanomaterials can be attributed to three (maybe four) mechanisms; neither of those is specific to nanomaterials:

- Release of metal ions (for metal containing soluble nanomaterials)
- Catalysing the formation of reactive molecules (e. g. ROS)
- Inflammation and loading of macrophages
- and possibly direct (mechanical) interaction with cellular structures

These primary effects are modulated by the distribution and persistence of the nanomaterial in the lungs (or in other tissues) and compartments inside the cell, resulting in different effects of different nanomaterials. At this time it is not exactly known which material properties direct the toxic effects. There is, however, no indication of a nano-specific toxicity per se. There are rather different effects and different potency of the different nanomaterials.

References

Landsiedel R, Ma-Hock L, Kroll A, Hahn D, Schnekenburger J, Wiench K, Wohlleben W (2010) Testing metal-oxide nanomaterials for human safety. Adv Mater 22: 1–27

Ma-Hock L, Gamer A, Landsiedel R, Leibold E, Frechen T, Sens B, Huber G, van Ravenzwaay B (2007) Generation and characterization of test atmospheres with nanomaterials. Inhal Toxicol 19: 833–848

Ma-Hock L, Burkhardt S, Strauss V, Gamer AO, Wiench K, van Ravenzwaay B, Landsiedel R (2009) Development of a short-term inhalation test in the rat using nano-titanium dioxide as a model substance. Inhal Toxicol 21: 102–118

Ma-Hock L, Treumann S, Strauss V, Brill S, Luizi F, Mertler M, Wiench K, Gamer AO, van Ravenzwaay B, Landsiedel R (2009) Inhalation toxicity of multi-wall carbon nanotubes in rats exposed for 3 months. Toxicol Sci 112: 468–481

Morfeld P, Treumann S, Ma-Hock L, Bruch J, Landsiedel R (2012): Deposition behaviour of inhaled nanostructured TiO_2 in rats: number distribution of particles by different lung lobes and fraction of particle diameters below 100 nm. Inhal Toxicol 24: 939-993.

Ravenzwaay B, Landsiedel R, Fabian E, Burkhardt S, Strauss V, Ma-Hock L (2009) Comparing fate and effects of three particles of different surface properties: Nano-TiO_2, pigmentary TiO_2 and quartz. Toxicol Lett 186: 152–159

1.6 Animal Studies on the Effect of Nanoparticles in Organs other than the Lungs

Uwe Heinrich

Fraunhofer Institute for Toxicology and Experimental Medicine

Hanover, Germany

Apart from their different kinetics (distribution in the organism), nanometer and micrometer particles of the same material do not seem to differ qualitatively regarding their toxic effects on the lungs. Based on the particle mass, which determines the dose, the inflammatory proliferative and tumour-inducing effects of nanoparticles are severer than those of microparticles. The clearance half-lives of nanoparticles in the lungs are also longer than those of microparticles.

This statement does not apply to non-soluble or poorly soluble nanoparticles. Their toxicity originates from the physicochemical particle properties and from the surface activity of the particles. There is hardly any evidence of a possible toxicity of such nanoparticles in organs other than the lungs. Numerous publications on nanoparticles mainly deal with the question in which organs other than the lungs such nanoparticles can be detected after inhalation.

The particle effect of nanoparticles from metal and their inorganic compounds is also determined by the degree of the bioavailability of the metal since the metal ions may have an effect of their own. The metal nanoparticle is thus a carrier for the metal ion. A high cellular concentration of toxic metal ions may form, particularly if the metal nanoparticle becomes bioavailable intracellularly.

Carbon nanotubes (CNT) are a group of nanomaterials that is not considered here. Because of their high biopersistence and possible occurrence in very different lengths and diameters, some nanotubes may also have the potential to induce mesotheliomas and lung tumours. No carcinogenicity tests or validated screening tests that can be used to rule out carcinogenicity are available for this group of nanomaterials. Therefore, the effect of such nanotubes might be compared with an effect of granular biopersistent particles.

A special group of nanotubes retains the structure of a considerably entangled agglomerate and does not segregate into individual nanotubes even after mechanical treatment and in suspension. If these nanotube agglomerates occur in a respirable size, they behave like granular biopersistent dusts, although they have a very low density and a great specific surface.

Publications of Effect Studies on Granular Biopersistent Nanodusts (GBND) and Metal Nanoparticles

The intranasal administration of carbon black nanoparticles in mice with primary particle sizes of 14 nm (Printex 90; Degussa) and 95 nm (lampblack; Degussa) and with BET surfaces (*B*runauer, *E*mmett and *T*eller theory) of 300 m^2/g

or 20 m^2/g in a dose of 62.5 µg/naris once per week for 4 weeks showed a significant increase in the mRNA expression of cytokines (IL-1beta and TNF-alpha) and chemokines (macrophage inflammatory protein CCL2, monocyte chemoattractant protein CCL3 and the chemokine ligand CXCL9, which is related to the Th 1 response) in the olfactory bulb only for Printex 90, but not for lampblack. No evidence of this mRNA expression was provided in the hippocampus of the treated animals for any of the carbon black particles used. The molecules expressed here all play a role in neurogenic immune response and inflammation (Tin-Tin-Win-Shwe et al. 2006).

After i. p. injection into mice in doses of 6.5 to 51.8 mg, nano TiO_2 (100 nm) was found in the liver, lung and kidney; no positive evidence was provided in the heart or brain. Histopathological effects in the different organs were found particularly in the spleen (increased neutrophil concentration and inflammation), in the liver (inflammation and fibrosis) and in the lung (increased occurrence of neutrophil cells, thickened alveolar septa, TiO_2 particles in pulmonary vessels and thrombosis). Liver enzymes in the blood were also increased in the two highest dose groups; however, these dose groups also showed increased mortality (Chen et al. 2009).

Pregnant mice were subcutaneously treated with suspended nano TiO_2 (particle size: 25–0 nm; anatase) on days 3, 7, 10 and 14 after mating. The male offspring were examined when they were 4 days or 6 weeks old. Evidence of TiO_2 in the testes and brain of the offspring was provided with the electron microscope and the associated energy dispersive X-ray spectroscopy. Aggregates of TiO_2 nanoparticles (100–200 nm) were detected in Leydig cells, Sertoli cells and spermatids of the testes of the offspring. A histopathological examination of the testicular morphology revealed clear changes in the 6-week-old offspring. Sperm production, sperm motility and the number of Sertoli cells were significantly reduced as compared with the controls. This describes an effect of treatment on spermatogenesis. TiO_2 was also detected in brain cells of the offspring (6 weeks). An increased number of cells with a positive reaction to apoptosis markers (caspase-3) was found in the olfactory bulb, and obstruction of small vessels and perivascular edema were described histopathologically (Takeda et al. 2009).

Rats were exposed to MnO nanoparticles (primary particle size: 3–8 nm; agglomerate particle size: 30 nm) in a whole-body exposure inhalation system for 6 hours/day, 5 days/week, for up to 12 days. The particles had a solubility of 1–1.5 % per day at a neutral pH. The exposure concentration was about 500 $\mu g/m^3$. Both TNF-alpha gene expression and TNF-alpha protein expression were significantly increased in the olfactory bulb and in various other brain regions. The gene for the macrophage inflammatory protein-2, for the glial fibrillary acidic protein and for the neuronal cell adhesion molecule was also significantly overexpressed in the olfactory bulb. Different approaches (comparative investigations of $MnCl_2$ with MnO; solubility tests of MnO using different pH levels) used in these studies demonstrated that the main fraction of manganese oxide reached the olfactory bulb in particle form (Elder et al. 2006).

In a study in pregnant mice, the gene expression was determined in the brain of the embryos and of the 1- and 2-day-old newborns after maternal subcutaneous injection of nano-TiO_2 (anatase). Changes in the expression of genes were found that were associated with encephalization, cell death, oxidative stress and the mitochondria during the perinatal period (Shimizu et al. 2009).

In addition to toxic effects in the lung, histopathological changes in the liver (bile-duct hyperplasia) were also described after inhalation (28 and 90 days) of silver nanoparticles (metallic silver) in a particle size of 18 nm count median diameter (CMD). Apart from the lung, the liver had the highest silver concentration as compared with the kidney, brain and blood. The silver concentrations were determined using an atomic absorption spectrophotometer. The solubility of these metallic silver particles was not specified (Sung et al. 2008; Sung et al. 2009).

Genotoxic effects in peripheral blood cells after i. p. injection of nano Al_2O_3 (primary particle size 30 and 40 nm; agglomerate size in the suspending medium 140–220 nm) were found in rats using the comet assay and micronucleus test. Al_2O_3 with a particle size of 50–200 µm did not show these findings (Balasubramanyam et al. 2009).

References

Balasubramanyam A, Sailaja N, Mahboob M, Rahman MF, Hussain SM, Grover P (2009) *In vivo* genotoxicity assessment of aluminium oxide nanomaterials in rat peripheral blood cells using the comet assay and micronucleus test. Mutagenesis 24: 245–251

Chen J, Dong X, Zhao J, Tang G (2009) *In vivo* acute toxicity of titanium dioxide nanoparticles to mice after intraperitoneal injection. J Appl Toxicol 29: 330–337

Elder A, Gelein R, Silva V, Feikert T, Opanashuk L, Carter J, Potter R, Maynard A, Ito Y, Finkelstein J, Oberdörster G (2006) Translocation of inhaled ultrafine manganese oxide particles to the central nervous system. Environ Health Perspect 114: 1172–1178. Erratum in: Environ Health Perspect. ug;114: 1178

Shimizu M, Tainaka H, Oba T, Mizuo K, Umezawa M, Takeda K (2009) Maternal exposure to nanoparticulate titanium dioxide during the prenatal period alters gene expression related to brain development in the mouse. Part Fibre Toxicol 6: 1–8

Sung JH, Ji JH, Yoon JU, Kim DS, Song MY, Jeong J, Han BS, Han JH, Chung YH, Kim J, Kim TS, Chang HK, Lee EJ, Lee JH, Yu IJ (2008) Lung Function Changes in Sprague-Dawley rats after prolonged inhalation exposure to silver nanoparticles. Inhal Toxicol 20: 567–574

Sung JH, Ji JH, Park JD, Yoon JU, Kim DS, Jeon KS, Song MY, Jeong J, Han BS, Han JH, Chung YH, Chang HK, Lee JH, Cho MH, Kelman BJ, Yu IJ (2009) Subchronic inhalation toxicity of silver nanoparticles. Toxicol Sci 108: 452–461

Takeda K, Suzuki K, Ishihara A, Kubo-Irie M, Fujimoto R, Tabata M, Oshio S, Nihei Y, Ihara T, Sugamata M (2009) Nanoparticles transferred from pregnant mice to their offspring can damage the genital and cranial nerve systems. J Health Sci 55: 95–102

Tin-Tin-Win-Shwe, Yamamoto S, Ahmed S, Kakeyama M, Kobayashi T, Fujimaki H (2006) Brain cytokine and chemokine mRNA expression in mice induced by intranasal instillation with ultrafine carbon black. Toxicol Lett 163: 153–160

1.7 Transport of Nanoparticles to the Brain: Concern for Neurotoxicity?

Andrea Hartwig

Karlsruhe Institute of Technology

Karlsruhe, Germany

There are several publications raising the question of whether there is concern for neurotoxicity of nanoparticles, summarized for example by Oberdörster et al. (2009). One important prerequisite to induce oxidative stress or inflammation in the central nervous system (CNS) would be a significant translocation of nanoparticles to the brain upon realistic exposure conditions. As stated before by Heinrich (this volume) systemic availability of inhaled nanoparticles outside the lung upon realistic exposure conditions appears to be very limited; additionally, nanoparticles would have to cross the blood brain barrier, which has not been demonstrated to occur *in vivo* yet. Nevertheless, one alternative way proposed for the potential transfer of nanoparticles to the brain consists in the passage through sensory nerves. Thus, for nanoparticles of less than 0.1 µm diffusion appears to be the main mechanism of disposition during nasal breathing, and significant fractions are deposited in all parts of the respiratory tract, namely the nasal, the tracheobronchial and the alveolar region. Within the nasal region, the smallest nanoparticles may behave similar to smell molecules and have the potential to be translocated along the sensory neuronal pathway to the olfactory bulb. Similarly, the nasopharyngeal and the tracheobronchial airways are supplied with sensory nerves as well, whereas their presence in the alveolar region of the lung is less clear (Oberdörster et al. 2009). Up to now, there are only few studies available demonstrating olfactory nerve nanoparticle translocation to the brain (Table 1).

As evident from Table 1, there is only one inhalation study demonstrating an inflammatory response, determined by a pronounced change in TNF-α-expression, after realistic inhalation exposure to MnO nanoparticles in rats. Here, inhalation experiments with rats at 500 µg/m^3 revealed higher concentrations of manganese in the olfactory bulb as compared to lung tissue; furthermore, pronounced changes in TNF-α gene and protein expression levels were observed specifically in the olfactory bulb as opposed to other brain regions (Elder et al. 2006). Even though further studies are needed, this example is interesting since epidemiological evidence points towards a pronounced neurotoxic potential especially of small manganese oxide particles generated predominantly during welding, which are likely to contain a large fraction of ultrafine particles. Thus, a tenfold lower MAK value has been established in 2010 for particles in the alveolar fraction (0.02 mg/m^3) as compared to the inhalable fraction (0.2 mg/m^3) (Hartwig 2010). These differences in neurotoxic potential can be explained either by higher systemic bioavailability of smaller particles via blood circulation and translocation through the blood brain barrier or via sensory

Table 1: Olfactory nerve nanoparticle translocation to the brain.

Type of nanoparticle	Species	Application	Fraction deposited	Biological effects in the CNS	Reference	Comments
Inhalation						
Mn oxide 3–8 nm (primary) 30 nm (agglomerate)	rat Fischer 344 male	**6 d** 465 ± 94 µg/m^3 6 h/d	olfactory bulb: 1.42 ng/mg* lung: 0.35 ng/mg* liver: 2.61 ± 1.61 ng/mg*		Elder et al. 2006	
		12 d 465 ± 94 µg/m^3 6 h/d	olfactory bulb: 1.75 ng/mg* lung: 0.4 ng/mg* liver: 2.91 ± 0.09 ng/mg*	TNF-α↑		
		control	olf. bulb: 0.5 ng/mg* lung: 0.18 ng/mg* liver: 2.78 ± 0.04 ng/mg*			
^{13}C < 100 nm	rat Fischer 344 male	**6 h** 170 µg/m^3 24 h postexposure	olf. bulb: 0.35 ± 0.17 µg/g lung: 1.39 ± 0.26 µg/g	inflammatory response not determined	Oberdörster et al. 2004	0.36 % of the inhaled aerosol translocated to the CNS
		3 d postexposure	olf. bulb: 0.35 ± 0.02 µg/g lung: 1.28 ± 0.27 µg/g			
		5 d postexposure	olf.bulb: 0.37 ± 0.08 µg/g lung: 0.83 ± 0.27 µg/g			

Type of nanoparticle	Species	Application	Fraction deposited	Biological effects in the CNS	Reference	Comments
		7 d postexposure	olf.bulb: 0.43 ± 0.08 µg/g lung: 0.59 ± 0.15 µg/g			
		control	olf.bulb: 0.01 ± 0.12 µg/g lung: 0.0 ± 0.3 µg/g			
^{192}Ir 15–20 nm	rat Wistar-Kyoto male	**1–1.5 h endotracheal intubation** 0.2 mg/m^3 21 d postexposure	0.35 ± 0.06 µg Ir mass = 3.5 ± 0.6 kBq in lung	inflammatory response not determined	Semmler et al. 2004	Peak of ^{192}Ir at day 7 in the brain, no further accumulation
		60 d postexposure	5.88 ± 0.76 µg Ir mass = 58.7 ± 7.6 kBq in lung			
		168 d postexposure	11.21 ± 1.71 µg Ir mass = 112.1 ± 17.1 kBq in lung			
nAu 30–110 nm	rat Wistar male	**7 d** 2 × 106 ± 7 % *NSPs/cm^3 6 h/d, 5 d	olf. bulb: 12 ng/g lung: 126 ng/g	inflammatory response not determined	Yu et al. 2007	significant accumulation of gold was detected in the lung and olfactory bulb

Type of nanoparticle	Species	Application	Fraction deposited	Biological effects in the CNS	Reference	Comments
		21 d 6 h/d, 5 d/w	olf. bulb: 13 ng/g lung: 387 ng/g	significant accumulation of gold was detected in the lung, esophagus, tongue, kidney, aorta, spleen, septum, heart and blood		
		control	olf. bulb: 4.4 ng/g lung: 5.5 ng/g			
Instillation						
TiO_2 80 nm Rutil	mouse CD-1(ICR) female	500 µg/mouse x 1 1 x every 2 d, x 5 (10 d) 1 x every 2 d, x 10 (20 d) 1 x every 2 d, x 15 (30 d) control	olf. bulb: increase gradually 65 ng/g* (control) to 200 ng/g* Hippocampus: 285 ng/g (30 d)*	TNF-α↑ IL-1β IL-6: no increase No antioxidative responses of brain	Wang et al. (2008)	very high dose (a total dose of 7.5 mg of nano TiO_2 instilled intranasally into mice would be equivalent to instilling 17.5 g into the nose of humans; Oberdörster 2009 b)
Co 25 nm	mouse CD-1(ICR) female	1 mg/kg bw 1 x every 2 d, x 3 48 h postexposure control	olf. bulb: 2.8 µg/g* brain: 17.6 ± 1.6 mg/g olf. bulb: 2.3 µg/g* brain: 16.7 ± 1.7 mg/g	inflammatory response not determined	Liu et al. (2009)	

Type of nanoparticle	Species	Application	Fraction deposited	Biological effects in the CNS	Reference	Comments
		40 mg/kg bw 1 x every 2 d, x 3 48 h postexposure	olf. bulb: 4.37 µg/g* brain: 19.8 ± 1.7 mg/g			Histopathology: olf. bulb severe lesions
		control	olf. bulb: 2.3 µg/g* brain: 19.0 ± 0.8 mg/g			
MPEG-PLA polymer 76 nm	rat Sprague-Dawley male	2 mg NM/kg 5, 10, 15, 30, 60, 120, 240 and 360 min post-administration	olf. bulb: NM ↑ brain: NM ↑	inflammatory response not determined	Zhang et al. 2006	
Fe_2O_3 280 nm	mouse CD-ICR male	40 mg/kg bw 24 h postexposure	olf. bulb: Fe↑ (31 %) brain stem sections: Fe↑ (21 %)	pathological changes of the hippocampus	Wang et al. 2007	very high dose
Carbon Black 14 nm (Printex 90)	mouse BALB/c male	125 µg/mouse 1 x every 28 d, x 4	not determined	olf. bulb: TNF-α↑ IL-1β↑ hippocampus: unchanged	Tin-Tin-Win-Shwe et al. (2006)	
95 nm (Flammruss 101)			not determined	olf. bulb: TNF-α↓ IL-1β↓		
Carbon Black 14 nm (Printex 90)	mouse BALB/c male	250 µg/mouse (single administration)	not determined	TNF-α↑	Tin-Tin-Win-Shwe et al. (2008)	

* values taken from the diagram; NM nanomaterial; MPEG-PLA diblock copolymer of methoxy poly(ethylene glycol)

nerve translocation from the nasal cavity. Within the brain cells, toxicity is most likely not a particle effect as such but rather due to the liberation of manganese ions leading to oxidative stress and related effects.

However, whether or not there will be significant transport of nanoparticles through the sensory nerve system will have to be investigated on a case-by-case basis. Care must be taken to discriminate between hazard and risk, i. e. the potential to reach the brain (hazard) and the question whether the extent of translocation of the respective nanoparticles to the brain is sufficient to elicit adverse effects (risk). Thus, effects derived from experiments with bolus-type delivery of nanoparticles such as nasal or tracheal instillation may provide valuable information on hazard but not on risk; similarly, high dose experiments are not representative for continuous low-dose exposure. Important for risk assessment appears to be not only the delivered dose per unit surface area of the respiratory tract, but also the dose rate, i. e. dose per unit time. One other decisive factor is the particle size, since only very small particles in the lower nanometer range will be able to traverse through sensory nerves; here, agglomeration and aggregation within the respiratory tract has to be taken into account. Furthermore, the impact of the corona formation has been stressed during the last years, also in the context of potential neurotoxic effects (Lynch and Dawson 2008). Thus, nanoparticles in biological media attract proteins and lipids, depending on their size, surface area, charge, surface hydrophobicity and further characteristics on one side and extra- and intracellular fluids on the other side. The corona formation appears to be a dynamic process, leading to an equilibrium of association and dissociation of proteins and/or lipids. At the end, the composition of the corona will be one important factor with respect to translocation of nanoparticles to secondary organs and cell entry (Lynch et al. 2009).

In summary, up to date there is no conclusive evidence that neurotoxicity may be a relevant endpoint for low-dose exposure towards nanoparticles, even though neurotoxic effects of specific types of particles cannot be excluded. Nevertheless, further research is needed providing data suitable for risk assessment of this important aspect of nanotoxicology.

References

Elder A, Gelein R, Silva V, Feikert T, Opanashuk L, Carter J, Potter R, Maynard A, Ito Y, Finkelstein J, and Oberdörster G (2006) Translocation of inhaled ultrafine manganese oxide particles to the central nervous system. Environ Health Perspect 114: 1172–1178

Hartwig (2010) Aerosols. List of MAK and BAT Values, Maximum concentrations and biological tolerance values at the workplace, Commission for the Investigation of Health Hazards of Chemical Compounds in the Work Area. Report 46, 179–187, Wiley-VCH, Weinheim

Liu Y, Gao Y, Zhang L, Wang T, Wang J, Jiao F, Li W, Liu Y, Li Y, Li B, Chai Z, Wu G, Chen C (2009) Potential health impact on mice after nasal instillation

of nano-sized copper particles and their translocation in mice. J Nanosci Nanotechnol 9: 6335–6343

Lynch I, Dawson KA (2008) Protein-nanoparticle interactions. Nanotoday 3: 40–47

Lynch I, Salvati A, Dawson KA (2009) What does the cell see? Nature Nanotechnol 4: 546–547

Oberdörster G, Sharp Z, Atudorei V, Elder A, Gelein R, Kreyling W, Cox C (2004) Translocation of inhaled ultrafine particles to the brain. Inhal Toxicol 16: 437–445

Oberdörster G., Elder A., Rinderknecht A. (2009) Nanoparticles and the brain: cause for concern? J Nanosci Nanotechnol. 9: 4996–5007

Oberdörster G (2009b) Safety assessment for nanotechnology and nanomedicine: concepts of nanotoxicology. J Internal Med 267: 89–105

Semmler M, Seitz J, Erbe F, Mayer P, Heyder J, Oberdörster G, Kreyling WG (2004) Long-term clearance kinetics of inhaled ultrafine insoluble iridium particles from the rat lung, including transient translocation into secondary organs. Inhal Toxicol 16: 453–459

Tin-Tin-Win-Shwe, Yamamoto S, Ahmed S, Kakeyama M, Kobayashi T, Fujimaki H (2006) Brain cytokine and chemokine mRNA expression in mice induced by intranasal instillation with ultrafine carbon black. Tox Lett 163: 153–160

Tin-Tin-Win-Shwe, Mitsushima D, Yamamoto S, Fukushima A, Funabashi T, Kobayashi T, Fujimaki H (2008) Changes in neurotransmitter levels and proinflammatory cytokine mRNA expressions in the mice olfactory bulb following nanoparticle exposure. Toxicol Appl Pharmacol 226: 192–198

Wang B, Feng WY, Wang M, Shi JW, Zhang F, Ouyang H, Zhao YL, Chai ZF, Huang YY Xie YN, Wang HF, Wang J (2007) Transport of intranasally instilled fine Fe 203 particles into the brain: Micro-distribution, chemical states, and histopathological observation. Biol Trace Elem Res 118: 233–243

Wang J, Liu Y, Jiao F, Lao F, Li W, Gu Y, Li Y, Ge C, Zhou G, Li B, Zhao Y, Chai Z, Chen C (2008) Time-dependent translocation and potential impairment on central nervous system by intranasally instilled TiO2 nanoparticles. Toxicology 254: 82–90

Yu LE, Lanry Yung LY, Ong CN, Tan YL, Balasubramaniam KS, Hartono D, Shui G, Wenk MR, Ong WY (2007) Translocation and effects of gold nanoparticles after inhalation exposure in rats. Nanotoxicology 1: 235–242

Zhang QZ, Zha LS, Zhang Y, Jiang WM, Lu W, Shi ZQ, Jiang XG, Fu SK (2006) The brain targeting efficiency following nasally applied MPEG-PLA nanoparticles in rats. J Drug Target 14: 281–290

1.8 Genotoxicity of Nanoparticles

Roel Schins

Leibniz Research Institute for Environmental Medicine

Düsseldorf, Germany

Introduction

Current understanding about the mechanisms of genotoxicity of nanoparticles is predominantly based on genotoxicity investigations performed with the particulate carcinogen quartz as well as poorly soluble particles (PSP) of low toxicity such as carbon black, and titanium dioxide. Together with carcinogenicity studies in rats, these investigations have lead to the introduction of the concepts of primary versus secondary genotoxicity of inhalable particles. This particle genotoxicity paradigm is of relevance in view of the observations that the tumourigenicity of PSP in rat lungs after chronic high exposures is associated with overload and persistent inflammation (Greim et al. 2001; Knaapen et al. 2004; Schins and Knaapen 2007).

Secondary genotoxicity refers to genetic damage that results from the oxidative DNA attack by reactive oxygen and nitrogen species (ROS/RNS) and possible other mediators that are being generated during particle-elicited inflammation from recruited and activated phagocytes (macrophages, neutrophils). This secondary genotoxicity is considered to involve a threshold; its value is set to be determined by the exposure concentration that will trigger inflammation and overwhelm antioxidant and DNA damage repair capacities in the lung (Greim et al. 2001). Primary genotoxicity can be defined as the elucidation of genetic damage by particles in the absence of inflammation. This primary genotoxicity may be further subdivided into direct and indirect pathways. Direct primary genotoxicity implies a direct physical interaction between nanoparticles and the genomic DNA. Indirect primary genotoxicity e. g. may result from the formation of ROS by nanoparticle-activated target cells, or from depletion of intracellular antioxidants (Schins and Knaapen 2007; Stone et al. 2009; Donaldson et al. 2010).

Secondary Genotoxicity

Key studies which have lead to the above particle genotoxicity paradigm are those by Driscoll and co-workers (1997). They investigated *in vivo* mutagenicity, in rat lungs 15 months after a single intratracheal instillation of different doses of crystalline silica, carbon black or titanium dioxide. It was observed that mutagenesis (determined by HPRT assay (hypoxanthin-phosphoribosyl-transferase assay) in the lung epithelial cells isolated from the lungs of the treated animals) was associated with the level of persisting inflammation (characterized as the %

of neutrophils in bronchoalveolar lavage fluid (BAL)) (Driscoll et al. 1997). The role of particle-induced inflammation in driving genotoxicity in rat lungs since then has been supported by further investigations, e. g. in intratracheal instillation studies in rats with quartz particles of different surface modification (native DQ 12 quartz, and DQ 12 coated with polyvinylpyridine-N-oxide or aluminium lactate). The extent of neutrophilic inflammation measured in BAL from the rats was associated with the level of DNA strand breakage measured by the *in vivo* comet assay in the lung epithelial cells from these animals (Knaapen et al. 2002), as well as with the frequency of micronuclei in the epithelial cells (Albrecht et al. 2008).

The role of inflammatory phagocytes (macrophages, neutrophils) in eliciting DNA damage and mutagenesis in neighbouring target cells is further supported by numerous *in vitro* studies, that used co-culture models of inflammatory cells and various other cell types including lung epithelial cells (reviewed in Knaapen et al. 2006). Although these *in vitro* studies indicate that the ROS generated by phagocytes are responsible for the genotoxic effects in the target cells, the precise mechanism may be more complex. Exemplary, Johnston et al. (2000) observed contrasting *in vivo* mutagenesis for crystalline (fine) silica versus amorphous silica (primary particle size 12 nm) in rat inhalation study. Despite the fact that a similar level of lung inflammation was triggered in the rat lungs because of differently chosen exposure concentrations for both particle types, only the crystalline silica caused increased HPRT mutations. The authors proposed that the strong apoptotic effects observed for the amorphous silica as well as potential differences in proliferative effects may have led to the observed differences. A further aspect which needs to be taken into account in the Johnston et al. (2000) study is the much larger solubility, and hence lower biopersistence of the amorphous silica, when compared to the crystalline silica. Further investigations are required to determine the precise mechanisms that drive *in vivo* mutagenesis in the inflamed lung.

Is the Genotoxicity Paradigm of Inhalable Particles Applicable to Nanoparticles?

Several observations provide support for the applicability of the particle genotoxicity paradigm to nanoparticles, that is, to those that are poorly soluble:

- The inflammatory potency of various poorly soluble particles in the lung has been shown to be proportional to the surface area of these materials (Oberdörster et al. 2005; Stoeger et al. 2006; Monteiller et al. 2007). In the knowledge that nanoparticles have an increased surface area per unit mass when compared to larger sized particles of the same chemical composition, this suggests that quantitative differences may exist in the threshold values for secondary between fine and nanosize particles: For nanoparticles, inflammation mediated genotoxic effect may occur at lower (cumulative) mass dose. However, it should be noted that no *in vivo* genotoxicity study has been published so far, that has demonstrated such quantitative difference.

- There is an increasing number of *in vitro* studies where genotoxic and mutagenic effects of specific types of nanoparticles has been shown in various cell types (reviewed by Landsiedel et al. 2009; several further studies such as those discussed below). In a number of these studies it was observed that nanosize particles were more potent in triggering genotoxicity than larger sized particles of the same chemical composition. Since such *in vitro* studies are performed in the absence of inflammatory cells, this indicates that primary genotoxicity of specific nanoparticles cannot be ruled out per se. It should be noted that among the various genotoxicity assays that are available to screen for potential chemical carcinogens, only few have been used to considerable extent with nanoparticles, i. e. the Salmonella Reverse Mutation Assay, the Micronucleus test and the alkaline comet assay (Stone et al. 2009).

Potential Mechanisms of Primary Genotoxicity

On the basis of mechanistic *in vitro* genotoxicity studies with (nano)particles, several mechanisms of primary genotoxicity have been proposed.

Best described and discussed is a mechanism whereby the particles cause an (increased) formation of intracellular ROS. For instance, fine crystalline silica particles have been shown to cause oxidative DNA damage induction in human lung epithelial cells at high treatment concentrations, in the absence of their translocation into cell nuclei. This effect could be abolished by inhibition of the respiratory chain, which suggests that primary genotoxicity of quartz may occur, albeit in an indirect manner resulting from the oxidative attack of the genomic DNA by mitochondria-derived reactive oxygen species (ROS) (Li et al. 2007). More recently, Xu and Hei (2009) described *in vitro* mutagenic effects of TiO_2 nanoparticles and C 60, and showed that these effects occurred in an indirect manner via the formation of peroxynitrite.

Apart from ROS/RNS mediated mechanisms, genotoxicity may result from various other mechanisms. These are however mostly under debate and not (yet) demonstrated in a concise manner. Potential mechanisms include a direct interaction of nanoparticles with the genomic DNA or interactions with structural and functional components of the mitotic spindle apparatus. Such mechanisms have been described and discussed for the particulate carcinogens asbestos as well as crystalline silica, and recently shown for some specific nanoparticles, e. g. nanosilver (Arshani et al. 2009). Recent investigations with specific carbon nanotubes suggest that a potential role for the negative charge of these materials in causing genotoxic effects via the disturbance of membrane stability (Cveticanin et al. 2010). A further potential mechanism whereby nanoparticles may cause genotoxic effects is through the inhibition of various DNA repair machineries. Yet another potential mechanism for nanoparticle genotoxicity was recently provided in a recent *in vitro* study by Bhabra et al. (2009). In this study, it was revealed that chromium-cobalt alloy nanoparticles (~30 nm) can cause "bystander-type" DNA damaging effects in human fibroblasts across an *in vitro* cellular barrier model (BeWo placental cells) likely via an involve-

ment of ATP and intercellular signalling (GAP junctions/membrane channels). Notably, in the study by Bhabra et al. (2009) the observed indirect intercellular DNA damaging effect was also observed with larger particles of the same chemical composition, which suggests that the observed effect is not a nano-specific phenomenon.

Final Remarks

Although secondary genotoxicity is the most plausible mechanism for potential genotoxic effects of poorly soluble/insoluble nanoparticles, potential primary genotoxicity cannot be entirely ruled out on the basis of current available *in vitro* findings. However it is important to take into account the relevance of the applied *in vitro* concentration in relation to the target cell type and mechanism investigated. Moreover, many of these studies have employed only limited genotoxicity measurements in relation to mechanistic investigations rather than obeying to recommended genotoxicity testing approaches. Unlike recommendations in various genotoxicity guidelines, many investigations with nanoparticles have been performed without inclusion of appropriate (positive) controls and/or were not carried out in appropriate dose-response range and in relation to cytotoxicity evaluation (Landsiedel et al. 2009; Stone et al. 2009; Donaldson et al. 2010).

References

Albrecht C, Knaapen AM, Cakmak G, Van Schooten FJ, Borm PJA, Schins RPF (2009) Intratracheal instillation of quartz in the rat model: Implications for the role of neutrophils in the induction of genetic instability in the lung. J Phys Conf Ser 151: 012046

Asharani PV, Low Kah MG, Hande MP, Valiyaveetil S (2009) Cytotoxicity and genotoxicity of silver nanoparticles in human cells. ACS Nano 3: 279–290

Bhabra G, Sood A, Fisher B, Cartwright L, Saunders M, Evans WH, Surprenant A, Lopez-Castejon G, Mann S, Davis SA, Hails LA, Ingham E, Verkade P, Lane J, Heesom K, Newson R (2009) Case CP. Nanoparticles can cause DNA damage across a cellular barrier. Nat Nanotechnol 4: 876–83

Cveticanin J, Joksic G, Leskovac A, Petrovic S, Sobot AV, Neskovic O (2010) Using carbon nanotubes to induce micronuclei and double strand breaks of the DNA in human cells Nanotechnology. 21:015102

Driscoll KE, Deyo LC, Carter JM, Howard BW, Hassenbein DG, Bertram TA (1997) Effects of particle exposure and particle-elicited inflammatory cells on mutation in rat alveolar epithelial cells. Carcinogenesis 18: 423–30

Donaldson K, Poland C, Schins RPF (2010) Possible genotoxic mechanisms of nanoparticles: criteria for improved test strategies. Nanotoxicol 4: 414–420

Duffin R, Tran L, Brown D, Stone V, Donaldson K (2007). Proinflammogenic effects of low-toxicity and metal nanoparticles *in vivo* and *in vitro*: highlight-

ing the role of particle surface area and surface reactivity. Inhal Toxicol 19: 849–856

Greim H, Borm P, Schins R, Donaldson K, Driscoll K, Hartwig A, Kuempel E, Oberdörster G, Speit G (2001) Toxicity of fibers and particles. Report of the workshop held in Munich, Germany, 26–27 October 2000. Inhal Toxicol 13: 737–754

Johnston CJ, Driscoll KE, Finkelstein JN, Baggs R, O'Reilly MA, Carter J, Gelein R, Oberdörster G (2000) Pulmonary chemokine and mutagenic responses in rats after subchronic inhalation of amorphous and crystalline silica. Toxicol Sci 56: 405–413

Knaapen AM, Borm PJA, Albrecht C, Schins RPF (2004) Inhaled particles and lung cancer, part A. Mechanisms. Int J Cancer 109: 799–809

Knaapen AM, Albrecht C, Becker A, Höhr D, Winzer A, Haenen GR, Borm PJ, Schins RP (2002) DNA damage in lung epithelial cells isolated from rats exposed to quartz: role of surface reactivity and neutrophilic inflammation. Carcinogenesis 23: 1111–1120

Knaapen AM, Güngör N, Schins RPF, Borm PJA, Van Schooten FJ (2006) Neutrophils and respiratory tract DNA damage and mutagenesis: a review. Mutagenesis 21: 225–236

Landsiedel R, Kapp MD, Schulz M, Wiench K, Oesch F (2009) Genotoxicity investigations on nanomaterials: Methods, preparation and characterization of test material, potential artifacts and limitations – Many questions, some answers. Mutat Res 681: 241–258

Li H, Haberzettl P, Albrecht C, Höhr D, Knaapen AM, Borm PJA, Schins RPF (2007) Inhibition of the mitochondrial respiratory chain function abrogates quartz induced DNA damage in lung epithelial cells. Mutat Res (Fund Mol Mech Mutagen) 617: 46–57

Monteiller C, Tran L, MacNee W, Faux S, Jones A, Miller B, Donaldson K (2007) The pro-inflammatory effects of low-toxicity low-solubility particles, nanoparticles and fine particles, on epithelial cells *in vitro*: the role of surface area. Occup Environ Med 64: 609–15

Oberdörster G, Oberdörster E, Oberdörster J (2005) Nanotoxicology: an emerging discipline evolving from studies of ultrafine particles. Environ Health Perspect 113: 823–839

Schins RP, Knaapen AM (2007) Genotoxicity of poorly soluble particles. Inhal Toxicol 19: 189–198

Stoeger T, Reinhard C, Takenaka S, Schroeppel A, Karg E, Ritter B, Heyder J, Schulz H (2006) Instillation of six different ultrafine carbon particles indicates a surface-area threshold dose for acute lung inflammation in mice. Environ Health Perspect 114: 328–333

Stone V, Johnston H, Schins RPF (2009) Development of *in vitro* systems for Nanotoxicology – Methodological Considerations. Crit Rev Toxicol 39: 613–626

Xu A, Chai Y, Nohmi T, Hei TK (2009) Genotoxic responses to titanium dioxide nanoparticles and fullerene in gpt delta transgenic MEF cells. Part Fibre Toxicol 6: 3

1.9 Metal-based Nanoparticles with Special Emphasis to Copper

Andrea Hartwig

Karlsruhe Institute of Technology

Karlsruhe, Germany

Many metal compounds have been shown to possess toxic and/or carcinogenic properties. Among them are also essential trace elements such as iron or copper, which on conditions of disturbed homeostasis, can cause cellular overload. One aspect having frequently been discussed in recent years is the question as to whether metal-based nanoparticles exert higher toxicity when compared to water-soluble metal compounds or microscale particles of the same metal content. This is of particular interest, since metal-based nanoparticles have manifold applications. For example, magnetic iron oxide nanoparticles are suitable for various biomedical applications, such as magnetic resonance imaging (MRI) in medical diagnostics, and they are present in numerous consumer products such as cosmetics, textiles and inks.

Copper is one example for which a number of published data, mainly from *in vitro* systems, exist. It has been shown that copper-based nanoparticles exert higher cytotoxicity and stimulate more intense inflammatory responses than do copper chloride and microscale copper particles based on the same copper content (Cho et al. 2011, Midander et al. 2009; Karlsson et al. 2008; Karlsson et al. 2009). Also, copper oxide was more toxic in cultured human laryngeal epithelial cells as compared to amorphous silicon dioxide (SiO_2) and ferric oxide (Fe_2O_3) of the same particle size: this argues against a mere impact of particle number and surface area, going along with a decreased antioxidative defence. The toxicity of the oxides was detected as decreased cell viability, generation of reactive oxygen species and alteration of the activity of antioxidant enzymes and the level of oxidized glutathione (Fahmy and Cornier 2009). A possible explanation for the greater toxicity of copper oxide might be a higher extracellular solubilisation of this particle. However, measurements of copper release and comparative investigations with water-soluble copper compounds provided no conclusive evidence in this regard. Instead, the intracellular bioavailability of copper may be decisive. Most likely nanoparticles as well as microscale particles are taken up by endocytosis and become deposited in the lysosomes. Here, due to the acidic pH, they are dissolved, thereby delivering large amounts of copper ions in close proximity to the nucleus. Even though this mechanism is the same for all particles small enough to get phagocytosed, nanoparticles may get dissolved more readily to give rise to higher concentrations of copper ions released intracellularly within a given time frame. Nevertheless, this hypothesis has still to be confirmed experimentally. The induction of both inflammatory responses and of oxidative DNA damage have been described as cellular effects mediated by copper oxide nanoparticles (Ahamed et al. 2010, Cho et al. 2011, Fahmy and

Cormier 2009, Studer et al. 2010). These results raise the question of whether similar effects occur *in vivo* under realistic exposure conditions. In support of the idea that Cu-containing nanoparticles are particularly toxic, they have been shown to be most potent (in comparison with NiO and ZnO nanoparticles) with respect to toxicity and inflammatory response in bronchoalveolar lavage fluid (BALF) cells after intratracheal instillation in rat lungs. Moreover, it was shown that the role that soluble ions released from the metal oxide nanoparticles play in the inflammatory effects of these nanoparticles is variable and specific to the metal oxide (Cho et al. 2011).

Furthermore, when comparing toxic effects related to oxidative stress in subcellular test systems, cell culture systems and after *in vivo* instillation, copper exerted the most pronounced activities of all nanomaterials tested (three different particles of TiO_2, Ag-, Cu-, Au-, C- and animated polystyrene-particles). Also, significant correlations between subcellular, cellular and *in vivo* systems on a surface-based dose and response metric were observed (Rushton et al. 2010).

Taken together, present experimental evidence suggests that metal-based nanomaterials need to be assessed on a case-by-case basis, since toxicity does not appear to be restricted to particle effects, but is also due to the intracellular release of potentially toxic metal ions. It has to be further emphasized that *in vivo* experiments have so far been performed via intratracheal instillation, which resembles a bolus-type delivery. This enables the ranking of hazard, but is not sufficient for risk estimation after chronic low dose inhalative exposure.

References

Ahamed M, Siddiqui MA, Akhtar MJ, Ahmad I, Pant AB, Alhadlaq HA (2010) Genotoxic potential of copper oxide nanoparticles in human lung epithelial cells. Bioch Biophys Res Commun 396: 578–583

Cho W-S, Duffin R, Poland CA, Duschil A, Oostingh GJ, Macnee W, Bradley M, Megson IL, Donaldson K (2011) Differential pro-inflammatory effects of metal oxide nanoparticles and their soluble ions *in vitro* and *in vivo*; zinc and copper nanoparticles, but not their ions, recruit eosinophils to the lungs. Nanotoxicology DOI: 10 3109/17435390 2011.552810

Fahmy B, Cormier SA (2009) Copper oxide nanoparticles induce oxidative stress and cytotoxicity in airway epithelial cells. Toxicol In Vitro 23: 1365–1371

Karlsson HL, Cronholm P, Gustafsson J, Möller L (2008) Copper oxide nanoparticles are highly toxic: a comparison between metal oxide nanoparticles and carbon nanotubes. Chem Res Toxicol 21: 1726–1732

Karlsson HL, Gustafsson J, Cronholm P, Möller L (2009) Size-dependent toxicity of metal oxide particles – a comparison between nano- and micrometer size. Toxicol Lett 188: 112–118

Midander K, Cronholm P, Karlsson HL, Elinh K, Möller L, Leygraf C, Wallinder IO (2010) Surface characteristics, copper release, and toxicity of nano- and micrometer-sized copper and copper(II)oxide particles: a cross-disciplinary study. Small 5: 389–399

Rushton EK, Jiang J, Leonard SS, Eberly S, Castranova V, Biswas P, Elder A, Han X, Gelein R, Finkelstein J, Oberdöster G (2010) Concept of assessing nanoparticle hazards considering nanoparticle dosemetric and chemical/biological response metrics. J Toxicol Environ Health 73: 445–461

Studer AM, Limbach LK, Duc LV, Krumeich F, Athanassiou EK, Gerber LC, Moch H, Stark WJ (2010) Nanoparticle cytotoxicity depends on intracellular solubility: Comparison of stabilized copper metal and degradable copper oxide nanoparticles. Toxicol Lett 197: 169–174

1.10 Common Denominators of Carbon Nanotubes

Jürgen Pauluhn

Bayer HealthCare – Dept. Inhalation Toxicology

Wuppertal, Germany

Nanotoxicology, a sub-specialty of particle toxicology, addresses the toxicology of nanoparticles (particles < 100 nm diameter at least in one dimension) which have been claimed to have some toxic effects that are unusual and not seen with larger micron-sized particles. Manufactured nanomaterials have attracted a great deal of attention due to their unique structural, chemical, and physical characteristics. Along with the excitements over the prospects of nanotechnology, there have been increasing concerns regarding the risks inhalation exposure to nanomaterials may pose (Donaldson et al. 2006; Stern and McNeil 2008). The pulmonary toxicity associated with these materials is likely to be related to several interrelated variables, namely structural factors (shape, size), specific surface properties and surface area as well as the tendency to agglomerate into closely packed micron-sized structures of nanoparticles which increase the void-space volume of agglomerated particles. Thus, depending on the nanomaterials addressed, "particles" may consist of micron-sized assemblies of nanoparticles which may or may not be disintegrated in the lining fluids of the lung. However, to disintegrate such packed, low density isometric or nanotubular structures van der Waals binding forces favouring the attaching and self-assembly process must be overcome. It is subject to challenge whether the forces available in biological systems cause a post-deposition disintegration of such agglomerates. In fact this has already been shown for nanostructured titanium dioxide, which is highly aggregated and agglomerated. Disagglomeration by lung surfactant has not been found (Maier et al. 2006).

Isolated nanotubular structures have been generated when using high dispersion energies and specialized media to disrupt adhesions mediated through van der Waals forces. Especially for nanotubes additional mechanical properties may come into play, i. e., whether they are smooth and thin enough to bend and to self-assemble into tangled, coil-like structures or whether the more rigid nanotubes have diameters large enough to prevent such processes to occur. More rigid/thick structures would then favour nanofibre formation.

These considerations demonstrate that nanomaterials are extremely diverse. To consider the diameter (of non-agglomerated substructures) alone as the key unifying variable appears subject to challenge since other important properties are not necessarily mirrored by this parameter. Apart from size, surface properties, and low solubility their tendency to self-assemble into low density agglomerated structures appears to be amongst the most critical variables because much less particle mass is needed to exceed the volumetric overload limit for the inhibition of macrophage-mediated clearance. Consequently, even for micron-sized, low-density agglomerates of NPs, on a mass-based metric, their

biopersistence in the lung is likely to be markedly higher than that of micron-sized high-density agglomerated particles.

Any unifying, most appropriate dose metric of NPs conferring both pulmonary biopersistence and toxicity has not been demonstrated yet. Hence, it is timely to analyse and to consider as to which extent current testing paradigms need to be modified in order to appropriately identify and rank the claimed unique hazards of nanomaterials. Some nanoparticle types seem to be able to translocate from their site of initial deposition to distant, extrapulmonary sites. However, little appreciation has been given to link the mere presence of particles at specific sites with associated adverse effects, including their toxicological significance. From the perspective of inhalation toxicology, it appears to be yet unresolved whether nanotoxicology has revolutionized particle toxicology and rejuvenated it or whether many of the reported characteristics that may confer toxicity are related to experimental shortcomings and non-inhalational testing strategies (Maynard 2007). The toxicokinetics ("partico-kinetics"), the distribution and bio-persistence of inhaled nanoparticles within the body have received relatively little attention so far.

Particles, Mode of Dosing, and Response

Poorly soluble particle toxicology is typically characterized by a series of changes leading eventually to lung injury. The extent of injury depends on the dose and mode of administration. The occurrence of artificial findings is highly dependent on the level of the control of dosing and particle shape/size. The administration of particles to the lung by inhalation requires aerosolization by mechanical dispersion. Extensive sonication (with ensuing increase of leachates into the solute) or the use of unusual vehicle systems is not required by this method. Moreover, inhalation exposure resembles more closely the human exposure patterns and minimizes artefacts occurring following bolus administration protocols. Either methodology may elicit comparable changes; however, especially for highly surface active, agglomerated hydrophobic materials the results obtained by the instillation of inhomogeneous particle suspensions may be highly contingent upon the specific conditions chosen. These may be related to both the instillation of a large bolus of vehicle containing surface active substances and the instillation of structures commonly too large to gain access to the pulmonary region by physiological pathways. A destabilization of pulmonary surfactant may occur due to high doses of surface active particles or by direct alveolar C-fibre stimulation. Sustained surfactant dysfunction may lead to injury of the alveolar gas exchange region which, secondarily, facilitates the translocation of particles into the lymphatic system and/or the systemic circulation.

Inhalation/aspiration/instillation studies with Carbon Nanotubes (CNTs), which are carbon allotropes, have been reported (Warheit et al. 2004; Shvedova et al. 2005, 2008). As evidenced by Baron et al. (2008), the degree and kind of aggregation of CNTs depends on the flexibility/rigidity of their nanotubular structures. Thin hydrophobic Multiwalled Carbon Nanotubes (MWCNTs) were

administered to rats either by single inhalation exposure (micronized dry dust) or by intratracheal instillation (suspension of micronized MWCNTs in saline). Marked differences in retained particle sizes could be demonstrated approximately one week after exposure/instillation, despite the fact that essentially identical micronized MWCNTs were used. In rats exposed to MWCNTs by inhalation (single 6 hour exposure to 11 and 241 mg/m³ followed by a 3 months postexposure period) histopathology revealed an accumulation of enlarged and/or foamy macrophages with dark cytoplasmatic spots. At 241 mg/m³, the intensity of some findings (bronchiolo-alveolar hypercellularity, focal septal thickening and focally increased septal collagen) was minimally increased in some rats at the end of the 3 months postexposure period. Distinct time-dependent differences between recovery days 28 and 90 were not apparent. In contrast, granulomas, extensive inflammation and fibrosis have been described to occur following the instillation of liquid suspensions of large CNT aggregates (Shvedova et al. 2005). Concurrent with published evidence (Shvedova et al. 2008), the inhalation route is considered the most appropriate method to reveal the potential hazards of these materials.

These examples demonstrate that results obtained with straightforward instillation techniques must be viewed critically and cautiously in the absence of data revealing the shape and dose of the particles administered to the lung or retained within the lung. Extrapulmonary particle translocation cannot be considered as intrinsic particle property as long as the extent of acute deterioration and injury of the air-blood barrier is not appropriately addressed and characterized.

Extrapulmonary Translocation to Lung Associated Lymph Nodes

Common mechanisms associated with the clearance of particulate material in the lung include the mucociliary escalator and phagocytosis by alveolar macrophages. Additionally, the lymphatic system has long been recognized as an additional pathway for alveolar particles clearance. The intra- and extrapulmonary lymphatic structures carry, store, and, in many instances, process a fraction of the alveolar deposit, participating in this way in the lung defense against inhaled particles.

The mammalian lung has two major lymphatic plexi, one forming a network within the connective tissue of the visceral pleura the other is forming a peribronchovascular network within the connective tissue surrounding the airways, arteries, and veins (Lauweryns and Baert 1977). The two plexi anastomose at the level of terminal bronchioles with valves toward the pleural plexus while the peribronchovascular lymphatics (bronchial associated lymphoid tissue BALT) have valves oriented toward the lung hilus (Miller 1947). Accordingly, granulomas may be preferentially occurring at intrapleural and/or BALT locations.

Microgranulomas were observed in BALT following inhalation exposure and lung instillation at equivalent lung burdens of α-quartz. Differences in the dis-

tribution of granulomatous lesions were described (Henderson et al. 1995). The authors conclude that the instillation technique is not appropriate for studies of the deposition patterns and clearance rates of particles or for characterizing the site of induced toxicity within the respiratory tract. Accordingly, the clearance pathway favouring the formation of granuloma is not specific to the size of particles per se and its occurrence and extent need to be related to the degree of pulmonary inflammation (and procedure of dosing). Interestingly, an association of pulmonary inflammation and changes in BALT was also observed in rats exposed by inhalation to MWCNTs for 8 weeks (6 hours/day, 5 days/week) at 0.4, 1.5 and 6 mg/m³. Despite focal collagen depositions at the bronchioloalveolar junctions (Sirius red stained sections), granuloma did not occur following this extended inhalation exposure period (Pauluhn, 210a).

Several studies in rodents have demonstrated that particles deposited in the lung, whether nano- or micron-sized, can translocate to the pulmonary interstitium (Brain 1986; Ferin and Feldstein 1978; Henderson et al. 1995). From there pulmonary lymph flows to the hilar lymph nodes and hence to the tracheobronchial and tracheal or paratracheal lymph nodes may also apply for interstitionalized particles. The walls of the pulmonary blood capillaries seem to be much less permeable than the lymphatic walls, suggesting that the lymphatics have a far more significant role in the translocation of particles than do the blood capillaries. Several experimental studies have proved that particles can be transported through the alveolar epithelium and that cell disruption appears to be an important factor (Lauweryns and Baert 1977). Theoretical models addressing the dynamics of the compartmental pulmonary translocation of biopersistent particles during or after inhalation exposure are reviewed and discussed in detail elsewhere (Stöber et al. 1994; Stöber and McClellan 1997).

Ferin and Feldstein (1978) investigated the relationship between the amounts of micron-sized TiO_2 in the lung at post-inhalation exposure/post-instillation days 1 and 25 and in the hilar lymph nodes (LALNs) on day 25. It was noted that the absolute amount of particles cleared from the lung into the lymph nodes can be substantially enhanced (20-fold) when exceedingly high doses are instilled. Thus, with increased particle load the amount of particles escaping the clearance by alveolar macrophages increases and hence the lymph node content is elevated. A precipitous increase in the lymphatic clearance occurred at 0.7 mg TiO_2/lung suggesting that above this level the containment of the deposited particles within the alveoli is less effective. Such increase in translocation was apparent following high dose intratracheal instillations but was absent following inhalation.

The interstitial/lymphatic translocation of an initial particle lung load of 10 mg TiO_2/lung (day 1) was analyzed following acute instillation in rats. A similar cumulative lung burden of the insoluble micron-sized ferric oxide magnetite (Fe_3O_4; BET: 10.5 m²/g) was attained during a nose-only inhalation exposure period of 4 weeks (6 hours/day, 5 days/week; Fe_3O_4 contains ≈70 % Fe). This accumulated lung burden caused a ≈40-fold lower clearance of particles from the lung into the lymph nodes than TiO_2 dosed intratracheally. This finding supports the notion that the repeated inhalation exposure to cumulative fractional

doses over time cannot reliably be modeled by single high-dose, bolus instillation techniques.

Increased translocation into the interstitium and lymph nodes is clearly associated with increased lung burdens and reduced elimination of particles from lung tissue of rats exposed at concentrations high enough to cause sustained pulmonary inflammation. Tissue iron increased during the postexposure period in controls due to organ growth. Despite the marked iron accumulation in LALNs evidence of particle "break-through" into other extrapulmonary organs (testes, liver and spleen) was not apparent to any appreciable extent. These findings suggest that particle-overloading conditions, defined as > 1 mg particle mass per gram lung, are attained at exposure levels exceeding 20 mg/m³. The elimination half-time for alveolar clearance in the non-overloading state (rats) has been reported to be in the range of 50–65 days (Donaldson et al. 2008; Stöber and McClellan 1997; Yeh et al. 1996). Collectively, an association of increased particle translocation into LALNs and pulmonary inflammation could be demonstrated. Concurrent with the other poorly soluble particles, pulmonary inflammation was verified by a dose-dependent increased influx of neutrophilic granulocytes in BAL.

Thus, intratracheal instillation techniques require not only a thoughtful selection of dose and vehicle system, but also a tight control of the dosing regime in regard to the size and shape of instilled particles. The non-uniformity of intratracheal bolus instillations may result in heavy, localized deposits of large particles with ensuing localized inflammatory responses and increased permeability of the epithelium. Accordingly, the occurrence of unexpected findings following instillation techniques should be accompanied by data not only categorizing the degree of pulmonary inflammation but also elucidating the kind, fate, and homogeneity of particles within the lung.

Extrapulmonary Translocation – Systemic Bioavailability

The empirical verification of the translocation of inhaled nanoparticles into the systemic circulation is complicated by many experimental factors (for details see Donaldson et al. 2006; Oberdörster et al. 2002; Stern and McNeil 2008) and is also dependent on the localized deterioration of the air-blood barrier as intimated above. The available evidence supports the view that systemic translocation does not occur to any appreciable extent at non-inflammatory exposure levels (Wiebert et al. 2006; Geiser et al. 2008; Möller et al. 2008). In general, hepatic Kupfer cells are thought to play a major role in clearing the particulate materials from the systemic circulation. Liver endothelial cells have also been shown to be important scavengers for circulating macromolecular waste products, including nanoparticulates (Moghimi et al. 1991; Ogawara et al. 1999). Sinusoids in the liver lobule consist of highly fenestrated endothelial cells and a basal lamina is lacking leading to an open connection between the sinusoidal lumen and the space of Disse with direct excess to the hepatocytes. Nanosized (50 nm) particles may be able to easily access hepatocytes directly, but 500 nm

sized particles may not (Ogawara et al. 1999). The amount of particles distributed to the liver, and to some extent also to the spleen and lung (after intravenous injection) has been shown to be particle-size dependent. This might be due to the difference in the capacity of the liver for the uptake of such microspheres. Overall, from a toxicological perspective, this published evidence suggests that the liver is the organ of choice to monitor empirically any "break-through" of particles from the alveolar-interstitial-lymphatic compartments into the systemic circulation.

Consistent with this hypothesis, the time-dependence of particle translocation (measured by the analytical determination of metallic tracers rather than the particle per se) into the liver tissue was analyzed in rats exposed to nano-sized MWCNTs. In contrast to micron-sized TiO_2 or Fe_3O_4 particles, even at the high exposure concentration of 241 mg MWCNTs/m³ (nose only exposure of rats for 1×6 h), a translocation of MWCNTs into the draining LALNs, evidenced by the determination of the MWCNT-associated tracer metal cobalt, did not occur during a postexposure period of 3 months. Minimally increased levels of tracer metal were found in the liver shortly after exposure but not after the 3 months postexposure period. This finding appears consistent with the acute inflammatory response observed at this time point. Determinations in other highly perfused organs were unobtrusive, except lung tissue which showed a concentration-dependent increase of the tracer metal with clearance over time. As shown in subacute inhalation studies in rats with nanosized isometric AlOOH, increased aluminum in extrapulmonary organs, except LALNs, could not be revealed. The compartmentalization of two different nanosized AlOOH particles (10 nm and 40 nm) with mass median aerodynamic diameters (MMADs) of 1.7 and 0.6 µm (actual exposure concentrations and GSD's identical) was more dependent on the aerodynamic diameter of agglomerated, micron-sized particles than on the geometric size of the primary particles. Theoretically, due to the void space in agglomerated particles, equal-mass 10 nm and 40 nm particles should have reciprocally increased displacement volumes (see below). Nonetheless, based on actual exposure concentrations, the time-course and magnitude of the associated pulmonary inflammatory responses were essentially similar, despite a marked difference in particle surface areas (for details see Pauluhn 2009 a, b). Moreover, at identical particle exposure concentrations, lung burdens were substantially higher when the MMAD was ≈0.6 µm as compared to ≈1.7 µm. Therefore, if technically feasible, inhalation studies with an MMAD less than 1 µm should be targeted to maximize the retained pulmonary dose. From these studies it is concluded that the pulmonary toxicity of nanosized, agglomerated AlOOH particles appears to be determined by the size of agglomerated particles while their fate is more dependent on the primary particle size. In regard to the toxicokinetics, the outcome is highly contingent upon the total lung burden and especially whether overloading and non-overloading conditions had been attained. These conclusions are coherent with published evidence (ILSI 2000; Pauluhn 2009 a, b, 2010 a, b).

To summarize, the translocation of NPs to extrapulmonary organs has been shown in research-scale studies (Geiser et al. 2005). Signal-mediated transport

via pores and non-receptor mediated uptake through "adhesive interactions" has been hypothesized (Rimai et al. 2000). Especially when focusing on the translocation of nanoparticles from pulmonary to extrapulmonary tissues, unexpected dispositional findings may incur either acute injury-related disturbances of the air-blood barrier system or related to particle-specific, adsorptive properties. Thus, systemic bioavailability appears to be primarily driven by pulmonary inflammation rather than inherent particle properties. These conclusions call for a balanced empirical evaluation of toxicokinetics and toxicodynamic factors. Needles to say, particles clearance half-times at non-overloading conditions are in the range of t 1/2 ≈50–60 days (Pauluhn 2009a, b, 2010 a, b). Hence, postexposure periods must be long enough to allow for normal or abnormal clearance processes to occur and to be manifest. Therefore, postexposure periods should not be shorter than one elimination t 1/2.

Particle-Induced Acute Lung Injury and Definition of Dose

The major objective of hazard identification is to reveal the specific hazards associated with inhalation exposure to NPs. Similarly, an additional objective is to rank the relative toxic potencies of different materials evaluated under standardized, highly controlled testing conditions. However, this requires a basic understanding of mechanisms involved with lung injury as well as a unifying dose metric. Accordingly, the choice of an appropriate measure of dose must be defined by the nature of the pathogenesis process (i. e., defined according to the mechanism of action) for the effect under consideration (Jarabek 1995). When accounting for the particle dose in the pool of cells accessible to bronchoalveolar lavage (BAL), it appears that the dose per BAL-cell is a better indicator of dose than lung tissue levels.

It is generally conceived that the conceptually better alternative to particle mass or number as a measure of dose would be the surface area/activity. Surface area rather than mass accounts for the fact that biopersistent particles can interact only by contact of their surface, determining an effective dose rate by a catalytic surface reaction rate that accumulates to an effective dose with increasing residence time in the target tissue (Stöber and McClellan 1997). However, a finite proportion of soluble fractions of particles may dissolve on contact with the lung and so do not contribute to "surface area dose" (apart from the fact of surface area-dependent facilitated dissolution). Along with these concerns and the risks exposure to nanomaterials may pose to workers, issues regarding the most appropriate unifying metric of dose are still unresolved (Maynard 2007). However, from an experimental perspective as well as the robustness of inhalation exposure data, mass-based metrologies are considered to be most expedient and least dependent on specialized equipment. Likewise, organ burdens commonly use the mass as primary metric. Therefore, exposure data using the same metric should be given preference for dosimetric comparisons.

It appears to be important to appreciate that the acute inflammatory pulmonary response at the site of initial deposition may initially be dependent on

the surface area/activity of the deposited particles which has already been substantiated by the analysis of respiratory patterns with the non-irritant, surface active, amorphous silica dry powder aerosol. On the other hand, concurrent with published evidence (Morrow 1988; Stöber and McClellan 1997), the retention-related sustained inflammatory response is likely to be more dependent on the particle-volume rather than surface area (Pauluhn 2009 a, b, 2010 a, b). In fact, this issue is complicated further as the surface area per se is not a unique characteristic of a particle. For instance, the specific surface area (BET, N_2 used as adsorbent) of AlOOH 40 nm and AlOOH 10 nm after drying and degassing (100 °C at 0.1 mbar for 16 hrs) was 46.3 and 159 m^2/g, respectively, while under other conditions of measurement (550 °C for 3 hrs) the BETs reported were 100 and 182 m^2/g, respectively. As long as the isotherms, actually available binding sites of key proteins or peptides and competitive factors present in the alveolar lining fluids are yet ill-defined, surface area per se may be an incomplete reflection of the potentially biologically active critical surface area. Hence, the biologically active surface area may vary from one circumstance to another.

Another often unique feature of nanoparticles is the low density of NP-agglomerates. Micron-sized agglomerated arrangements of closely packed nanoparticles increase the void-space volume and must be added to the composite volume of phagocytized particles. Consequently, much less particle mass is needed to exceed the volumetric overload limit for the inhibition of macrophage-mediated clearance, which is estimated to start at ≈60 μm^3 per alveolar macrophage (Morrow 1988). Loaded alveolar macrophages may be considered immobile at 10-times or thereabouts of volumetric loading. While the specific density of primary particles is commonly well defined, equivalent data for agglomerated particles are less defined. Accordingly, for lower than unit density agglomerated particles that are not disintegrated upon deposition, the geometric diameter (dgeo) may become larger than the aerodynamic diameter (dae = dgeo × agglomerated density1/2) and both the particle volume ($v = dgeo\ 3 \times \pi/6$) and particle surface area ($sa = dgeo\ 2 \times \pi$) increase in proportion to the geometric diameter. Based on Morrow's hypothesis of the volumetric overload of alveolar macrophages, the particle volume rather than surface area appears to be the most critical metric. Hence, agglomerated nanoparticles present in micron-sized form may cause a volumetric overload of alveolar macrophages at lower exposure doses as compared to their micron-sized crystalline counterparts.

The loose structures of thin-walled, tangled MWCNTs can be readily characterized in terms of their aerodynamic behaviour (daer) by cascade impactor analyses. Otherwise, their tangled, coiled structures of self-assembled nanotubes are somewhat difficult to describe. A quite similar type of self-assembly process has been demonstrated for Single Walled CNTs (Baron et al. 2008). The coiled assembly of thin-walled nanotubes appears to be conserved in alveolar macrophages. Accordingly, for MWCNTs smooth and thin enough to bend and self-assemble, the metric of choice appears to be the mass-based aerodynamic properties and the volume of coiled particle-like structures and not necessarily the number concentration and length distribution of nanotubes (after vigorous

dispersion in media with highly specialized properties to maximize the disaggregating process. Harmonized methodologies to determine the bulk density which, as a matter of fact, reflects the true agglomerate density by well-defined pyknometric procedures are urgently needed.

The impact of the residual catalyst cobalt (Co) on pulmonary toxicity was examined in identical MWCNTs, one of them was depleted of Co by washing with diluted hydrochloric acid followed by extensive rinsing with water and drying at 200 °C. By using this procedure surface bound (or non-bound) Co was removed from the MWCNTs without affecting the matrix-bound catalyst. The magnitude and time-course of the pulmonary inflammatory response (influx of PMNs) was indistinguishable. Hence, in regard to the sustained pulmonary response to inhaled and retained MWCNTs, the structure per se appears to be more important than surface activity or content of redox-active transitional metals.

Collectively, existing evidence from different types of isometric particles and self-assembling MWCNT structures appears to support a conclusion that even within one single class of nanomaterials very diverse material properties exist leading eventually to different biological responses. Particle-like structures of tangled, thin CNTs need to be distinguished from the more fibre-like thick-walled, rigid nanofibers. With regard to retention related long-term effects, the particle displacement volume and associated protracted clearance appear to be important variables.

Hazard Identification of Nanoparticles

With few exceptions, most data generated so far in context with nanostructured, engineered materials utilized single intratracheal or pharyngeal instillation techniques and high doses that raise the question about physiological relevance. Information on biopersistence and disposition following inhalation exposure is scarce. Recent reviews have emphasized that the lack of definitive inhalation studies that would avoid the potential for artifactual effects of large mats and agglomerates formed by CNTs during instillation procedures (Donaldson et al. 2006; Shvedova et al. 2008).

The stable, homogeneous, and day-by-day reproducible aerosolization of nanoparticles in general and CNTs in particular for inhalation studies is immensely difficult and experimentally demanding. MWCNT have a strong tendency to bundle together and to form tangled, coiled assemblies. Due to the limited dustiness of bulk material, micronization is therefore required to make inhalation testing of MWCNTs possible.

For the MWCNT inhalation studies presented in this paper, the dustiness of the bulk material was increased by careful micronization using a Centrifugal Ball Mill S 100. Grinding jars contained agate balls (at low concentrations: 2 of 30 mm balls, at higher concentration: 50 of 10 mm balls). The micronization lasted 20 min at 500 revolutions/min. The characterization of the test specimens before and after micronization demonstrated that the physical characteristic of

the bulk material was not affected to any significant extent, with the exception of the mean length of tubes (after dispersion in specialized media). Scanning electron microscopy (SEM) of the bulk and micronized MWCNTs did not reveal isolated tubes or granular break-off products in exposure atmospheres. The length of the tubes was determined after dispersion in ethanol using ultrasonic treatment (rt, 5 min, 35 kHz) followed by analysis with transmission electron microscopy (TEM) using AnalySIS pro version 3.2 to estimate length of tubes. The mean tube length in the bulk and micronized material was 1024 ± 628 nm and 309 ± 334 nm, respectively. Similarly, the d 50 (median of the particle size distribution) of the bulk and micronized material (median volume diameter measure by laser diffraction, MS 2000 Hydro S) was 500 nm and 5 nm, respectively. BETs of micronized, nondispersed and dispersed MWCNTs were 257 and 259 m^2/g, respectively. The bulk density of the bulk and micronized material was 0.156 and 0.109 mg/cm^3, respectively. The ζ-potential (Malvern Zetasizer 3000HSA) measured over a pH-range from 1–11 was not affected by micronization. Cobalt concentrations were identical in the bulk and micronized material which substantiate that no enrichment of Co-rich granular brake-off material occurred. Following dispersion into inhalation chambers, the cobalt concentrations were minimally reduced in filter samples from inhalation chambers (from 0.46 % to 0.38 %) relative to the bulk product. The catalyst (Co) appears to be matrix rather than surface associated as demonstrated by XPS (X-ray Electron Spectroscopy) (Pauluhn 2010 a).

As already highlighted by Warheit et al. (2008), the most important issue in nanotoxicology is to adequately characterize the nanomaterials prior to toxicological experimentation, after the dispersion in air and what type of structure is eventually retained in the lung. As detailed above, any additional (mechanical) procedure being applied to make such materials amenable to testing in inhalation bioassays must be utilized with due caution in order to maintain potentially critical factors of the test material, such as shape, surface properties, and state of agglomeration. This needs to be accompanied by extensive analytical verification to demonstrate that an analytically verified critical structural feature rather than an ill-characterized artefact is causative for the effects observed. CNT-related toxicity may be linked to both aerodynamic and geometric properties which require complementary methods for meaningful determinations. Likewise, it must be demonstrated that procedure-specific, artifactual structural entities or properties were not produced. In this context it is important to recall that carbon nanotubes may differ appreciably from one manufacturer/production process to another. Specific surface fictionalizations may overrule structural properties. Hence, the procedures used to convert the nanostructure into any 'testable' form may affect the outcome of toxicological testing as well. To exclude potential artefacts to occur, costly and elaborate analytical verifications have to be applied.

Much research has focused on the attempt to create homogeneous dispersions of nanoparticles (NPs) and CNTs in various carrier systems (Donaldson et al. 2006). Their unique properties NPs may cause interferences especially in static assay systems (Stern and McNeil 2008). This interference could also lead

to the adsorption of substrates present in the lining fluids of the lung, especially when instilled as one single high-dose bolus. Undoubtedly, although elaborate and technically demanding, the advantage of inhalation studies is that artifactual carrier systems are not required and that the concentration and physical properties of inhaled particles can readily be analytically characterized and controlled at breathing zone level of exposed animals using established procedures. Some experimental examples are shown below.

Micron-sized crystalline quartz (DQ 12; BET: 3.2 m^2/g), ultrafine carbon black (Printex® 90, CB; BET: ≈300 m^2/g), and MWCNTs (BET: 253 m^2/g) were compared at similar concentrations following a single 6-hour nose-only inhalation exposure. Rats of the control were nose-only exposed to air only. Pulmonary responses were examined by bronchoalveolar lavage (BAL) on postexposure days 7, 28, and 90. For intraluminal changes the most accurate quantitation of pulmonary inflammation can be achieved by this method (Donaldson et al. 2006). The precise composition of exudate probed by BAL depends on the cause of the injury at the site at which it occurs. However, the possibility of sampling errors cannot be excluded due to the greater adherence of highly activated cells and more focal lesions may not necessarily be adequately accessed by the lavage procedure applied.

Inter alia, the yield of sampled cells can be affected by the age of rats, number of lavage cycles, and whether excised lungs, whole lungs in situ or parts of lungs are lavaged. The average number of cells recovered per gram of lung from rats using 12 washes was reported to be in the range of $4.8–5.7 \times 10^6$ cells/g lung (Brain and Frank 1968 a, b). The methodological procedures used in this study, i. e., using two lavage cycles each with a single volume of 5 ml/rat and cycle (20 ml/kg), provided a yield of $5.1 \pm 1.4 \times 10^6$ cells/g lung (air control, male Wistar rats). This demonstrates that a representative population of cells and the maximum feasible number of cells was collected by the lavage method used. It has been demonstrated that even twelve saline washings appeared to have a negligible effect on the histologic appearance of the lung as viewed with the light microscope and that it was nearly impossible to distinguish between washed and unwashed lungs (Brain and Frank 1968 a, b). The findings presented by Pauluhn 2009 a, b also challenge the current recommendation for the need of absolute polymorphonuclear leukocyte cell (PMN) counts from BAL analyses (which means relative cytodifferentiation multiplied by total BAL cell counts). Pauluhn has shown that, depending on the degree of activation of BAL cells, approximately 20 % of the total cells could be retrieved by lavage. Taking into account the interlaboratory variability of lavage procedures, a similar value (≈14 %) was reported by Rehn et al. (1992). This also means that total lung particle burdens may not be equated to interstitialized particle burdens. Pauluhn's data appear to support the notion that lung burdens necessarily are mirroring the non-lavaged cellular compartment and not the parenchymal compartment. Suffice it to say, especially in rats (Brown et al. 2005), this sustained sequestration of overloaded/activated alveolar macrophages will eventually deteriorate the barrier function of the alveolar structures with associated long-term inflammatory response.

Distinctive morphological features in the development of fibroblastic/myofibroblastic foci at subepithelial mesenchymal levels may also occur subsequent to pulmonary injury and inflammation. These areas of active fibrogenesis play a crucial role in the progressive pulmonary fibrosis. Such changes require histopathology for analysis. Accordingly, either assay could be the more sensitive under a given circumstance. Thus, the two approaches are complementary and are used to best advantage in concert. However, due to its simplicity and expedience, the primary focus in this comparative study was on conventional endpoints in BAL that integrate the inflammatory response elicited by particles deposited in the pulmonary region (Driscoll et al. 1991; Pauluhn and Rosenbruch 2003; Porter et al. 2004; Warheit et al. 1991; 2005).

Selected pro-inflammatory cytokines and chemokines were compared with integrating inflammatory endpoints. Time-profiles and particle-specific responses differed appreciably between pro-inflammatory and inflammatory endpoints. Therefore, although invaluable for mechanistic studies, pro-inflammatory factors need to be interpreted with caution, especially in the absence of back-up methodologies demonstrating the toxicological significance of changes. Furthermore, this comparison demonstrates that a postexposure period limited to 1 month only does not clearly reveal the self-perpetuating and self-amplifying type of pulmonary inflammation following DQ 12 exposure.

The information provided following acute inhalation exposure/intratracheal instillation appears to provide little, if any, relevance to occupational exposure. Poorly soluble particles may elicit a surface area-dependent destabilization of the air-blood barrier with ensuing inflammatory response. However, with these types of poorly soluble materials, acute responses at high concentrations similar to those emerging from acute inhalation/instillation studies are unlikely to occur in the workplace environment. Due to the initial overloading-dependent inhibition of clearance, the analysis of time-course-related changes is an interesting academic exercise, an elaborate but mandatory exercise. However, the assessment of workplace hazards appears to require regimens similar to those present at the workplace. This can only be accomplished by repeated inhalation exposure studies (Pauluhn 2010 a, b).

Neutrophils in BAL have been shown to be amongst the most sensitive endpoints to probe for isometric particle- and CNT-induced changes. Based on this endpoint the thin-walled tangled MWCNTs examined followed the anticipated paradigm of low-density particles. After 2-months of inhalation exposure (6 hours/day, 5-times/week) rats elaborated statistically significant increases in BAL-PMN counts at 0.4 mg/m³ and above while the exposure to 0.1 mg/m³ did not cause an increased recruitment of cells or neutrophils. Likewise, histopathology was unobtrusive at this exposure level. So far, mesothelial changes have been shown to occur only using rigid CNTs and bolus pharyngeal aspiration techniques.

Conclusions

The comparison of inhalation studies with micron-sized isometric particles, agglomerated isometric nanoparticles, and nanostructured MWCNTs demonstrate similar basic principles, viz. that the relative biopersistence and inflammogenicity are the driving factors of pulmonary toxicity. Due to the cumulative nature of dose and effects toxicology tests must be devised to clearly distinguish these two aspects. This means, a highly biopersistent low-toxic CNT may lead to higher lung burdens (and associated inflammation) as compared to highly-toxic nanostructures with negligible biopersistence. Moreover, it has to be appreciated that most of the particle-related oxidative burden originates from the increased recruitment of inflammatory, activated PMNs rather than particle surfaces per se. As exemplified for high surface area MWCNTs, some types of pulmonary toxicity may already occur shortly after single inhalation exposures. Therefore, the design of toxicity studies must envisage two modes of actions, namely the acute toxicity due to the putative adsorptive depletion of essential homeostatic factors involved in surfactant homeostasis and secondary responses. Any change of these factors may increase extravascular leakage, associated with a dysfunction of the air-blood barrier. On the other hand, volumetric particle overload may trigger retention-related responses which then affect the biopersistence and long-term sequelae. A state-of-the-art test design should clearly disentangle these two mechanisms by postexposure periods of adequate duration which means at least 1–2 multiples of the clearance half-times (t 1/2 ≈60 days) at non-overload and mild-overload conditions. Empirical data appear to suggest that new testing paradigms need not be invented for the evaluation and assessment of inhalation toxicity of nanoparticles. Repeated inhalation studies still appear to be incumbent on inhalation toxicologists to demonstrate safe exposure levels. However, new methods may be required to better characterize the bulk density and particle volume of aggregated or self-assembled materials with less than unity density.

In regard to CNTs multiple variables may account for toxicity. This toxicity is clearly cumulative dose, structure (fibrillar, fibre-like, coiled and tangled assemblies), and/or surface functionalization related (the latter may have significant impacts on biopersistence). Impurities of transitional or rare earth metals, whether they are biosoluble/leachable from the CNT matrix, may be important modulating factors. So far, the structural complexity as well as the lack of mechanism-of-toxicity based characterization methods can neither define critical structural entities to define toxicity nor have toxicity test procedures been able to show robust common denominators of toxicity from different materials. This issue appears to be complicated further as the CNT structure per se has to be altered to make the structure dispersible in air or liquids. This also means, new structural entities can possibly be generated by the specific procedure applied. These considerations demonstrate that common denominators of risk cannot be defined yet.

References

Baron PA, Deye GJ, Chen BT, Schwegler-Berry DE, Shvedova AA, Castranova V (2008) Aerosolization of single-walled carbon nanotubes for an inhalation study. Inhal Toxicol 20: 751–760.

Brain JD (1986) Toxicological aspects of alterations of pulmonary macrophage function. Ann Rev Pharmacol Toxicol 26: 547–565

Brain JD, Frank NR (1968a) The relation of age to the numbers of lung free cells, lung weight, and body weight in rats. J Gerontol 23: 58–62

Brain JD, Frank NR (1968b) Recovery of free cells from rat lungs by repeated washings. J Appl Physiol 25: 63–69

Brown JS, Wilson WE, Grant LD (2005) Dosimetric comparisons of particle deposition and retention in rats and humans. Inhal Toxicol 17: 355–385.

Donaldson K, Aitken R, Tran L, Stone V, Duffin R, Forrest G, Alexander A (2006) Carbon nanotubes: a review of their properties in relation to pulmonary toxicity and workplace safety. Toxicol Sci 92: 5–22

Driscoll KE, Lindenschmidt RC, Maurer JK, Perkins L, Perkins M, Higgins J (1991) Pulmonary response to inhaled silica or titanium dioxide. Toxicol Appl Pharmacol 111: 201–210

Ferin J, Feldstein ML (1978) Pulmonary clearance and hilar lymph node content in rats after particle exposure. Environ Res 16: 342–352

Geiser M, Rothen-Rutishauser B, Kapp N, Schürch S, Kreyling W, Schulz H, Semmler M, Im Hof V, Heyder J, Gehr P (2005) Ultrafine particles cross cellular membranes by nonphagocytic mechanisms in lungs and in cultured cells. Environ Health Perspect 113: 1555–1560.

Geiser M, Casaulta M, Kupferschmid B, Schulz H, Semmler-Behnke M, Kreyling, W (2008) The role of macrophages in the clearance of inhaled ultrafine titanium dioxide particles. Am J Respir Cell Mol Biol 38: 371–376.

Henderson RF, Driscoll KE, Harkema JR, Lindenschmidt RC, Chang IY, Maples KR, Barr EB (1995) A comparison of the inflammatory response of the lung to inhaled versus instilled particles in F 344 rats. Fundam Appl Toxicol 24: 183–197

ILSI (International Life Science Institute) (2000) The relevance of the rat lung response to particle overload for human risk assessment: A workshop consensus Report – ILSI Risk Science Institute Workshop Participants. Inhal Toxicol 12: 1–17

Jarabek AM (1995) Consideration of temporal toxicity challenges current default assumptions. Inhal Toxicol 7: 927–946

Lauweryns JM, Baert JH (1977) Alveolar clearance and the role of the pulmonary lymphatics. Am Rev Respir Dis 115: 625–683

Maier M, Hannebauer B, Holldorff H, Albers P (2006) Does lung surfactant promote disaggregation of nanostructured titanium dioxide? J Occup Environ Med 48: 1314–1320

Maynard AD (2007) Nanotechnology: The next big thing, or much ado about nothing? Ann Occup Hyg 51: 1–12

Miller WS (1947) Lymphatics. In: Miller WS (2nd ed) The Lung , Ed. Thomas CC, Springfield, IL, USA: 89–118

Moghimi SM, Porter CJH, Muir IS, Illum L, Davis SS (1991) Non-phagocytic uptake of intravenously injected microspheres in the rat spleen. Influence of particle size and hydrophilic coating. Biochem Biophys Res Commun 177: 861–866

Möller W, Felten K, Sommerer K, Scheuch G, Meyer G, Meyer P, Häussinger K, Kreyling WG (2008) Deposition, retention, and translocation of ultrafine particles from the central airways and lung periphery. Am J Respir Crit Care Med 177: 426–432.

Morrow PE (1988) Possible mechanisms to explain dust overloading of the lungs. Fundam Appl Toxicol 10: 369–84

Oberdörster G (2002) Toxicology of ultrafine particles: *In vivo* studies. Philos Trans R Soc Lond A 358: 2719–2740

Ogawara K-I, Yoshida M, Higaki K, Kimura T, Shiraishi K, Nishikawa M, Takakura, Y, Hashida M (1999) Hepatic uptake of polystyrene microspheres in rats: Effect of particle size on intrahepatic distribution. J Controlled Release 59: 15–22

Pauluhn J, Rosenbruch M (2003) Inhalation toxicity of propineb. Part I: results of subacute inhalation exposure studies in rats. Inhal Toxicol 5: 411–434

Pauluhn J (2009a) Pulmonary toxicity and fate of agglomerated 10 nm and 40 nm aluminum oxyhydroxides (AlOOH) following 4-week inhalation exposure of rats: toxic effects are determined by agglomerated, not primary particle size. Toxicol Sci 109: 152–167

Pauluhn J (2009b) Retrospective analysis of 4-week inhalation studies in rats with focus on fate and pulmonary toxicity of two nanosized aluminum oxyhydroxides (boehmite) and pigment-grade iron oxide (magnetite): The key metric of dose is particle mass and not particle surface area. Toxicology 259: 140–148

Pauluhn, J. (2010a). Subchronic 13-week Inahlation Exposure of Rats to Multiwalled Carbon Nanotubes: Toxic Effects at determined by Density of Agglomerate Structure, not fibrillar Structures. Toxicological Sciences 113: 226–242.

Pauluhn, J. (2010 b). Multi-walled Carbon Nanotubes (Baytubes®): Approach for Derivation of Occupational Exposure L Regulatory Pharmacology and Toxicology 57: 78–89.

Porter DW, Hubbs AF, Mercer R, Robinson VA, Ramsey D, McLaurin J, Khan A, Battelli L, Brumbaugh K, Teass A, Castranova V (2004) Progression of lung inflammation and damage in rats after cessation of silica inhalation. Toxicol Sci 79: 370–380

Rehn B, Bruch J, ZouT, Hobusch G (1992) Recovery of rat alveolar macrophages by bronchoalveolar lavage under normal and activated conditions. Environ Health Persp 97: 11–16

Rimai DS, Quesnel DJ, Busnaia AA (2000) The adhesion of dry particles in the nanometer to micrometer range. Colloids Surf A Physicochem Eng Aspects 165: 3–10

Shvedova AA, Kisin ER, Mercer R, Murray AR, Johnson VJ, Potapovich AI, Tyurina YY, Gorelik O, Arepalli S, Schwegler-Berry D, Hubbs AF, Antonini J, Evans DE, Ku BK, Ramsey D, Maynard A, Kagan VE, Castranova V, Baron P (2005) Unusual inflammatory and fibrogenic pulmonary responses to single-walled carbon nanotubes in mice. Am J Physiol Lung Cell Mol Physiol 289: L 698–708

Shvedova AA, Kisin E, Murray AR, Johnson VJ, Gorelik O, Arepalli S, Hubbs AF, Mercer RR, Keohavong P, Sussman N, Jin J, Yin J, Stone S, Chen BT, Deye G, Maynard A, Castranova V, Baron PA, Kagan VE (2008) Inhalation vs. aspiration of single-walled carbon nanotubes in C 57BL/6 mice: inflammation, fibrosis, oxidative stress, and mutagenesis. Am J Physiol Lung Cell Mol Physiol 295: L 552–565

Stern ST, McNeil SE (2008) Nanotechnology safety concerns revisited. Toxicol Sci 101: 4–21

Stöber W, Morrow PE, Koch W, Morawietz G (1994) Alveolar clearance and retention of inhaled insoluble particles in rats simulated by a model inferring macrophage particle load distributions. J Aerosol Sci 25: 975–1002

Stöber W, McClellan RO (1997) Pulmonary retention and clearance of inhaled biopersistent aerosol particles: Data-reducing interpolation models and models of physiologically based systems. A review of recent progress and remaining problems. Crit Rev Toxicol 27: 539–598

Warheit DB, Carakostas MC, Hartsky MA, Hansen JF (1991) Development of a short-term inhalation bioassay to assess pulmonary toxicity of inhaled particles: comparisons of pulmonary responses to carbonyl iron and silica. Toxicol Appl Pharmacol 107: 350–368

Warheit DB, Laurence BR, Reed KL, Roach DH, Reynolds GA, Webb TR (2004) Comparative pulmonary toxicity assessment of single-wall carbon nanotubes in rats. Toxicol Sci 77: 117–125

Warheit DB, Brock WJ, Lee KP, Webb TR, Reed KL (2005) Comparative pulmonary toxicity inhalation and instillation studies with different TiO_2 particle formulations: impact of surface treatments on particle toxicity. Toxicol Sci 88: 514–524

Warheit BD (2008) How meaningful are the results of nanotoxicology studies in the absence of adequate material characterization? Toxicol Sci 101: 183–185

Wiebert P, Sanchez-Crespo A, Falk R, Philipson K, Lundin A, Larsson S, Möller W, Kreyling WG, Svartengren M (2006) No significant translocation of inhaled 35-nm carbon particles to the circulation in humans. Inhal Toxicol 18: 741–747

Yeh HC, Cuddihy RG, Phalen RF, Chang IY (1996) Comparisons of calculated respiratory tract deposition of particles based on the proposed NCRP model and the new ICRP66 model. Aerosol Sci Technol 25: 134–140

1.11 Epidemiological Data

Dirk Pallapies

Institute for Prevention and Occupational Medicine of the German Accident Insurance

Bochum, Germany

Epidemiological Studies

A comprehensive review by Schulte et al. (2009) did not report any epidemiological studies that have specifically recorded health effects caused by synthetic nanomaterials. The studies available on exposures involving nanoparticles in an occupational setting and in the environment – welding fumes and ultrafine carbon or titanium dioxide particles, on the one hand, and air pollution in general, on the other hand – demonstrate which end points also need to be considered in view of "nano"-induced effects. However, they are not suitable for a specific assessment of dose-response relationships, as will be explained in detail below.

As described by Schulte et al. (2009), the target organs that need to be investigated are primarily the lungs – with regard to both functional and malignant diseases – and the cardiovascular system as well as neurological effects. Since the number of persons regularly exposed to synthetic nanomaterials is relatively small and, in many cases, the exposure itself took place only recently and for a short period, it cannot be expected that epidemiological studies with conclusive results on potential (mainly carcinogenic) effects resulting from prolonged exposure will be available in the next few years.

In welding, nanoparticles are only one component of exposure, whereas larger particles and especially those components that are dependent on the welding material used, such as metals, account for considerable parallel exposure. This makes it impossible to assess the specific effects of nanoparticles.

WHO International Agency for Research on Cancer Monograph Working Group IARC (Baan et al. 2006) as well as the MAK Commission (Greim 1999) considered the epidemiological evidence of the carcinogenicity of carbon black to be inadequate. At the same time, it was pointed out that no data were available that would allow the characterization or quantification of exposure to primary ultrafine particles. In a review, Valberg et al. (2006) also concluded that no consistently increased lung cancer risks or dose-response relationships could be derived from the major studies with high carbon black exposures.

In 2006, titanium dioxide was evaluated by IARC (Baan et al. 2006) with the same result: inadequate evidence on the basis of epidemiological data. It was explained that none of the epidemiological studies had been designed to assess the potential effect of the particle size (fine or ultrafine) or of the coating materials. The MAK Commission also assessed the data on titanium dioxide (Hartwig 2009) as follows:

The available epidemiological studies provide no reliable evidence of an increased lung cancer risk after prolonged exposure to dust from fine titanium dioxide. However, in view of the methodological problems of some of these studies, it is currently not possible to make a final statement as to the carcinogenicity of titanium dioxide in humans.

Therefore, no reliable conclusions about the effect of nanoparticles can be drawn from these studies.

Studies from the Environmental Sector

Several studies that also deal with the effect of ultrafine dusts are available from the environmental sector.

Exposure assessment is an essential problem in these studies, too. The working group around Peters (Peters et al. 2005), for example, generally used the total number of all particles as an indicator of exposure to ultrafine dust and thus nanoparticles. They argued that ultrafine particles account for the largest fraction of particles in numerical terms. Moreover, measurements of exposures in environmental studies are not person-related in most cases, but are to reflect the concentrations at a certain place at which certain "events" such as myocardial infarctions or deaths were recorded at very different times after exposure measurement. In the above-mentioned study by Peters et al. (2005), no association was found between the total particle count and myocardial infarctions that had occurred from a few hours up to 5 days after exposure. In 2005, Peters et al. concluded that there was little evidence of a relationship between exposure to ultrafine particles and the exacerbation of cardiovascular diseases but referred to the following studies by Wichmann et al. (2000) and Pekkanen et al. (2002).

In the study by Wichmann et al. (2000), which tried to characterize exposures to ultrafine particles in more detail by means of a wide range of estimates and model calculations, borderline significant associations were found between exposure to ultrafine particles (and also larger ones and SO_2, for example; the latter was interpreted as an artefact by the authors) and mortality especially in the period up to 4 or 5 days after exposure. (Typically, in these time-series studies, various periods ranging between 0 and 5 days after a specific measurement are analyzed and the significant results then highlighted.) One problem of these studies is the collinearity of various exposures and the effects can therefore not be assigned to a clearly defined single exposure – even with optimum adjustment.

In the study by Pekkanen et al. (2002), the number of ultrafine particles was recorded with an electric aerosol spectrometer. A significant association between concentrations of ultrafine particles (and also other particles and of NO_2 and CO) and ST-segment depressions in electrocardiograms (ECGs) during exercise tests of persons with coronary heart disease who lived within a 5-kilometer radius of the monitoring site was observed 2 days, but not 0, 1 or 3 days after exposure.

Lanki et al. (2008) found no association between exposure to ultrafine particles and ST-segment depressions in a small study group after a few hours.

De Hartog et al. (2003) investigated cardiac and respiratory symptoms of persons with coronary heart disease and revealed an association with ultrafine particles only for the symptom "avoidance of activities".

Another study by von Klot et al. (2005) reported a slight, but borderline significant association (RR 1.026; 95 % CI 1.005–1.048) between the total particle count, as well as particulate matter < 10 µm (PM_{10}), CO, NO_2 and O_3, and hospital admissions for cardiac reasons – this time on the day of exposure measurement.

The same study group (Lanki et al. 2006) described associations between total particle count and acute myocardial infarction on the same day, but they were not significant and were only observed in 3 of the 5 study centres, most consistently one day after exposure for a subgroup of fatal cases aged below 75 years.

Another publication by this group (Forastiere et al. 2005) dealt with out-of-hospital coronary deaths in Rome and described a significant association for the total number of particles on the same day (as well as for PM_{10} and CO); however, no association was found for mortality observed on the following three days.

Kettunen et al. (2007) reported a just not significant association between the concentration of ultrafine particles and fatal stroke on the following day, but only for the season from May to September.

Penttinen et al. (2001) observed weak inverse, but mainly non-significant associations between ultrafine particle concentrations in Helsinki and the PEFR (peak expiratory flow rate) among a group of 54 adult asthmatics. The study group seems to have been essentially identical with that of 57 asthmatics of another publication by the same authors (Penttinen et al. 2001), in which they also established an effect of ultrafine particles, although they could not definitely separate it from effects of NO, NO_2 or CO.

McCreanor et al. (2007) carried out a crossover study among 60 mild to moderate asthmatics in London, with probably the best exposure assessment to date. Volunteers walked along Oxford Street (considerable exposure mainly to diesel engine emissions) for 2 hours or through Hyde Park. During this time, exposure was recorded via sampling devices installed on a pushcart accompanying them. Lung function and immunological parameters of the volunteers were recorded. An about 5 % higher reduction in lung function parameters and a small decrease in the pH of the exhaled breath condensate were observed after walking on Oxford Street. The authors found a borderline significant association with exposure to ultrafine particles, but also with $PM_{2.5}$, elemental carbon and NO_2. No clinically relevant symptoms occurred.

Rückerl et al. (2006) and Delfino et al. (2008) also published studies in which biomarkers of inflammation, antioxidative activity and coagulation were investigated and occasional associations were described.

In summary, it must be pointed out that no consistent effects have been observed in environmental epidemiological studies to date, particularly as regards

the time of occurrence after exposure. In most cases, individual measurement data of exposure to ultrafine particles (and to other air pollutants) is missing; moreover, some studies use only the total number of particles as an index of ultrafine particles. Since the concentrations of many air pollutants are collinear, it is unclear which parameter is most probably causally related to the endpoint even if there are signs of effects on health. Other possible relevant confounders, especially such as noise or socio-economic status, have only been taken into account insufficiently or not at all.

Therefore, these studies can hardly be used for the assessment of the effects of nanoparticles.

Clinical Studies

In addition, clinical studies with short-term exposure to nanoparticles are available.

Pietropaoli et al. (2004) found no effects on lung function or signs of inflammatory effects on the airways either in healthy or asthmatic volunteers after 2-hour exposure to ultrafine carbon particles at concentrations of 10 or 25 µg/m³. After exposure of 16 healthy volunteers to a level of 50 µg/m³ while engaging in physical exercise on a bicycle ergometer for 15 min every half hour, mild reversible effects of borderline significance ($p = 0.04$ as compared with air) were observed: reduction in $FEF_{25–75}$ (forced expiratory flow) of 4.34 ± 1.78 % and in CO diffusing capacity of 1.76 ± 0.66 ml/min/mm Hg. There were no consistent differences in symptoms, induced sputum or exhaled NO, nor were there any signs of inflammatory effects on the airways.

Reactive hyperaemia of the forearm and venous nitrate and nitrite levels were determined by means of venous occlusion plethysmography among the above-mentioned 16 healthy volunteers 3.5, 21 and 45 h after exposure (Shah et al. 2008). As compared with air, absence of reactive hyperaemia was only observed 3.5 hours after ultrafine particle exposure (9.31 ± 3.41 vs. 1.09 ± 2.55 ml/min/100 ml; $p = 0.03$), venous nitrate and nitrite levels decreased slightly after ultrafine particle exposure whereas there were no significant differences for blood pressure or other parameters.

In another publication based on the same clinical study (Frampton et al. 2006), alterations in leukocyte distribution and expression of adhesion molecules associated with exposure to the particles were only described after physical exercise. As also assessed by the authors, the differences after exposure to ultrafine carbon particles were so small that adverse health effects were not expected.

Beckett et al. (2005) compared the effects of 2-hour exposure to ultrafine zinc oxide particles (500 µg/m³) and fine zinc oxide particles of the same mass and air among 12 healthy adults. No acute systemic effects on various respiratory, haematological or cardiovascular endpoints were observed.

Whereas the above studies used artificially generated nanoparticles of a certain substance, Gong Jr. et al. (2008) exposed 17 healthy and 14 asthmatic

volunteers for 2 hours to concentrated ultrafine particles collected in a Los Angeles suburb with substantial motor vehicle pollution. According to the authors, inhaled ultrafine particle counts (mean 143 000/cm^3 with a range of 39 000–312 000/cm^3) were 7 to 8 times higher than ambient levels. Although a number of lung function parameters, symptoms, exhaled NO concentrations, ECG and inflammatory markers in peripheral blood and sputum were evaluated, only very sporadic associations with exposure to particles were found. The described effects such as a 0.5 % decrease in arterial oxygen saturation or a 2 % decrease in FEV_1 (forced expired volume) on the morning after exposure are clinically insignificant at least on an individual level and might also be incidental findings.

Seen as a whole, clinical studies have up to now not provided definite evidence of effects specifically mediated by nanoparticles.

Occupational Medical Case Report

Song et al. (2009) reported the development of progressive lung fibrosis in seven female Chinese printers. The authors related clinical symptoms to nanoparticle exposure, although they occurred after massive exposure to a paste (an ivory-coloured, soft polyacrylic ester mixture), which was sprayed under pressure to coat polystyrene surfaces heated up to 100 °C in a windowless room of about 70 m^2 – with smoke development. The workplace conditions are very likely responsible for the lung damage and symptoms observed in the female workers, but the information available does not allow any conclusion with regard to a potential contribution of nanoparticles to the observed health effects.

References

Baan R, Straif K, Grosse Y, Secretan B, El Ghissassi F, Cogliano V (2006) Carcinogenicity of carbon black, titanium dioxide, and talc, WHO International Agency for Research on Cancer Monograph Working Group. Lancet Oncol 7(4): 295–296

Beckett WS, Chalupa DF, Pauly-Brown A, Speers DM, Stewart JC, Frampton MW, Utell MJ, Huang LS, Cox C, Zareba W, Oberdörster G (2005) Comparing inhaled ultrafine versus fine zinc oxide particles in healthy adults: a human inhalation study. Am J Respir Crit Care Med 15, 171: 1129–1135

Delfino RJ, Staimer N, Tjoa T, Polidori A, Arhami M, Gillen DL, Kleinman MT, Vaziri ND, Longhurst J, Zaldivar F, Sioutas C (2008) Circulating biomarkers of inflammation, antioxidant activity, and platelet activation are associated with primary combustion aerosols in subjects with coronary artery disease. Environ Health Perspect 116: 898–906

Forastiere F, Stafoggia M, Picciotto S, Bellander T, D'Ippoliti D, Lanki T, von Klot S, Nyberg F, Paatero P, Peters A, Pekkanen J, Sunyer J, Perucci CA (2005) A

case-crossover analysis of out-of-hospital coronary deaths and air pollution in Rome, Italy. Am J Respir Crit Care Med 172: 1549–1555

Frampton MW, Stewart JC, Oberdörster G, Morrow PE, Chalupa D, Pietropaoli AP, Frasier LM, Speers DM, Cox C, Huang LS, Utell MJ (2006) Inhalation of ultrafine particles alters blood leukocyte expression of adhesion molecules in humans. Environ Health Perspect 114(1): 51–58

Gong H Jr, Linn WS, Clark KW, Anderson KR, Sioutas C, Alexis NE, Cascio WE, Devlin RB (2008) Exposures of healthy and asthmatic volunteers to concentrated ambient ultrafine particles in Los Angeles. Inhal Toxicol 20(6): 533–545

Greim H (1999) Industrieruße (Carbon black) in Form atembarer Stäube, Deutsche Forschungsgemeinschaft, Toxikologisch-Arbeitsmedizinische Begründungen von MAK-Werten, 29. Lieferung, Wiley-VCH Verlag, Weinheim, 1–45

Hartwig A (2009) Titaniumdioxid (einatembare Fraktion), Deutsche Forschungsgemeinschaft, Toxikologisch-Arbeitsmedizinische Begründungen von MAK-Werten, 47. Lieferung, Wiley-VCH Verlag, Weinheim,1–61

de Hartog JJ, Hoek G, Peters A, Timonen KL, Ibald-Mulli A, Brunekreef B, Heinrich J, Tiittanen P, van Wijnen JH, Kreyling W, Kulmala M, Pekkanen J (2003) Effects of fine and ultrafine particles on cardiorespiratory symptoms in elderly subjects with coronary heart disease: the ULTRA study. Am J Epidemiol 157(7): 613–623

Kettunen J, Lanki T, Tiittanen P, Aalto PP, Koskentalo T, Kulmala M, Salomaa V, Pekkanen J (2007) Associations of fine and ultrafine particulate air pollution with stroke mortality in an area of low air pollution levels. Stroke 38: 918–922

von Klot S, Peters A, Aalto P, Bellander T, Berglind N, D'Ippoliti D, Elosua R, Hörmann A, Kulmala M, Lanki T, Löwel H, Pekkanen J, Picciotto S, Sunyer J, Forastiere F (2005) Health Effects of Particles on Susceptible Subpopulations (HEAPSS) Study Group. Ambient air pollution is associated with increased risk of hospital cardiac readmissions of myocardial infarction survivors in five European cities. Circulation 112: 3073–3079

Lanki T, Hoek G, Timonen KL, Peters A, Tiittanen P, Vanninen E, Pekkanen J (2008) Hourly variation in fine particle exposure is associated with transiently increased risk of ST segment depression Occup Environ Med 65: 782–786

Lanki T, Pekkanen J, Aalto P, Elosua R, Berglind N, D'Ippoliti D, Kulmala M, Nyberg F, Peters A, Picciotto S, Salomaa V, Sunyer J, Tiittanen P, von Klot S, Forastiere F (2006) Associations of traffic related air pollutants with hospitalisation for first acute myocardial infarction: the HEAPSS study. Occup Environ Med 63: 844–851

McCreanor J, Cullinan P, Nieuwenhuijsen MJ, Stewart-Evans J, Malliarou E, Jarup L, Harrington R, Svartengren M, Han IK, Ohman-Strickland P, Chung KF, Zhang J (2007) Respiratory effects of exposure to diesel traffic in persons with asthma. N Engl J Med 357: 2348–2358

Pekkanen J, Peters A, Hoek G, Tiittanen P, Brunekreef B, de Hartog J, Heinrich J, Ibald-Mulli A, Kreyling WG, Lanki T, Timonen KL, Vanninen E (2002) Particulate air pollution and risk of ST-segment depression during repeated submaximal exercise tests among subjects with coronary heart disease: the Exposure and Risk Assessment for Fine and Ultrafine Particles in Ambient Air (ULTRA) study. Circulation 106: 933–938

Penttinen P, Timonen KL, Tiittanen P, Mirme A, Ruuskanen J, Pekkanen J (2001) Number concentration and size of particles in urban air: effects on spirometric lung function in adult asthmatic subjects. Environ Health Perspect 109: 319–323

Penttinen P, Timonen KL, Tiittanen P, Mirme A, Ruuskanen J, Pekkanen J (2001) Ultrafine particles in urban air and respiratory health among adult asthmatics. Eur Respir J 17: 428–435

Peters A, von Klot S, Heier M, Trentinaglia I, Cyrys J, Hörmann A, Hauptmann M, Wichmann HE, Löwel H (2005) Particulate air pollution and nonfatal cardiac events. Part I. Air pollution, personal activities, and onset of myocardial infarction in a case-crossover study. Res Rep Health Eff Inst 124: 1–66; discussion 67–82, 141–148

Pietropaoli AP, Frampton MW, Hyde RW, Morrow PE, Oberdörster G, Cox C, Speers DM, Frasier LM, Chalupa DC, Huang LS, Utell MJ (2004) Pulmonary function, diffusing capacity, and inflammation in healthy and asthmatic subjects exposed to ultrafine particles. Inhal Toxicol 16: 59–72

Rückerl R, Ibald-Mulli A, Koenig W, Schneider A, Woelke G, Cyrys J, Heinrich J, Marder V, Frampton M, Wichmann HE, Peters A (2006) Air pollution and markers of inflammation and coagulation in patients with coronary heart disease. Am J Respir Crit Care Med 173: 432–441

Schulte PA, Schubauer-Berigan MK, Mayweather C, Geraci CL, Zumwalde R, McKernan JL (2009) Issues in the development of epidemiologic studies of workers exposed to engineered nanoparticles. J Occup Environ Med 51: 323–335

Shah AP, Pietropaoli AP, Frasier LM, Speers DM, Chalupa DC, Delehanty JM, Huang LS, Utell MJ, Frampton MW (2008) Effect of inhaled carbon ultrafine particles on reactive hyperemia in healthy human subjects. Environ Health Perspect 116: 375–380

Song Y, Li X, Du X. Exposure to nanoparticles is related to pleural effusion, pulmonary fibrosis and granuloma (2009) Eur Respir J 34: 559–567

Valberg PA, Long CM, Sax SN. Integrating studies on carcinogenic risk of carbon black: epidemiology, animal exposures, and mechanism of action (2006) J Occup Environ Med 48: 1291–1307

Wichmann HE, Spix C, Tuch T, Wölke G, Peters A, Heinrich J, Kreyling WG, Heyder J (2000) Daily mortality and fine and ultrafine particles in Erfurt, Germany part I: role of particle number and particle mass. Res Rep Health Eff Inst 98: 5–94

2 Summary and Conclusions

Andrea Hartwig

Karlsruhe Institute of Technology

Karlsruhe, Germany

Since nanomaterials are increasingly used in industrial and consumer products, a science-based risk assessment is highly required. The aim of the MAK working group was to summarize current scientific evidence needed for risk assessment of nanomaterials with respect to workplace exposure. Within this task, the principal issue was the identification of critical reactions of toxicological concern and whether or not there are modes of action unique for nanomaterials as compared to particles in the microscale range. In general, current evidence suggests that nanoparticles evoke the same toxic reactions, i. e. inflammation and oxidative stress, as do their counterparts in the micrometer alveolar fraction. Nevertheless, there are pronounced quantitative differences in the extent of the toxic reactions at a given dose, including those related to carcinogenicity under conditions of particle overload (for details see Gebel (2011)), and perhaps also qualitative differences in translocation to different targets *in vivo*. Since the goal was risk assessment and not hazard identification, emphasis was put on available data allowing the establishment of dose-response relationships with respect to exposure and biological effects, i. e. toxicokinetic and toxicodynamic interactions, as a basis for the setting of occupational exposure limits.

2.1 Characterization of Nanomaterials and Exposure Assessment

One indispensable prerequisite for the risk assessment concerns the assessment of the extent of exposure towards nanomaterials. This provides a major challenge in several aspects. Nanoparticles differ from larger particles in their tendency to form agglomerates and aggregates. Even though agglomerates appear macroscopically as one particle, they may break down in primary particles in biological systems. In contrast, particles within aggregates are firmly fused together, providing a surface area smaller than the sum of the primary particles. This raises several questions. First, what is the biologically and thus toxicologically relevant measure? Even though there is no definite answer to this question, relevant parameters are size, shape, surface area and surface properties. Furthermore, the so called protein corona generated *in vivo* appears to be of major importance for the transport and translocation of the respective nanoparticles. The second aspect concerns the measurement of particles within exposure assessment. In the case of microscale and larger particles the mass is usually given as mg/m^3. However, since nanoparticles exhibit a far higher particle to mass ratio or surface area to mass ratio, the measurement based on mg/m^3